KINETIC ANALYSIS OF THE CONTRIBUTION OF BASE FLIPPING TO THE SUBSTRATE SPECIFICITY AND CATALYTIC ACTIVITY OF HUMAN ALKYLADENINE DNA GLYCOSYLASE

By

AARTHY C. VALLUR

A DISSERTATION PRESENTED TO THE GRADUATE SCHOOL
OF THE UNIVERSITY OF FLORIDA IN PARTIAL FULFILLMENT
OF THE REQUIREMENTS FOR THE DEGREE OF
DOCTOR OF PHILOSOPHY

UNIVERSITY OF FLORIDA

2004

This work is dedicated to my family whose unshakable belief in me made me aspire.

ACKNOWLEDGMENTS

My gratitude to my parents exceeds expression. They always instilled in me the will and desire to achieve, aspire and hope in my abilities. I am indebted to my husband for being an enormous source of support and encouragement through the trying years of graduate school. I would also like to acknowledge the mentorship of Dr. Linda Bloom, for the countless lessons I learnt from her and the very rewarding years I spent in her lab. Beyond that, acknowledgements will not be complete without recalling the inspiration I derived from my excellent uncle and aunts, all my teachers through school and college and my dear friends, notably, Balaji Krishnaprasad of Gainesville.

TABLE OF CONTENTS

page

LIST OF TABLES

LIST OF FIGURES

Abstract of Dissertation Presented to the Graduate School
of the University of Florida in Partial Fulfillment of the
Requirements for the Degree of Doctor of Philosophy

KINETIC ANALYSIS OF THE CONTRIBUTION OF BASE FLIPPING TO THE SUBSTRATE SPECIFICITY AND CATALYTIC ACTIVITY OF HUMAN ALKYLADENINE DNA GLYCOYSLASE

By

Aarthy C. Vallur

December 2004

Chair: Linda B. Bloom
Major Department: Biochemistry and Molecular Biology

Human alkyladenine DNA glycosylase (AAG) removes a variety of alkylated and deaminated bases from double stranded DNA to initiate base excision repair of damaged adenines. The crystal structure of AAG shows that the enzyme uses a characteristic base flipping mechanism and does so by using Tyr-162 to intercalate through the minor groove and occupy the space vacated by the flipped out substrate. The purpose of this dissertation is to further understand the contribution of base flipping to the specificity and efficiency of AAG.

A Y162S mutant showed undetectable activity on hypoxanthine (Hx) and *1, N^6*-ethenoadenine (εA) substrates. A Y162F mutant showed 2-fold reduced activity on Hx but the activity of the mutant was rescued by a "DNA mutation", in which the thymine (T) opposite Hx was replaced by diflorotoluene (F) with which Hx cannot base pair. The

reduced activity of the Y162F mutant on εA was not rescued by the same "DNA mutation".

Other changes were made to affect the stability of Hx in DNA in an attempt to understand the importance of flipping to AAG activity on Hx. When Hx•T was placed between strong base stacking G-C partners, excision of Hx was reduced and required 4 times the AAG needed to saturate the excision of the same amount of Hx•T placed between weak base stacking T-A partners. When T was replaced by F, excision of Hx in both sequence contexts was enhanced, but the enhancement with the G-C stacking partners was greatest, up to 10-fold and enhancement with T-A stacking partner was modest. When T was replaced by C with which Hx forms Watson- Crick bonds excision was poor and the stacking partners did not matter.

The above results went on to show that AAG could use the Tyr-162 mediated flipping mechanism to specifically bind and use the flipping mechanism as an important step in recognizing the substrate. Factors that affect the flipping equilibrium which is the first step in catalysis, like the stability of the damaged base in DNA will also affect the capacity of the enzyme to remove the damaged base, ultimately. The sequence context of the damaged base may be a determining factor in its recognition by DNA glycosylases and hence in the initiation of its repair by the base excision repair pathway.

CHAPTER 1
BACKGROUND AND SIGNIFICANCE

The Problem of Chemical Reactivity of Bases

The bases in DNA can undergo chemical modifications which can alter the genetic code and cause disturbances in the helical structure of DNA. Like any unsaturated, heterocyclic compound, a base in DNA can fall prey to attacks by water, reactive oxygen species and many endogenous and environmental agents (*1-6*). These chemical changes account for around 20,000 damages/cell every day. Almost a quarter of these arise due to the hydrolysis of the *N*-glycosidic bond between the base and the deoxyribose sugar leading to abasic or apurinic/apyrimidinic (AP) residues in DNA. Purines are more susceptible to hydrolysis of the *N*-glycosidic bond at an *in vivo* rate of >4500 depurinations/ cell (*3, 7*) whereas depyrimidination by hydrolysis occurs at a rate of less than that of depurinations. Abasic sites are extremely mutagenic and cytotoxic since they can lead to replication blocks and DNA strand breaks if not repaired (*8*). Deamination is another consequence of hydrolysis in normal bases.

Oxidation is a major source of damage to bases. DNA bases have electrophilic carbons that can undergo oxidation to form mutagenic lesions, primary of which is 7,8-dihydro-8-oxoguanine (8-oxoG) (*6, 9*). Pyrimidine glycols and formamidopyrimidines are also products of oxidative damage (Figure 1-1). Oxidative metabolism leads to the accumulation of free radicals and products of lipid peroxidation like aldehydes which can form etheno adducts with adenine, guanine and cytosine (*3*). Alkylation damage is also

brought about by S-adenosyl methionine, an abundant methyl donor in cells, which can react with the ring nitrogens of purines (*3*) (Figure 1-1).

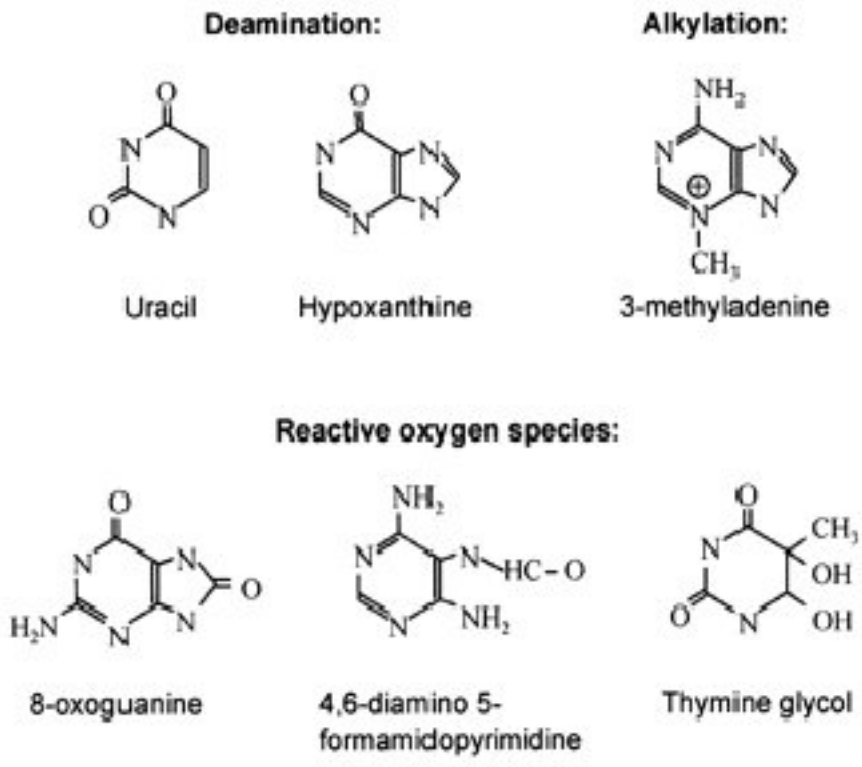

Figure 1-1. Structures of damaged bases, commonly encountered in DNA. Deamination, alkylation and oxidation are chemical changes that contribute to damaged bases in DNA (*See text*)

Other cellular agents that can react with bases include nitric oxide and its derivatives. Nitric oxide (NO·) is an important second messenger in the body and is involved in many functions including pathways signaling neurotransmission and arterial wall relaxation (*10*). Nitric oxide is highly reactive with oxygen and forms nitrous anhydride which can deaminate the primary amino groups of cytosine, 5-methyl cytosine, adenine and guanine (*11, 12*). NO induced deamination of cytosine, 5-methyl cytosine and guanine can lead to GC→AT transitions, which are the primary mutations seen with NO·. of the three, guanine has the greatest susceptibility to NO· induced deamination,

which modifies dG to xanthine (*13*). NO· induced deamination of dA to hypoxanthine, which can result in AT→GC transitions. Spencer *etal* observed significant accumulation of xanthine and hypoxanthine as the predominant lesions and a significant number of single strand breaks in HBE-1 cells, a human bronchial cell line, when the cells were exposed to 1mM nitrite at times greater than 60 min (*14*). More in vivo studies with cultured muscle nervous tissue cell lines, in which nitric oxide has important functions is needed to learn about the degree and prevalence nitric oxide-induced deamination.

Base Excision Repair- All Roads Lead to DNA

The base damages discussed above are small chemical changes that do not disrupt the structure of DNA drastically. But the problem of accumulating even small damages in a vast sea of base pairs that make up the genome posts many challenges to the integrity of the genome. Many pathways have evolved to repair damaged DNA and restore genomic integrity, of which the repair of small, chemically damaged bases falls on the base excision repair pathway (BER) (*15-20*). Initiation of BER is accomplished by a damage-specific DNA glycosylases, which recognize its substrate and then excise the C1'-N glycosidic bond between the base and the sugar (Figure 1-2). This leaves behind an abasic residue in DNA, which is then processed by an AP endonuclease to create a nick 5' to the abasic site. DNA glycosylases are thus very important in sustaining base excision repair and ensuring its success. Up to eight human proteins have been reported to have DNA glycosylase activity. The substrate specificity of glycosylases is wide, with some glycosylases being selective for one substrate only while others have a broader substrate range. Examples for glycosylases specific for one damaged base only are UDG (uracil) and hOGG1 (8-oxoguanine) while hAAG which can act on various adenine lesions is a good example for glycosylases that can act on a group of substrates (*16*). In

addition to having C1'-N glycosylase activity, some glycosylases also have an additional AP lyase activity. These are called bifunctional glycosylases in contrast to the former, which are monofunctional glycosylases.

Bifunctional glycosylases, also called the Class I AP endonucleases, utilize an enzyme amino group as a nucleophile to form a Schiff- base intermediate with the abasic site which then undergoes either a β or a β-δ elimination reaction to leave a nick. β-elimination leaves an α-β unsaturated aldehyde with the 3'- phosphate and when followed by δ-elimination (Figure 1-2), leaves just a 3'- phosphate residue which cannot be extended by a polymerase (*21*). These 3'- termini can be acted on by a Class II AP endonuclease, which processes the 3'- phosphate residue to leave a 3'- OH residue which can then be extended by a polymerase. Repair is then completed when a DNA polymerase replaces the nucleotide and a DNA ligase seals the 3'-OH and 5'- phosphate termini. Some bifunctional glycosylases like the hOGG1 and the bacterial FPG also have deoxyribophosphatase (dRPase) activity which can hydrolyze the abasic sugar- phosphate residue (*22*). The major Class II endonucleases in *E. coli* are Exo III and Endo IV, Exo III being responsible for 90% of the activity under normal physiological conditions (*23, 24*) while Endo IV takes over during periods of oxidative and nitrosative stress (*25, 26*). The mammalian homolog of Exo III is the human AP endonuclease I (aka APEX, APEI, Ref I), which is responsible for 95% of AP endonuclease activity in humans (*22, 27, 28*).

After the action of the Class II endonuclease in humans, deoxyribosephosphate lyase (dRPlyase) activity and synthesis to fill the gap is carried out by polymerase β (Pol β). After this, DNA ligase III, which interacts with Pol β through the XRCC1 protein, seals the nick to restore the original sequence in DNA. It is significant to note that Pol β

lacks the proofreading activity of replicative polymerases and is prone to a relatively high frequency of errors during incorporation, to the tune of 1 mismatched nucleotide per 3000-5000 residues (*29*). These errors occur despite an induced fit mechanism in the active site of Pol β. Two combined events ensure error free gap filling by Pol β. First, DNA ligase III discriminates against joining ends with a 3' mismatch thereby, allowing for excision of the wrong residue and replacement of the mismatched residue (*30*). Second, just like replicative polymerases act as holoenzymes with separate subunits encoding varied functions, a distinct human 3' exonuclease can cleave the mismatched 3' residue and allow for replacement. Recently, a human homolog of the *E. coli* Pol III holoenzyme component, Dna Q exonuclease, has been identified, which can correct Pol β errors during BER and hence can be a major candidate for error free repair (*31*). Such a proof- reading step will guarantee that correction of endogenous DNA damage does not by itself contribute to a high frequency of mutations.

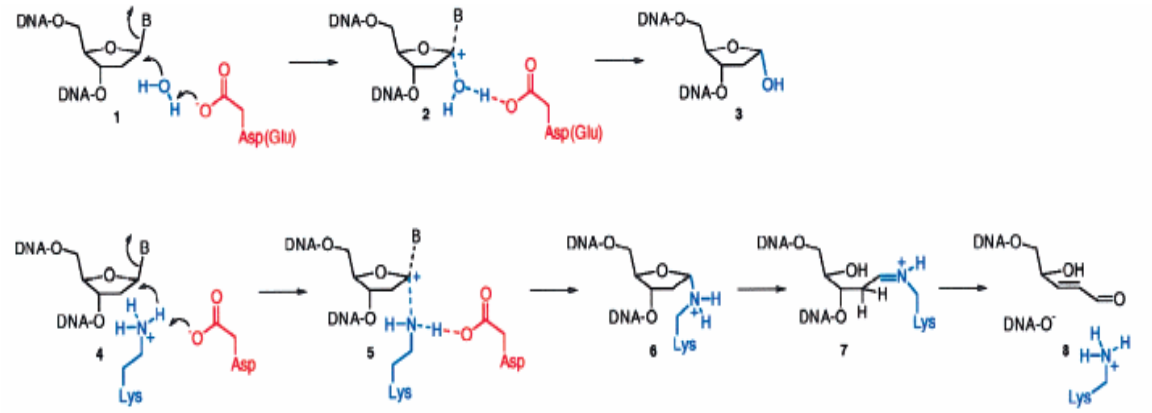

Figure 1-2. Mechanism of action of mono- and bi-functional DNA glycosylases. The first 3 steps illustrate excision of the C1-N glycosyl bond by nucleophilic attack by activated water in mono- functional DNA glycosylases like UDG. Steps 4- 8 illustrate the formation of a Schiff-base intermediate between a lysine residue and the sugar followed by β-δ elimination.(Figure adapted from *Scharer, O.D and Jiricny, J*, Bioessays, *23:270-281*, 2001)

Patch Size in Base Excision Repair

An alternative BER pathway to the single nucleotide replacement synthesis carried out by Pol β has been observed in eukaryotes. This pathway involves the replacement of around 4-19 nucleotides by DNA polymerase mediated strand displacement (*32, 33*) and has been seen to require FEN1 and PCNA (*34*). One possible need for this long- patch pathway could be the presence of termini which are resistant to the dRP lyase activity of Pol β (*35, 36*). In this case, a more processive polymerase may cause strand displacement and leave FEN1 to cleave the flap. The resulting nick is sealed by DNA ligase I. In reconstitution assays it was shown that, in the presence of PCNA and FEN1, Pol β can also carry out long- patch repair (*32, 37, 38*), suggesting that the role of PCNA may not be to support processive replication, but activation of FEN 1 (*37*). There is speculation that the BER initiating DNA glycosylase may influence the choice of patch size.

An added complexity is the observation that other factors may influence the patch size. Sung and Mosbaugh used a closed, circular plasmid with a site- directed uracil or ethenocytosine (εC) in *E coli* and studied the resulting patch size (*39*). In reconstitution experiments with various BER proteins, they discovered that DNA ligase mediated end-joining was the slowest step and also observed, short, long and very long patch repair. Increasing the ligase to polymerase ratio biased synthesis towards short- patch repair. With long time periods, longer patches (> 20 nucleotides) were observed (*39*).

The idea that the steps in BER are coordinated has been given a lot of thought due to the complicated interplay of proteins and mounting evidence delineating the interactions between enzymes catalyzing successive steps. Interactions between APE1 and Pol β (*40*), Pol β and XRCC 1 (*41, 42*), Pol β and ligase 1 (*43*) and XRCC1 and PARP (*44*) have been reported. The role of PARP in BER may be accidental but

nevertheless important, as it is known to be a sensor for nicks in DNA and interacts with XRCC1 (*44, 45*). Moreover, PARP knockouts are highly sensitive to methylnitrosourea, which leaves behind BER substrates in DNA (*46*). There is also evidence for some functional interactions between glycosylases and APE1. This step- wise coordination may be important in bringing substrates and enzymes together and also protecting the cell from the harmful abasic sites that accumulate as intermediates in BER.

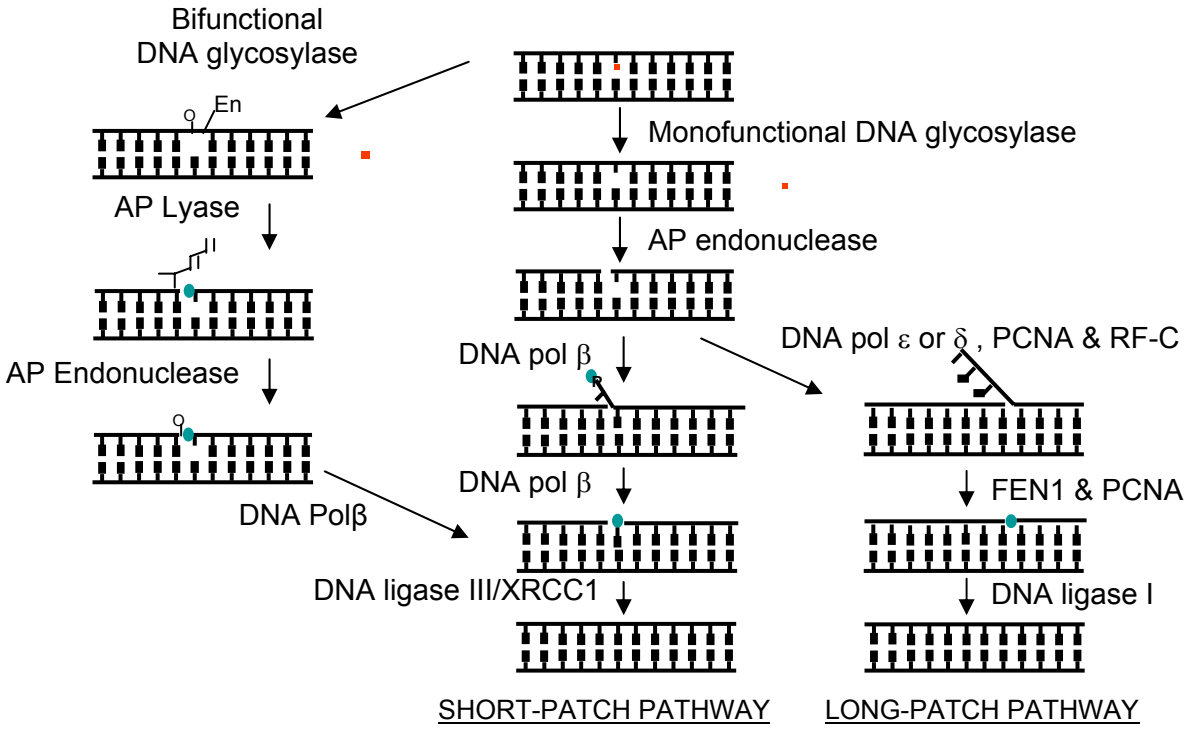

Figure 1-3. Base excision and repair by different pathways. Base excision, initiated by a damage specific DNA glycosylase can lead to resynthesis by either the short patch pathway, in which one nucleotide is resynthesized or long patch pathway, in which anywhere from 4-20 nucleotides are resynthesized. Mono- and bi-functional glycosylases leave behind different 3' termini which are processed by AP endonucleases or Pol β. Abbreviations: XRCC1- X-Ray Cross Complementation protein, PCNA- Proliferating Cell Nuclear Antigen, FEN1- Flap-Endonuclease1, RF-C- Replicating Factor- C.

Though it is reasonable to assume that DNA glycosylases are localized to the nucleus where they function, it is also important to address the problem of damage to mitochondrial DNA, especially given its proximity to the oxidative phosphorylation system. It has been found that many eukaryotic DNA glycosylase mRNAs like those coding uracil DNA glycosylase (UDG) (*47*), human 8-oxoguanine DNA glycosylase (hOGG1) (*48*) and the human MutY homolog (MYH) (*49*) are alternatively spliced to encode nuclear and mitochondrial versions of the protein (*50*). Two additional DNA glycosylase activities have been reported to be localized only to mitochondria, MtODE and MtGendo (*51, 52*). These act on oxidatively damaged bases. More research is needed to reconstitute the BER pathway in the mitochondria and identify other proteins and splice variants for other components of the pathway.

CHAPTER 2
HUMAN ALKYLADENINE DNA GLYCOSYLASE- THE MASTER FLIPPER

Alkylating agents constitute one of the major offenders of the integrity of bases in DNA. Alkylated purines are mutagenic, especially susceptible functional groups in purines being the N7 of guanine and the N3 of adenine. Though commonly resulting from environmental and chemotherapeutic agents, alkylation damage can also result as a by- product of cellular activities. A unique suicidal enzyme, O^6-methylguanine methyl transferase directly reverses O^6-methyl guanine lesions which are highly prone to mispairing with thymine (*53, 54*). Most other alkylated bases are removed by specific DNA glycosylases and alkylated base- specific glycosylases have been cloned in almost all species studied, including bacteria, yeast, mice and humans. With the discovery of UDG by Lindahl and coworkers in 1974 (*55*), came the awareness about the need for more glycosylases to play a role in base excision repair. Research since has identified *E. coli* glycosylases responsible for removing 3-methyladenine (3-meA) and other cytotoxic alkyl purines (*56-58*). In 1982, Goldthwait and co- workers identified two distinct glycosylases responsible for excising 3-meA, a 3-meA DNA glycosylase I constitutively expressed from the tag gene and a 3-meA glycosylase II which is encoded by the inducible alkA gene (*59*). The tag gene product was specific for 3-meA while the alkA product showed a broad substrate range including 3-meA, 3-meG and 7-meG. Subsequently, alkylpurine glycosylase activities have been identified and purified from S. cerevisiae (MAG), mice (MPG) and humans (AAG). Alkyladenine DNA glycosylase (AAG) was identified as the human equivalent of E. coli AlkA and could complement tag

and alkA deficient strains. It was independently characterized by three groups who alternatively named it as alkyladenine DNA glycosylase (AAG) (*60*), methylpurine DNA glycosylase (MPG) (*61*) and alkyl-N-purine DNA glycosylase (ANPG) (*62*). It has been the only alkyl purine glycosylase discovered in humans so far. In 1993, Vickers *et al* localized the human AAG gene between the α- globin gene cluster and the telomere of the short arm of chromosome 16 (chr16p) (*63*). Working with a colon adenocarcinoma cell line (HT29) and a human erytholeukemia cell line (K562), they identified the gene as comprising five exons whose representation differed in the 5' end from the cloned cDNA reported earlier by Samson *et al* (*60*). Rafferty and co- workers, in 1994, screened a λgt11 human placental cDNA library with a probe derived from the original sequence and identified two alternative cDNAs, which differed in seven N-terminal residues (*64*). They concluded that these were likely to be splice variants differing in exon usage and could be important in accounting for some properties such as cellular localization and binding properties of the protein. In a search for more information on the expression of AAG, O Connor's group located the basal promoter within 80 bases of the start codon of exon 1 in HT-29, K562 and 3T3 cell lines (*65*). They also identified some putative transcription factor binding sites in the promoter region, including those for N-MYC, SP1, USF-1 and CBP. In super shift assays, N-MYC and SP1 were found to bind and super shift the promoter region (Figure 2-1). It was also reported that expression of the AAG gene was cell- cycle dependent. The expression was seen to increase during G1, remain elevated during synthesis and then decrease to basal levels. This was consistent with DNA synthesis and the need for repairing replicating DNA. Other BER enzymes like APE1 and

Pol β have been found to be induced upon accumulation of DNA damage. Whether AAG is also induced requires more extensive in vivo studies to ascertain.

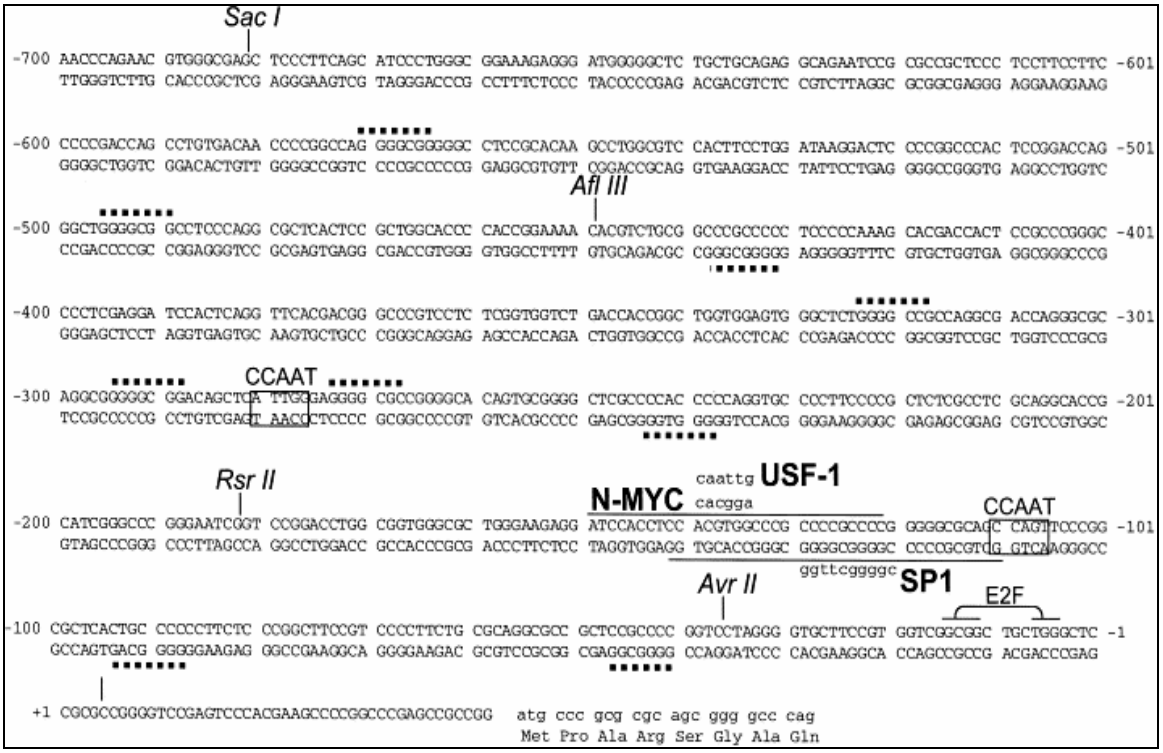

Figure 2-1. Basal promoter region of the AAG gene. Putative binding sites for several transcription factors like USF-1, SP1, N-MYC and CBP were noticed *(Adapted from Bouziane et al, Mutation Research, 2000, 461:15-29)*

AAG knockout Mice and Implications for Repair

Questions remained as to the precise biological effects of methyladenines in the cell and the possible role of protection by AAG activity. Given the broad substrate range observed for the mouse 3-MeA glycosylase (MPG), homozygous *AAG* knockout mice were generated by two groups and examined for phenotypes that can make the role of AAG clearer. Engelward *et al*, reported in 1997 that AAG was the major 3-MeA glycosylase in at least 4 different tissues, namely, liver, kidney, testes and lungs in these mice (*66*). Mouse embryonic fibroblasts that were deficient in AAG were more sensitive

to Me-Lex, an alkylating agent that generates 3-MeA specifically in DNA, than the wild type AAG producing fibroblasts. AAG was also found to be the only glycosylase responsible for removal of Hx when tested in the testes, kidney and lung tissues. It was also the major activity responsible for excising εA lesions, but it is interesting to note that though no other εA glycosylase activity was noticed in testes and kidney, there was a minor degree of εA excision noticeable in the lungs of the $AAG^{-/-}$ mice.

Elder *et al* also published the generation and effects of the $AAG^{-/-}$ genotype (*67*). They reported an increased frequency of MMS- induced mutations in the *hprt* gene of splenic T- lymphocytes after a single MMS dose of 150mg/kg. These mutations were mostly AT→TA transversions (47%) with some GC→TA transversions (27%). The mutation frequency was about 10-fold higher than the background. When analyzed, they found an accumulation of 3-MeA and methylated guanines in the hprt gene up to a 24hr period after MMS treatment, but found that O^6-MeG and O^4-MeT which are also formed at lower frequencies by MMS were efficiently cleared in the knock out (*ko*) cells lacking MPG activity. A reason for the cytotoxicity of 3-MeA and 7-MeG are their labile glycosylic bonds depurinating at a higher rate leading to abasic sites in the DNA. O^6-MeG and O^4- MeT are highly prone to mispairing and creating single base changes. O^6-MeG and O^4- MeT seem to be cleared by another redundant activity, possibly by the nucleotide excision repair (NER) machinery or another DNA glycosylase. Elder *et al* concluded that the importance of AAG may be more than the need to protect against 3-MeA and 7- MeG. It may be more important to protect the genome from its other substrates, Hx, which is highly mutagenic and can cause AT→GC transitions and *εA*,

which is also promutagenic. Both these lesions have stable glycosidic bonds and may be the primary target for AAG.

One remarkable feature of both these knockout mice was that both strains were active, viable, and fertile and did not show any other abnormalities, prompting the conclusion that either the spontaneous lesions that are the targets of AAG were not lethal when unrepaired or that other glycosylases/repair pathways can assist to handle these lesions. This is important because there is evidence that, in yeast, NER can process some AAG substrates and can also act on some other methylated substrates like O^6-MeG. It was recently reported that human AAG can interact with the human RAD23 proteins, which are involved in recognition of damaged bases in DNA in NER and that the interaction can functionally affect AAG binding and excision activity on Hx containing DNA (*68*). Nevertheless, the AAG knockout model is the first glycosylase/BER homozygous knockout model available to better understand the complex pathway. Knockouts of other downstream enzymes in BER have proved embryonic lethal, possibly due to the general requirement of enzymes like Pol β and APE1 for processing all products of glycosylase action. These enzymes may also have other roles to perform and any possible complementation in activity by the NER pathway may not be sufficient to make up for the loss of these enzymes in the knockout cells. Loss of individual DNA glycosylases, on the other hand, may be much easier to complement by other DNA glycosylases or pathways. Hence, homozygous knockout models of individual DNA glycosylases, like the AAG knockout mice discussed above, may be useful in generating heterozygous crosses to study the effect of the BER machinery and its interplay with other repair machineries.

Diversity in Substrate Choice- Uniqueness of AAG

E. coli AlkA, mouse and human AAG have all been found capable of removing a diverse range of substrates unlike many other DNA glycosylases which are specific for one damaged base only. AAG was first identified as a 3-MeA glycosylase and hence named so (*60, 62*). But later, it was discovered to be able to remove 7-MeG, 8-oxoG, Hx and *εA* bases *in vitro (69-71)*. The $AAG^{-/-}$ mice demonstrated that it was the major glycosylase responsible for the removal of 3-MeA, Hx and *εA*. 8-oxoG may not be an AAG target since it was removed efficiently in the AAG ko cells probably by its own dedicated glycosylase, OGG1 (*72*). So being able to excise out at least 4 structurally diverse substrates in the cell raises the question of whether catalytic efficiency is compromised for substrate diversity. Methylated adenines and guanines can arise spontaneously *in vivo* from the action of methyl donors like SAM. Methyl adenines are unstable and spontaneously depurinate at a higher rate than normal purines, leading to cytotoxic abasic sites in DNA, in addition to having the ability to block replication forks. Hx is deaminated adenine, formed by the action of nitric oxides and its derivatives in the cell. Nitric oxide is an important second messenger and is also released by activated macrophages. Hx is highly mutagenic. *εA* on the other hand is formed by the action of lipid peroxidation products in the cell and the action of the common hepatocarcinogens, vinyl chloride and ethyl carbamate (*62, 73, 74*). In COS7 cells, 70% of *εA* lesions led to mutations. So, the biological cost of compromised catalytic efficiency for substrate diversity can be immense, making AAG a uniquely gifted enzyme. How one active site can be tailor- made to fit these diverse substrates is difficult to imagine. Extensive biochemical work done by our group show that, AAG-mediated excision is sensitive to

the base pairing partner of the damaged base, and the extent sensitivity varied with the identity of the damaged base (*75, 76*).

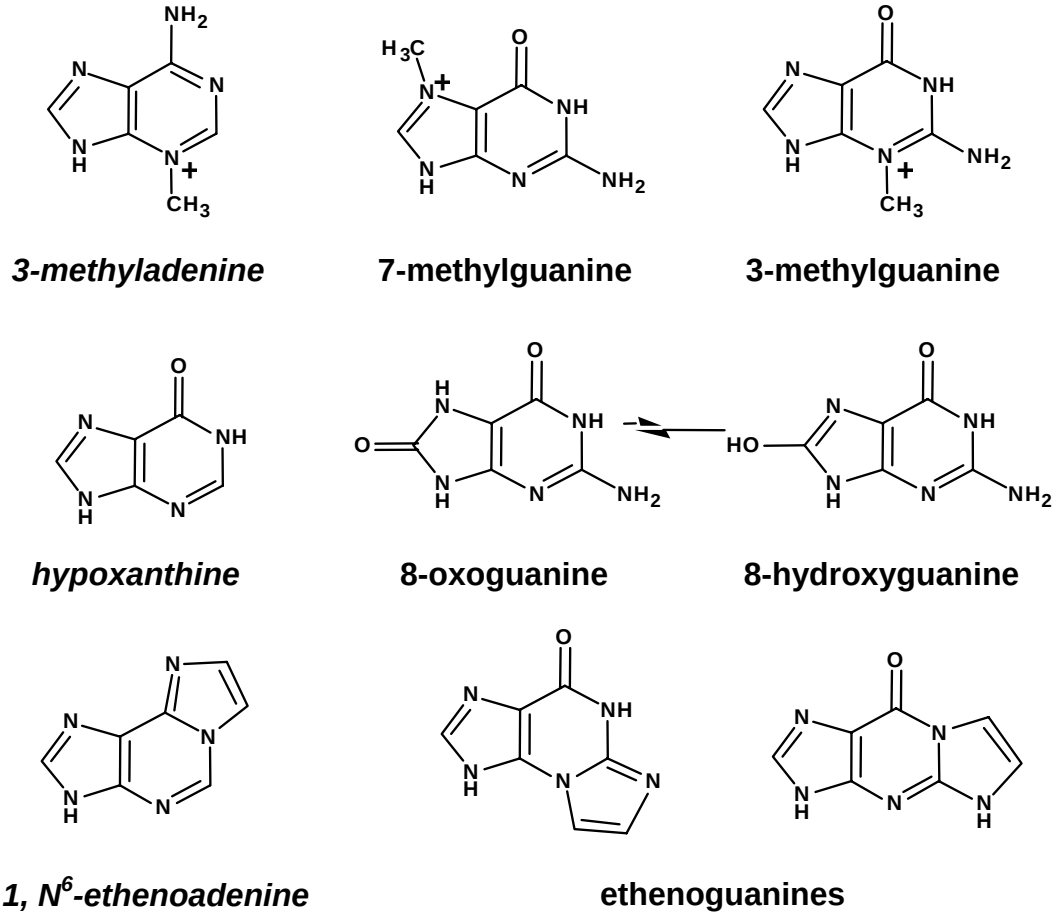

Figure 2-2. Bases found to be *in vitro* substrates for AAG. 3-methyladenine, 7-methyl guanine, hypoxanthine and *1, N^6*-ethenoadenine were found to be excised by AAG in *$AAG^{-/-}$* cells and are italicized for emphasis.

Crystal Structure of AAG and Implications for Catalysis

The diverse substrate specificity of AAG and the fact that it is the only known alkylpurine excising glycosylase makes it an interesting protein whose structure can not only tell us more about general glycosylase action but also about the complicated nature of substrate recognition used by AAG. Lau *et al* reported two crystal structures of AAG,

one bound to a pyrrolidine abasic site analog (*77*) and another of the catalytically inactive AAG mutant bound to one of its substrates, ethenoadenine (*78*). Both have contributed enormously to the understanding of AAG and have provided a tremendous boost to research on AAG and its mechanism of action. The first reported structure was a 2.7Å crystal structure of an enzymatically active fragment of AAG lacking the first 79 amino acids in the N-terminal, bound to a pyrrolidine abasic nucleotide, which is a potent inhibitor of the glycosylase activity. This structure showed AAG as a single domain containing seven α helices and eight β strands. β3β4, in the core of the protein, protrude as a β hairpin that inserts into the minor groove of the bound DNA, and displaces the target nucleotide, in this case the pyrrolidine. The displacement is made possible by insertion of Tyr-162, so that it intercalates in the space occupied by the nucleotide, which is then flipped out of the helix into the enzyme's active site binding pocket. This flipping mechanism was first identified in the cytosine methyl transferases (*79, 80*) and has also been consistently observed as the binding mechanism of choice for BER proteins like glycosylases (*81-83*) and endonucleases (*84, 85*).

In the AAG-DNA complex the B-form DNA duplex is kinked away from the protein where Tyr-162 intercalates, by about 22° and is held by two clusters of basic residues that contact the DNA backbone on either side of the flipped out residue. The extent of the buried DNA surface, as measured with a 1.4Å probe was 1034Å. This is similar to that observed with the UDG-DNA complex (*81*). The flipped out pyrrolidine is looped out of the helix by rotation of the P-O5' bond and the O3'-P bond of the phosphodiester backbone on either side of the nucleotide. The intercalating Tyr162 pushes out the opposite T19 residue 1.5 Å into the major groove. No specific contacts

between the opposing T19 and enzyme residues are visible in the flipped- out nucleotide-AAG structure. Met-164 and Tyr-165 located in the β hairpin, fill the minor groove and push against the deoxyribose moieties of T19 and T9, thereby widening the minor groove by almost 2 Å, 3' to the flipped out pyrrolidine. This 3' distortion may help AAG to scan the DNA unidirectionally.

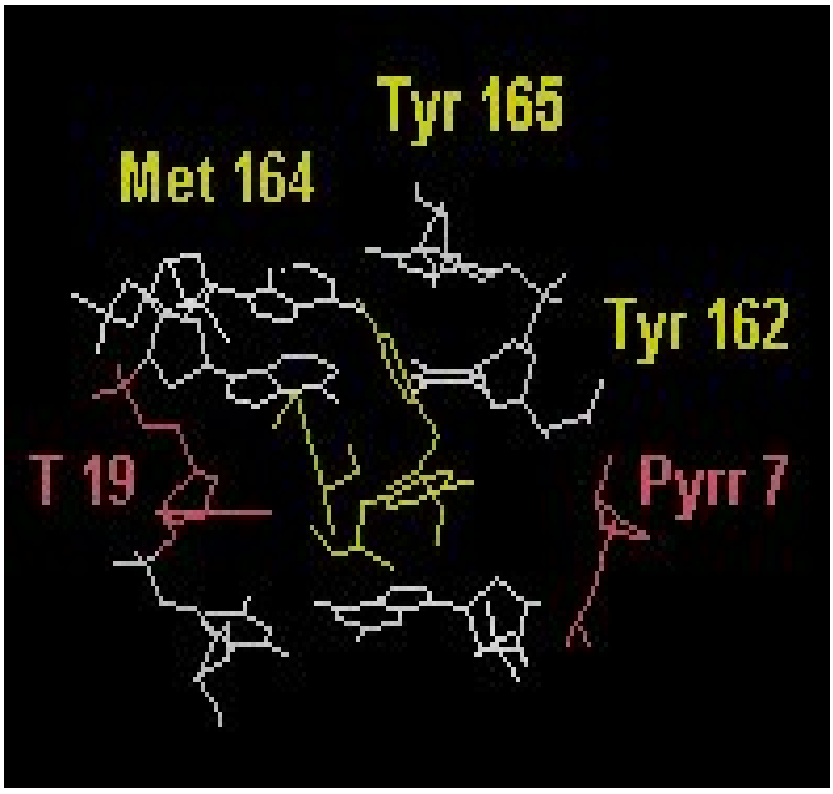

Figure 2-3. Residues that intercalate into the minor groove when AAG flips the pyrrolidine abasic analog (*Pyrr 7*). *Tyr-162* is fully intercalated between Guanine 6 and Thymine 8, while Thymine 19 (*T19*) is pushed into the major groove. *Met-164* and *Tyr-165* widen the minor groove.

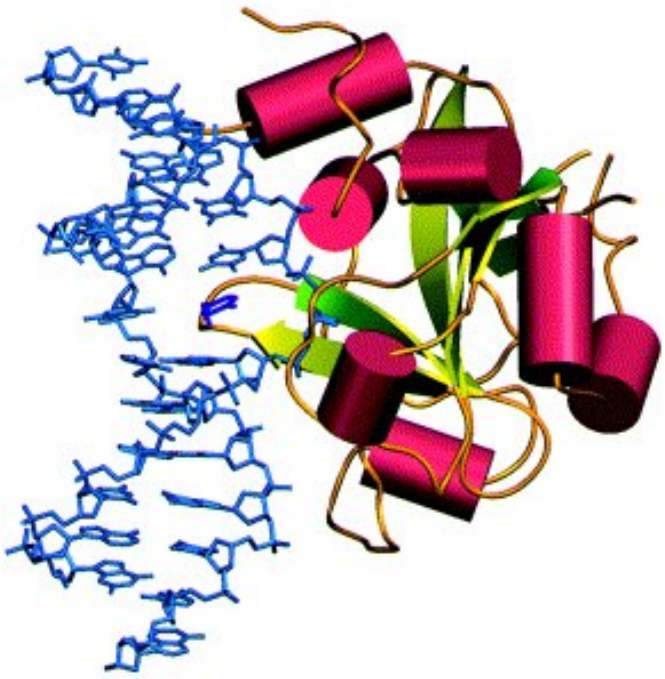

Figure2-4. Crystal structure of AAG bound to a pyrrolidine abasic nucleotide. The enzyme binds by intercalating Tyr-162 into the minor groove and flips out the abasic nucleotide into the active site. Enzyme residues widen the minor groove *(see text) (Adapted from Lau etal, Cell 95, 249- 258, 1998)*

The active site shows a central water molecule well positioned for a nucleophilic attack on the glycosyl bond of the flipped- out nucleotide. It is linked by a hydrogen bonding network with the pyrrolidine nucleotide and the side chains of Glu-125 and Arg-182 and the main chain carbonyl of Val-262. Glu-125 acts as a general base by deprotonating the water and thereby activating it for attack. Tyr-127 stabilizes Glu-125 by forming hydrogen bonds and may also stack against the base. The 2.1 Å crystal structure of AAG bound to *εA* gives a clearer picture of how a substrate is bound in the active site. In this structure, Tyr-127 stacks against *εA* while another active site tyrosine, Tyr-159 makes an edge to face stacking interaction with the *εA*. The flipped- out base itself is rotated 85° about its glycosyl bond away from the double helix. It is remarkable that these active site residues located in the buried core of AAG are conserved among the

other putative alkylation repair glycosylases identified in *Borrelia burgdorferi* (*86*), *Bacillus subtilis* (*87*), *Arabidopsis thaliana* (*88*), and *Mycobacterium tuberculosis* (*89*). The other important family of DNA glycosylases, of which *E. coli* AlkA, *S. cereviseae* MAG and human OGG1 are members, binds DNA and flips out the target base through a structurally conserved helix- hairpin- helix motif and use an aspartate as the catalytic residue, though there is no obvious sequence homology in this family of glycosylases. Whereas no AAG homologs have been noticed yet, in terms of its structural or sequence details, the conserved active site residues point out that proteins with similar folds may employ similar catalytic mechanisms, especially given the divergence of the glycosylases that share these conserved residues, in contrast to the structural homology seen in the HhH family of glycosylases.

The crystal structure also gives a hint of how AAG could achieve substrate specificity given its diverse substrate range; yet exclude normal purines from its active site. Positively charged substrates like 3-MeA and 7-MeG are electron deficient and hence, they may be bound and excised by using the aromatic π-electron stacking strategy in which, aromatic residues in the active site like Tyr-127 stack favorably with the flipped out base, thereby stabilizing it for excision. This method of sandwiching electron deficient bases between aromatic residues is a hallmark of many methylated base binding proteins such as AlkA and several mRNA binding proteins (*82, 90*). Add to it the intrinsic instability of the glycosylic bond in these bases, effective excision is more probable. But this same strategy may not work for neutral bases like Hx or εA. The εA-AAG crystal structure shows that εA is accommodated in the active site by a combination of aromatic stacking and hydrogen bonds between the main chain amide of His-136 and

the N^6 of the flipped out base. The stacking offers a lone pair of electrons which would not be possible if the base was adenine. In the same manner, the O^6 of Hx can accept a hydrogen bond from His-136, although guanine can do the same, its N^2 amino group will clash with the side chain of Asn-169, thereby restricting access to both normal purines but allowing both neutral substrates. This strategy for fitting the flipped nucleotide in the active site allows AAG to both screen for the right substrate and accommodate only the right substrate for excision, once flipped.

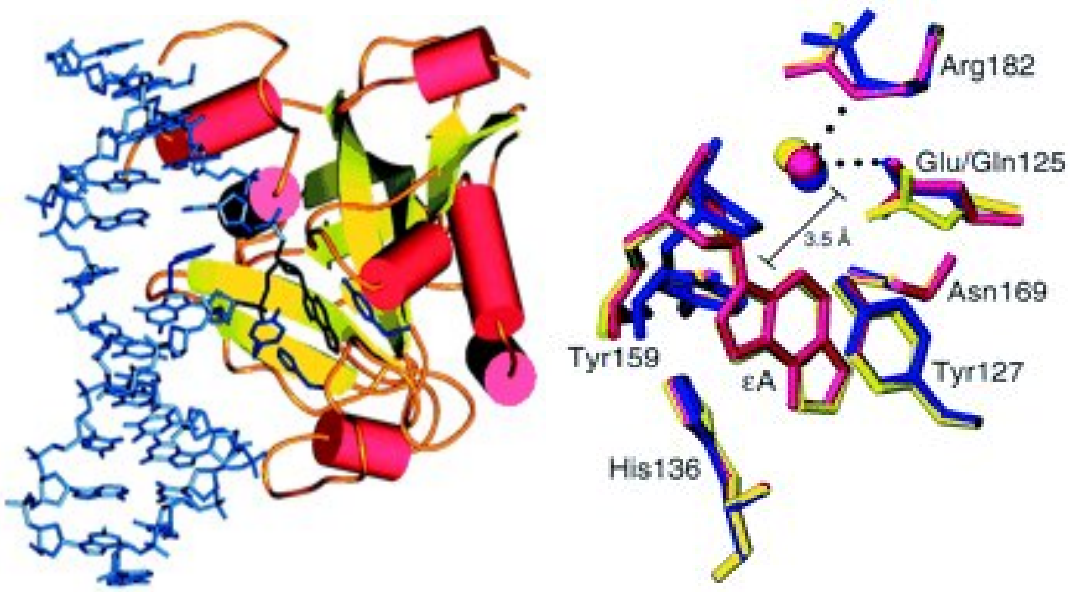

Figure 2-5. Crystal structure of E125Q bound to εA (left panel). The black εA is flipped into the active site, where it stacks between Tyr-159, His-136.and Tyr-127. The active site is clearly shown in the right panel. The orientation of the flipped out εA relative to the catalytic residue and the water molecule is shown in a superposition of the active sites of E125Q/ εA (green), wild- type AAG/ εA (pink.) and wild- type AAG/ pyrrolidine abasic site (blue) (Adapted from Lau et al, Proc. Nat. Acad. Sci. USA 97-13573, 2000)

Relevance of Studying Flipping in AAG

Role of Tyr-162 in Flipping

The flipping mechanism facilitated by insertion of Tyr-162 into the minor groove, is indicative of both how tight binding is achieved by AAG and how specific binding

may be achieved. The limited DNA contacting surface seen in the crystal structure and the absence of any specific contacts between the opposite base and enzyme residues also increases speculation on how important Tyr-162 mediated intercalation is to the overall efficiency of substrate binding by AAG. In contrast, *E. coli* UDG, which flips out uracil from DNA, makes extensive contacts with the phosphodiester backbone of the DNA and involves a "pinch-push-pull" mechanism to extrude the uracil from the DNA into the active site (*85*). In this model, UDG, scans along the DNA using its leucine finger .When a U-G wobble base pair is detected by the leucine, the Ser- Pro loops compress the phosphodiester backbone extensively, kinking the DNA to almost 45°, thereby pinching the DNA to gain access to the uracil. This pinching gives the needed force for the leucine to intercalate into the minor groove thus, "pushing" the uracil out of the helix where it is "pulled" into the active site by specific hydrogen bonding interactions. The last two steps can happen in either order. It is clear how protein- DNA interactions other than leucine insertion can contribute to flipping uracil by UDG. But these interactions seem to be largely missing from the AAG crystal structure, in which we do not see extensive compression or kinking of the DNA to the extent seen with UDG. In addition, leucine mutations to alanine or glycine reduced UDG activity to 10% and 1% respectively (*91-93*). In a similar attempt to test the functional significance of Tyr-162 , mutants and wild-type AAG were expressed in a *S. cerevisiae* strain lacking the endogenous yeast MAG1 and tested for resistance against the alkylating agent MMS. In contrast to the wt AAG, the Y162A mutant made yeast very sensitive to MMS, pointing out that maybe the mutation may have rendered AAG unable to bind and hence excise alkylated bases. In contrast mutations to the two other residues, Met-164 and Tyr-165, which are also part of

the β-hairpin, and which are shown to assist flipping by destabilizing the base pair next to the flipped out base, did not confer MMS sensitivity to the yeast cells (*78*). Mutation of Tyr-162 to Ser reduced AAG activity to undetectable levels, in kinetic studies done by us (*75*). So the importance of Tyr-162 to the process of flipping could be significant and in the absence of other factors that could affect DNA binding, must also contribute to the overall catalytic efficiency of the enzyme in ways more extensive than what is known from UDG.

Locating Substrates In DNA- Needle in a Haystack

The crystal structure offers no plausible explanation of how the daunting task of identifying its substrates amidst millions of bases is accomplished in the vast genome with its complex hierarchy of structures. It does make sense though, to expect AAG to use Tyr-162 intercalation to scan the DNA or possible substrates. Since AAG substrates are not known to distort the backbone extensively, a partial unstacking of the nucleotides may be needed for AAG to identify its substrate, as proposed for AlkA (*77*). Once a nucleotide is thus flipped, the disproportionate rigidity produced by Met- 164 and Tyr-165 may help the protein progressively flip nucleotides in the 3' direction, thereby scanning the minor groove for substrates. Once a base is recognized, the interactions in the active site may include or exclude the base as a substrate for excision. This two- step recognition may also help AAG preserve its substrate diversity. An added complexity comes from the reports that, though AAG does not seem to make any specific contacts with the opposite base, it is sensitive to the opposite base in terms of binding and excision proficiency (*75, 76*). These findings further enhance the need to understand the mechanism of AAG may achieve substrate diversity, given the different properties of the substrates it excises.

A systematic analysis of the biochemistry of flipping and its effects will be very useful in understanding the mechanism of action of AAG and inching closer to the unsolvable riddle of how glycosylases find their substrates in the vast genome. This dissertation attempts to address the issue of the contribution of flipping to the activity of AAG. A systematic, biochemical approach to analyzing the effects of mutating Tyr-162 on flipping efficiency and the contribution of local DNA sequence context to flipping efficiency was undertaken. The kinetic interpretation of the resulting observations reveals important biological implications about the contribution of flipping to the specificity and the catalytic efficiency of AAG (*75*). The conclusions drawn from this dissertation and the reagents developed to conduct the research will be valuable in dictating further studies on AAG mechanism and action.

CHAPTER 3
EXPERIMENTAL PROCEDURES

Cloning and Expression of Human Alkyladenine DNA Glycosylase Δ79 (AAGΔ79) and Its Mutants

A deletion mutant of AAG that is missing the first 79 amino acids from the N-terminus (AAGΔ79) was constructed using PCR, as already published (*75, 76*). Deletion of this unconserved N-terminal region has been shown to have no effect on either base excision or DNA binding activities of the enzyme, but the truncated protein is more soluble at low ionic strength. All site-directed mutants were made in the coding sequence of this truncated gene using the Transformer Site-directed mutagenesis kit (BD Biosciences Clontech, Palo Alto, CA). The primers used to generate the desired mutations were also engineered to contain a silent mutation that created a restriction site to facilitate screening of clones.

Subcloning of hAAGΔ79–E125Q into pET-15b Vector

The hAAGΔ79 constructs were cloned into pET-14b vectors and were used to transform *E. coli* BL21 (DE3) cells. The hAAGΔ79 –E125Q mutant was subcloned into a pET-15b vector due to its incompatibility with the pET-14b vector. The pET-15b vector has a multiple cloning site with a T7 promoter sequence and the *lac* operator sequence, which can allow for more controlled expression of the cloned gene and hence help get over the incompatibility problems seen with pET-14b. The E125Q gene sequence along with an upstream ribosome binding site was subcloned into the Xba1 and the BamH1 restriction sites (Figure 3-1). The vector was transfected into DH5-α cells and the plasmid

was isolated from the cells. The sequence and alignment of the E125Q gene was checked by sequencing. All other AAG mutants were cloned into pET-14b vectors.

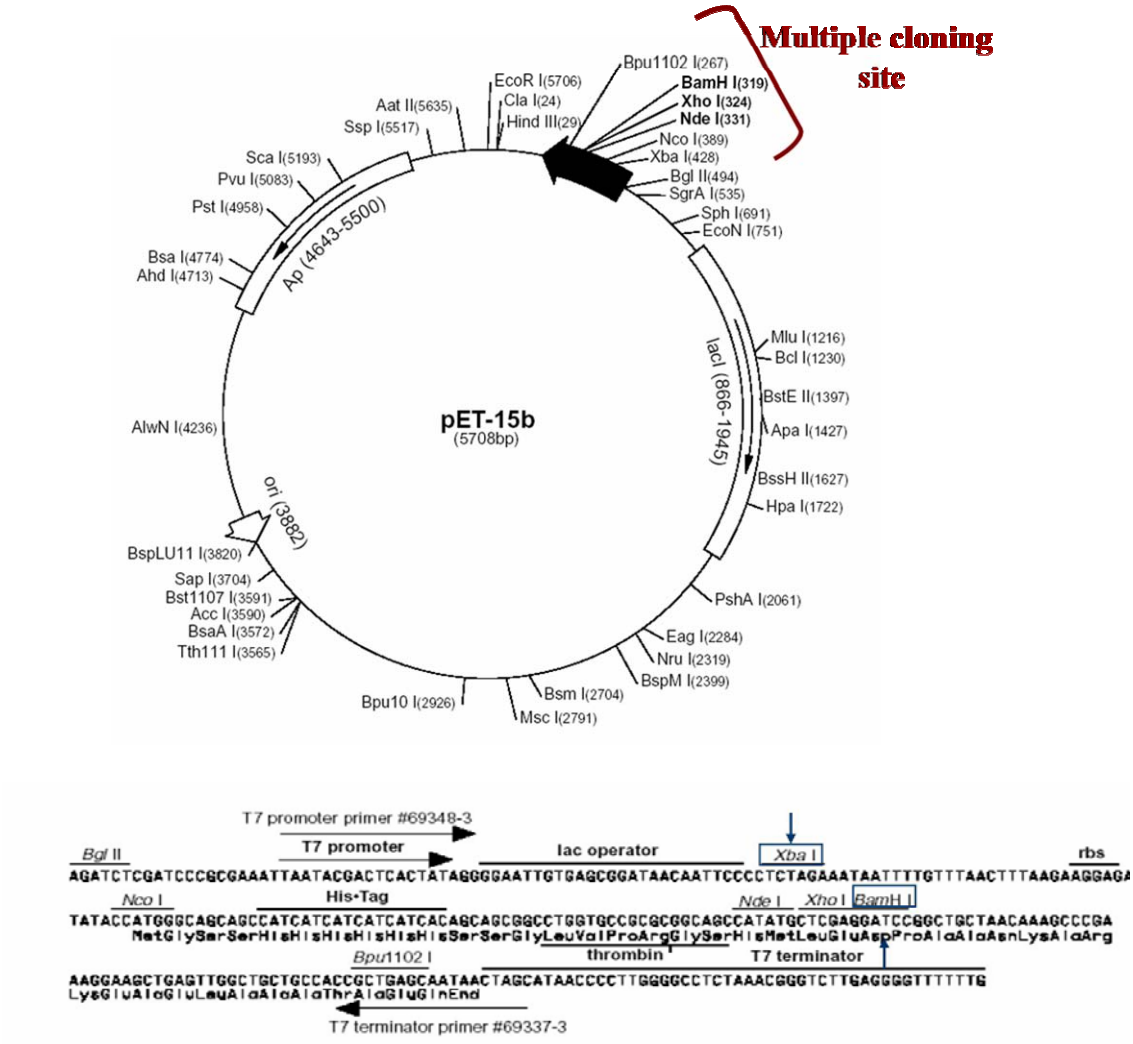

Figur 3-1. The map showing the multiple cloning site and the other features of the pET-15b vector. The multiple cloning site and its components are shown in the sequence below the map. The restriction sites used to subclone the E125Q gene, the Xba1 and the BamH1 sites are highlighted in blue with arrows.

The transformed cells were plated on 2xYT plates containing 100µg/mL ampicillin and grown for 16-20 hours at 37°C. A 10-mL aliquot of fresh 2xYTcontaining 100µg/mL ampicillin was inoculated with a single colony of transformed cells and grown at 37°C with vigorous shaking (200 rpm) to A_{600} of 0.5-0.8 and then stored at 4°C overnight. The

next day, the cells were spun down and washed two times with 2xYT- 100μg/mL ampicillin (10mL per wash) and then resuspended in fresh media. The washed cells were used to inoculate 3 liters of fresh, autoclaved 2xYT- μg/mL ampicillin. Cells were grown with shaking (200rpm) at 37°C to A_{600} =0.5. The cells were then cooled to 20- 25°C in the cold room. The cells were then induced with a 0.4mM final concentration of isopropyl β-thiogalactopyranoside (IPTG) and allowed to express at room temperature (20-25°C) with shaking for an additional 8 hours. Cells were then harvested by centrifugation at 5000rpm for 30 minutes at 4°C using a JLA-200 rotor (Beckman). The cell pellets were drained thoroughly and were stored at -80°C until needed. The pellets can be stored at -80°C from at least 16 hours up to a week for maximum protein yield.

Purification of Human Alkyladenine DNA Glycosylase Δ79 and Mutants

The frozen pellets were weighed and resuspended on ice in cold buffer A (50mM sodium phosphate, pH 7.4, 1mM EDTA, 70mM KCl, 10% glycerol, 0.5% 2-mercaptoethanol, 1μg/mL pepstatin A, 1μg/mL leupeptin, 0.1μg/mL PMSF) Approximately 3mL of buffer per gram of pellet was used. The resuspended pellets were then pooled into pre-chilled conical tubes and were lysed in a Aminco-SLM Instruments French press after loading into a 40K cell (30mL capacity) and pressing at medium (700psig) followed by maximum pressure (2550psig). The press was repeated again to ensure thorough lysing. The pressed cells were immediately placed on ice and centrifuged at 10, 000 rpm for 45 minutes in pre-chilled plastic tubes at 4°C using a JA-20 rotor (Beckman). The supernatant, containing the soluble protein was then pooled into a pre-chilled conical tube and placed on ice. All further purification steps were carried out at 4°C and the protein fractions were always kept on ice.

The pooled supernatant was loaded on to a 200mL diethylaminoethyl (DEAE) cellulose (Sigma) anion- exchange column using a peristaltic pump. The DEAE cellulose was batch equilibrated with several changes of 125mM sodium phosphate(pH 7.4) before packing until the material reached a pH of 7.4- 8.0. It was then packed in a column and further equilibrated to pack and flow at a rate of 2mL/ min. using two column volumes of buffer A without the protease inhibitors. After loading the supernatant on to the column, the column was washed with one column volume of buffer A with protease inhibitors. AAG which has a calculated pI of 9.1 will not bind to the DEAE and hence elutes in the wash. This step is useful in removing the vast amounts of DNA from the supernatant. The flow-through fractions were collected in pre-chilled conical tubes placed on ice. They were then loaded at 2mL/ min onto a 5mL Hi-Trap sulfopropyl sepharose (Hi Trap S) cation exchange column (Amersham Pharmacia Biotech) using an Amersham Pharmacia Biotech FPLC system. The column was previously washed in 2 column volumes of 1M KCl to strip any protein stuck and then equilibrated in 5 column volumes of buffer A. AAG binds to the column under these conditions. An 80mL gradient from 70 to 500mM KCl in buffer A was then used to elute AAG from the Hi trap column. AAG usually eluted at approximately 250-300mM KCl. Fractions of 1.8mL were collected and stored on ice. The fractions eluting at 250- 300mM KCl were analyzed by SDS-PAGE for the presence of AAG and those fractions that contain AAG were pooled and concentrated to 1- 2mL in an Amicon Ultracentrifugation Stirred cell (Model 8010) using a 5000D cut-off Polyethersulfone membrare, wetted in nanopure water. The concentrated fractions were then loaded on to a 125mL Sephacryl S-200 HR gel filtration column, at 0.5mL/ min using an Amersham Pharmacia Biotech Gradifrac system.

Previously, the column was isocratically developed at 1mL/ min with buffer B (25mM Tris, pH 7.5, 200mM KCl, 1mM EDTA, 1mM dithiothreitol and 5% v/v glycerol). Fractions were collected by washing the loaded fractions with buffer B. The fractions corresponding to the AAG peak were then analyzed by SDS-PAGE and the AAG containing fractions were pooled and concentrated as before to approximately 1.5 ml final volume. The purified, concentrated AAG was then dialysed against two changes of pre- chilled storage buffer(50mM HEPES, pH 8.0, 100mM KCl, 1mM EDTA, 1mM dithiothreitol and 37.5% v/v glycerol), in a 12, 500 cut-off dialysis membrane, for atleast 4 hours each. The final protein yield was determined by A_{280} measurements against a storage buffer blank using the published AAG extinction co-efficient of (27, 099 $M^{-1}cm^{-1}$). The dialyzed, pure AAG was dispensed into pre- chilled eppendorf tubes as 8- 10μL aliquots and stored at - 80°C. The purity of the protein was assessed by staining a SDS- PAGE gel with sypro-red dye.

Typically, fresh aliquots were taken from the -80°C for an experiment. Any protein leftover from the used stock was stored at -20°C and used within 3 days of storage. Serial dilutions of the stocks were done in cold AAG storage buffer prior to an experiment.

Synthesis and Purification of Oligonucelotides

Synthetic oligonucleotides were made on an ABI 392 DNA synthesizer using standard β-cyanoethylphosphoramidite chemistry and reagents from Glen Research (Sterling, VA). The oligonucleotides were cleaved after synthesis from the solid support by treatment with fresh ammonium hydroxide and were forced into collection vials with argon flush. The collected oligonucleotides contained base-protected products and other partial synthesis products. The protecting groups were removed by placing the vial into a

55°C sand bath for 12-16 hours. The deprotected oligos were then concentrated to dryness in a Savant Hi-Speed centrifugal vacuum system. The dried oligonucleotides were resuspended in 50% glycerol for purification by denaturing PAGE.

The samples were then resolved on a 12% polyacrylamide gel containing 8M urea, by loading around 40- 60 nM DNA per lane. The bands corresponding to the right sized product were visualized by UV shadowing and cut out from the gel. The DNA was eluted by shaking the gel slices in 8-15 mL of sterile NTE buffer (50mM Tris, pH 7.5, 50mM NaCl and 1mM EDTA), at room temperature. The buffer was changed every 8 hours three times and the eluted DNA was pooled. The pooled DNA was then passed through a 0.2-μm syringe filters (Acrodisc) to remove the gel remnants before dialyzing in a 3500 MW cut-off dialysis tubing (Spectropor) against 4L of nanopure water, changing water every 8 hours, 3 times. The dialyzed DNA was concentrated to approximately 1.5mL final volume and then quantitated using A_{260} measurements and calculated extinction co-efficients (*94, 114*). The oligonucleotides were then aliquoted and stored at -80°C.

Radio-labeling of Substrates and Annealing to Complement

DNA substrates strands containing the damaged nucleotide were 5'end-labeled with $[\gamma]^{32}$P-ATP using T4-kinase. A typical 50-μL reaction consisted of 2μM single-stranded 25mer containing the damaged base, labeling buffer (50mM HEPES, pH 8.0, 100mM KCl, 6.4mM $MgCl_2$), 30μCi $[\gamma]^{32}$P-ATP (Amersham) and 1 unit of T4 kinase (Invitrogen) at 37°C for at least one hour. The kinase was then inactivated by placing the tube at 95°C for 5 minutes. A 2-fold excess of the unlabeled complement was added to ensure complete annealing of all the labeled substrate. Annealing was performed by thoroughly heating the mixture to 85°C to remove all secondary structure and then slowly

cooling to room temperature to aid the formation of the most stable duplex. Typically 10% of the total DNA substrate was labeled when using a final DNA concentration of 2μM. When a final concentration of 200nM substrate was used, with all other parameters remaining constant typically almost 100% of the substrate was labeled. For freshly labeled substrate, optimum times of exposure for good signal ranged from 6-8 hours. Increasing times of exposure were used for older labels, ranging from 10-16 hours.

Single Turnover Excision Assay for Glycosylase Activity

To provide a measure of the chemistry of the enzyme, single turnover conditions in which a known amount of substrate DNA was incubated with a vast excess of AAG, were used. Single turnover conditions provide a measure of a step occurring after substrate binding and before product dissociation, which in this case is presumed to be the chemistry step. Another reason for doing single turnover kinetics for assessing activity is that, in preliminary steady- state experiments, it was observed that AAG could not recycle to excise all the substrate present and hence seemed to be product inhibited in some way. Saturating conditions were used to assess glycosylase activity. Typically, either 50nM labeled duplex DNA (10% labeled) or 5nM labeled duplex DNA (100% labeled) were used as substrate in the AAG assay buffer, consisting of 50mM HEPES pH 8.0, 100mM KCl, 0.5mM EDTA, 0.25mM DTT and 9.5 % v/v glycerol. At 37°C, the assay was started by adding AAG, typically anywhere from 4-to 20-fold excess AAG over substrate was used depending on the saturating concentration for that particular substrate, which were determined empirically by titrations. At various time points, from 30 seconds to 80 minutes, a 4μL aliquot of the reaction was withdrawn and quenched in 0.2M NaOH and chilled to stop the glycosylase activity. The rest of the assay relies on

the fact that the abasic site after glycosylase action exists in equilibrium between the hemiacetal and the aldehyde forms of the deoxyribose. The aldehyde form is labile to base and heat and undergoes β-elimination to yield a single stranded 5' labeled product upon denaturation, indicative of AAG mediated excision of the substrate base. After quenching and chilling, the tubes were heated at 95°C for 10-15 minutes to ensure complete β-elimination. The samples are then diluted with 2 volumes of loading buffer consisting of 95% formamide and 20 mM EDTA. Unreacted substrates were separated from cleaved products by PAGE on 12 % denaturing gels (8M urea, 1XTBE). The dried gel was exposed to a phosphor screen and visualized using a phosphorimager (Storm, Molecular Dynamics). Only the DNA with the 5'-label is visible under these conditions, resolved between a faster migrating 13mer product of AAG activity and a slower migrating, unexcised 25mer substrate. The bands were then analyzed using Image Quant software, which enables to quantify the β-emissions. The number of counts is proportional to the amount of DNA in the band. The background radioactivity was controlled for by averaging the analyzed bands with the counts in region of the gel which has no DNA. The product formed over time P_t was plotted over time using Kaleidagraph software. The plot was fit to a single- exponential rise Equation- 3-1, using non- linear regression.

$$P_t = A_0 (1 - e^{-k_{obs}t}) \qquad \text{(Eqn 3-1)}$$

Where, A_0 and k_{obs} are the amplitude of product formed and observed rate of the exponential rise, respectively.

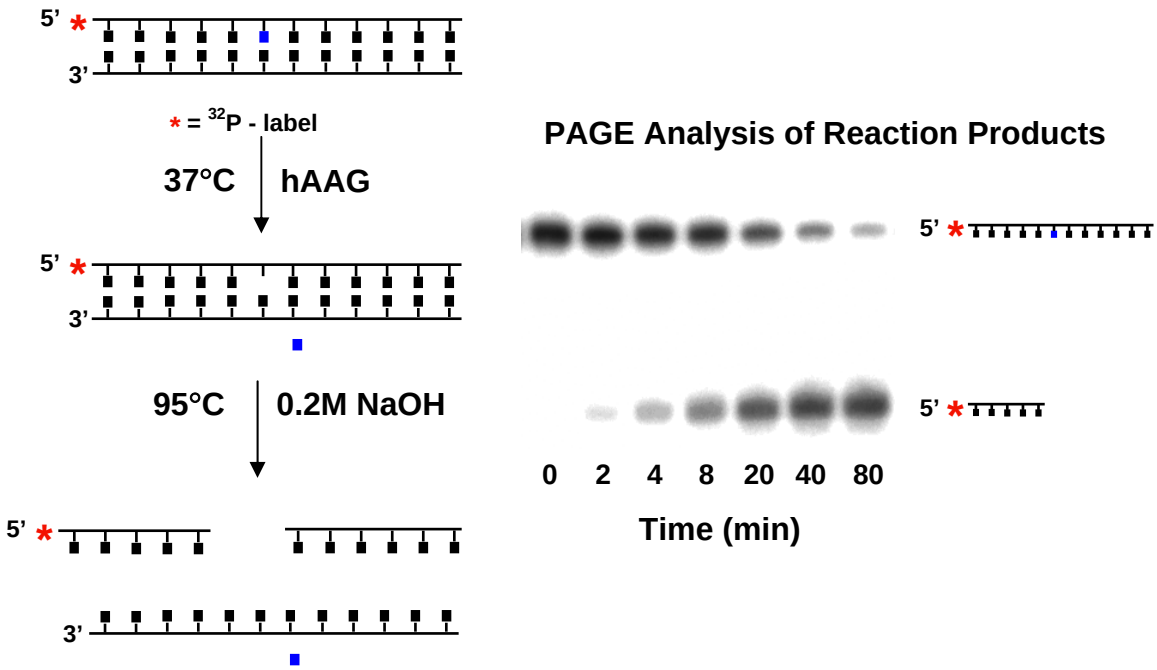

Figure 3-2. A schematic of the excision assay and a sample gel for resolution of products from substrates. The glycosylase action, followed by base and heat exposure, causes complete β-elimination to yield a 13-mer product, which is resolved on the gel from the 25-mer substrate. The 0 min time point is the no AAG control which also serves as the background control for spontaneous generation of basic sites during the assay.

Multiple Turnover Assays for Glycosylase Activity

Under multiple turnover conditions, concentrations of DNA (50nM) was in excess of AAG (1-20nM) were used. Other assay conditions and procedures were the same as for the single turnover assays described above. To ensure total denaturation of the DNA after heating, twice the volume of Formamide/EDTA was used..

Electrophoretic Mobility Shift Assay (EMSA) for AAG binding activity

Concentrations of labeled duplex DNA used to observe the binding properties of AAG were the same as used in the excision assays. Because, AAG was capable of

excising the damaged base, a catalytically inactive mutant of AAG, E125Q, in which the catalytic residue Glu-125 was mutated to a Gln was used. This mutant has identical binding properties to the wild type AAG, but cannot excise the glycosidic bond. The EMSA consists of resolving bound versus free species on a non- denaturing PAGE, to give a higher molecular weight, slower migrating bound species and free, faster migrating species. Ideally, 50nM DNA was incubated on ice with 0 to 1600nM E125Q for 10 minutes and loaded on to a 6% non-denaturing PAGE, which was then run at 8V/cm for 180 minutes at 4°C, to prevent overheating of the fragile gel. When 5nM DNA was used, 0 to 160 nM E125Q was used. The dried gels were analyzed by phosphorimaging and ImageQuant software as in the excision assays to obtain free over bound DNA. DNA bound was plotted over concentration of E125Q and fit to a quadratic equation (Equation 3- 2) to get apparent binding constants (K_d)

$$[ED_{total}] = \frac{E_0 + D_0 + K_d - \sqrt{(E_0 + D_0 + K_d)^2 + 4E_0D_0}}{2} \qquad \text{(Eqn 3-2)}$$

Melting Temperature (Tm) Measurements For Duplex DNA

Melting temperatures of duplex DNA substrates were calculated using the Thermal program for DNA melting in the CARY-3 Bio-UV-visible spectrophotometer (Varian Australia Pty Ltd., Australia). A temperature controller (Peltier) was used to create a controlled rise in temperature. DNA substrates containing the damaged base were annealed to equal concentrations of the complementary strand containing T, F or C opposite the damaged base in 50mM HEPES pH 8.0, 100mM KCl and 0.5mM EDTA, to a final duplex concentration of 4μM. Annealed DNA was diluted 6 times into masked cuvettes with caps to prevent evaporation during melting. The dilution gave a final concentration of 0.67μM, which was determined to be the minimum concentration

required to give an initial absorbance of 0.2, so as to be within the range of the Beer-Lambert law of absorbance. The temperature was increased from 35°C to 65°C at a rate of 0.5°C per minute. T_m values were calculated by taking the first derivative of the melting curve. T_m values correspond to the maximum value of the first derivative. Control experiments were done using temperature increase rates of 0.25, 0.5 and 1°C per minute. Rates of 0.25 and 0.5°C per minute gave consistent results.

Fluorescence Assay For Ethenoadenine-AAG Binding and Excision

εA is intrinsically fluorescent(*94*) and has an excitation λ_{max} at 310nm with an emission λ_{max} at 405nm (Figure 3-3). The fluorescent properties of εA were used to monitor the binding and excision of AAG in real time. The fluorescence emission of εA is considerably quenched when in double stranded DNA, but upon binding and excision of the glycosylic bond by AAG, fluorescence emission is increased in intensity in a time based pattern indicative of AAG activity.

Duplex DNA (100nM) containing εA as the damaged base was incubated with saturating enzyme concentrations. For measuring binding in the absence of excision, 400-1600nM E125Q was used in standard AAG buffer, in which 0.5M HEPES was replaced by 0.5M Bicine(pH 8.0) as HEPES was found to be slightly fluorescent at the UV range. Replacing HEPES with Bicine did not affect AAG activity, as measured in ^{32}P glycosylase assays. Binding reactions were carried at 25°C. To observe excision, AAG was used in the same concentrations as in the binding measurements and the reaction was carried out at 37°C. εA fluorescence was monitored over time in a quartz cuvette. Data was collected using a Photon Technology Inc. QuantaMaster fluorimeter using a 75W xenon- arc lamp. The band pass was set at 4nm with the excitation and emission

monochromators set at 310nm and 410nm, respectively. Although the theoretical λ_{max} for emission was found to be 405nm, reactions were monitored at 410nm to avoid the tryptophan fluorescence interference due to the protein at this wavelength. Each concentration titration was done as a separate reaction. Buffer only and DNA only background signals were recorded for all spectra, before adding the enzyme and starting the reaction.

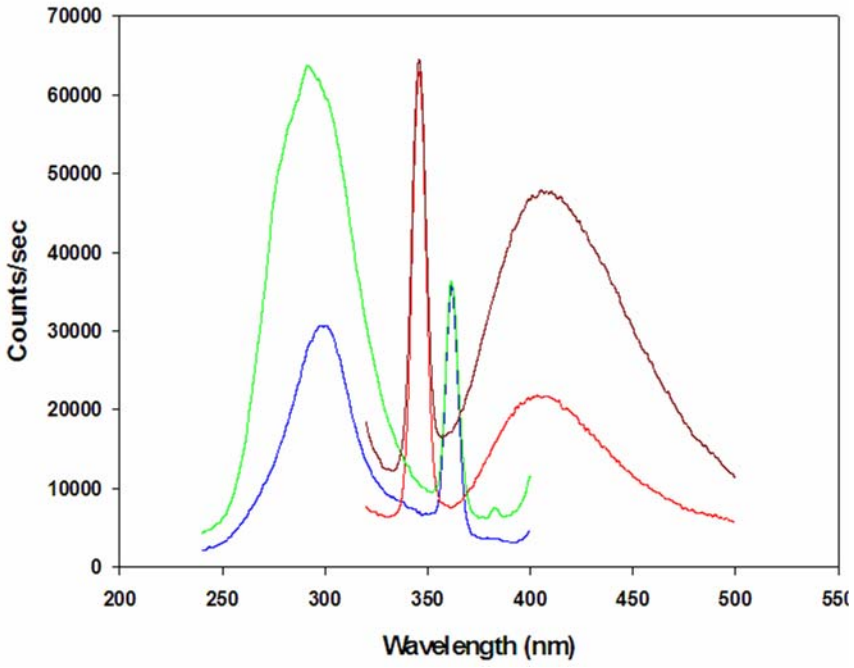

Figure 3-3. Fluorescent properties of 100nMεA when in double stranded DNA and after excision by 400nM AAG at 37°C for 60 minutes. The *blue and green* spectra are excitation spectra, before and after excision by AAG, while the *red and brown* spectra are emission spectra, before and after excision b y AAG. The λ^{max} for excitation and emission are given by the peaks (*see text*).

Stopped-flow Fluorescence to Observe Flipping of εA by AAG

Since binding appeared to be too fast to measure by hand- mixing in the cuvette, stopped-flow measurements were done to observe binding and flipping in real time. DNA containing εA, at a final concentration of 200nM, was added to AAG at a final

concentration of 100, 200 or 400nM in standard AAG buffer at 20°C in a Biologic Stopped-flow fluorimeter. Excitation was set at 310nm and emission was measured in the 2-channel mode using 380nm cut on filters. Traces were taken for each reaction with 4 traces per channel, giving a total of 8 traces per mixing. The same number of traces was taken for the DNA only and AAG only controls for subtracting the backgrounds. Maximum number of traces was taken to increase the signal to noise ratio as much as possible. These traces were then averaged to obtain the final signal, which was plotted against time to obtain a 5000millisecond time based binding curve. The data was not fitted, but the change in fluorescence intensity was taken as a measure of binding and flipping of εA.

CHAPTER 4
EFFECTS OF HYDROGEN BONDING WITHIN A DAMAGED BASE PAIR ON THE ACTIVITY OF WILD-TYPE AND DNA-INTERCALATING MUTANTS OF HUMAN ALKYLADENINE DNA GLYCOSYLASE

Structural studies of AAG (*95, 96*) and other DNA glycosylases have revealed that a nucleotide "flipping" mechanism is used for damaged base recognition and excision in which the damaged base is flipped out of the DNA helix and bound in an enzyme active site. In these nucleotide-flipped DNA glycosylase•DNA complexes, an enzyme amino acid side chain is inserted into the base stack at the site vacated by the flipped base and may assist in nucleotide flipping by pushing the damaged base from the helix. It is believed that DNA glycosylases actively flip damaged bases out of the helix rather than passively capturing bases that have transiently adopted extrahelical conformations. This active nucleotide flipping mechanism is supported by detailed kinetic studies of *E. coli* uracil DNA glycosylase which show a two-step binding mechanism where UDG initially binds DNA to form a non-flipped protein•DNA complex prior to flipping uracil from the helix (*97*).

Many questions remain about how nucleotide flipping enables DNA glycosylases to discriminate between damaged and undamaged bases. For DNA glycosylases that have a narrow substrate specificity, a mechanism in which a "tight fit" of the damaged base in the enzyme active site allows the DNA glycosylase to discriminate between damaged and undamaged bases seems probable. For example, UDG excises only uracil from DNA and mutation of enzyme residues that form specific interactions with U alters the specificity of the enzyme so that it can excise C and T (*96, 95*). On the other hand,

for DNA glycosylases that excise a structurally diverse group of damaged bases such as AAG, a mechanism for damaged base recognition and excision that depends solely on specific interactions between enzyme binding pocket residues and a damaged base seems unlikely. Damaged bases excised, by AAG including 3-methyladenine, 1,N^6-ethenoadenine (εA), hypoxanthine (Hx), and 7-methylguanine, have no obvious structural features in common that would allow the enzyme to distinguish between damaged and undamaged bases. In addition, the efficiency of excision by AAG is dependent on the base pairing partner for some damaged bases (*76*) even though the enzyme makes no specific contacts with the base pairing partner in the crystal structures (*77, 78*). This base pair specificity of AAG further suggests that substrate specificity is governed by a mechanism that involves more than the fit of the damaged base in the enzyme binding pocket.

To further define the mechanisms of damaged base recognition and excision by AAG, the question of how nucleotide flipping contributes to the efficiency of base excision by AAG was addressed using two general approaches. First, site-directed mutations that were predicted to reduce the efficiency of nucleotide flipping were made to the DNA intercalating Tyr-162 residue of AAG. Second, hydrogen bonding interactions within the damaged base pair were removed by substitution of a non-hydrogen bonding partner, difluorotoluene (F), for thymine to increase the efficiency of nucleotide flipping by reducing the stability of the damaged base within the helix. Difluorotoluene is isoteric to thymine but lacks the hydrogen bonding potential due to the substitution of the hydrogen bonding groups of thymine with electronegative fluorine (Figure 4-1). Kool and co- workers who designed F as a thymine analog found that it was

a substrate of replicative polymerases and can be inserted into a growing strand just like thymine, making it a valuable tool for use in replication and repair studies (*105, 106*). Since AAG substrates are damaged adenine bases encountered opposite T, F is a good reagent to use as a non- hydrogen bonding partner as it was a thymine analog. Experiments were designed to investigate the effect of the Tyr-162 mutation on AAG activity and the effects of the "DNA mutation" in which T was replaced with F, on the activities of both wild type and mutant AAG.

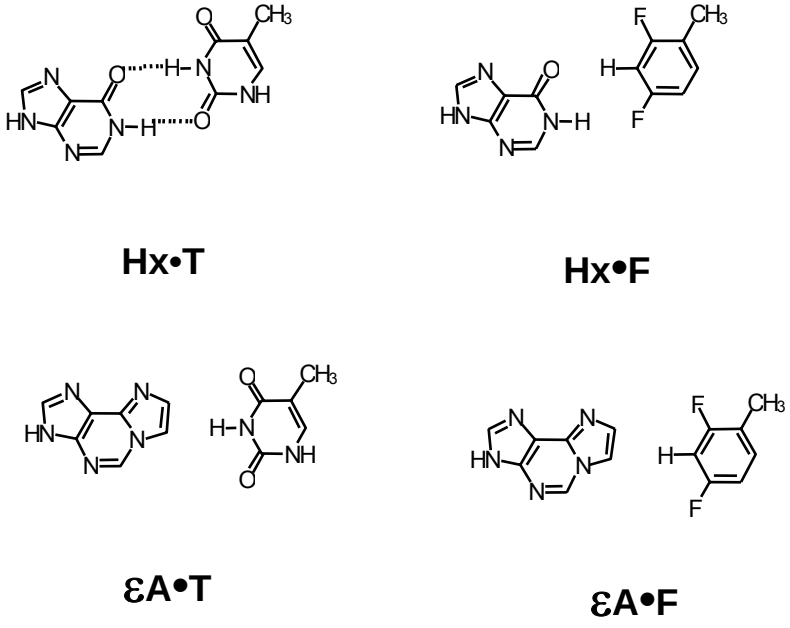

Figure4-1. Chemical structures of hypoxanthine and 1, N^6-ethenoadenine paired with thymine and difluorotoluene. F cannot form hydrogen bonds with Hx. Neither T nor F cannot hydrogen bond with εA.

DNA Substrates and Sequences

The two AAG substrates used in these experiments were Hx and εA. DNA duplexes were 25 nucleotides long, with the damaged bases in position 13, base paired with either T or F, with the rest of the sequence remaining perfectly complementary. The

DNA substrates were always duplexes, since AAG was found to be incapable of binding or excision on single stranded DNA. The substrate DNAs were named based on the central damaged base and its base pairing partner, as Hx•T, Hx•F, εA•T or εA•F. The sequences of the DNA substrates are tabulated in Table 4-1.

Table 4-1. Sequences of DNA substrates and positions of damaged base pairs

Upper strand	5'-GCG TCA AAA TGT NGG TAT TTC CAT G-3' (N= Hx or εA)
Lower strand	5'-CAT GGA AAT ACC XAC ATT TTG ACG C-5' (X= T or F)

Mutations to Tyr-162 and Projected Consequences

To assess the contribution of the DNA-intercalating Tyr-162 residue to the base excision activity of AAG, Tyr-162 was converted to Ser and Phe by site-directed mutagenesis to generate two mutant proteins, Y162S and Y162F, respectively. A catalytically inactive double mutant, Y162F/E125Q, was made for DNA binding experiments. Converting the Tyr-162 residue to Ser removes the aromatic ring generating a smaller amino acid side chain that should not be able to penetrate the DNA helix as deeply when intercalated. Mutation of Tyr-162 to Phe removes the hydroxyl group but leaves the aromatic ring intact to intercalate into the DNA base stack. These differences in insertion are illustrated in Figure 4-2 as cartoons in which Tyr-162 is replaced by Ser or Phe, as seen in the crystal structure. Figure 4-2 is not an actual structure but is meant to indicate possible differences in intercalation between Tyr-162 and the two amino-acids by simple replacement and not to indicate any other properties they may affect such as flipping. To see whether these intercalating differences will be translated into flipping inefficiencies is the goal of this mutational analysis.

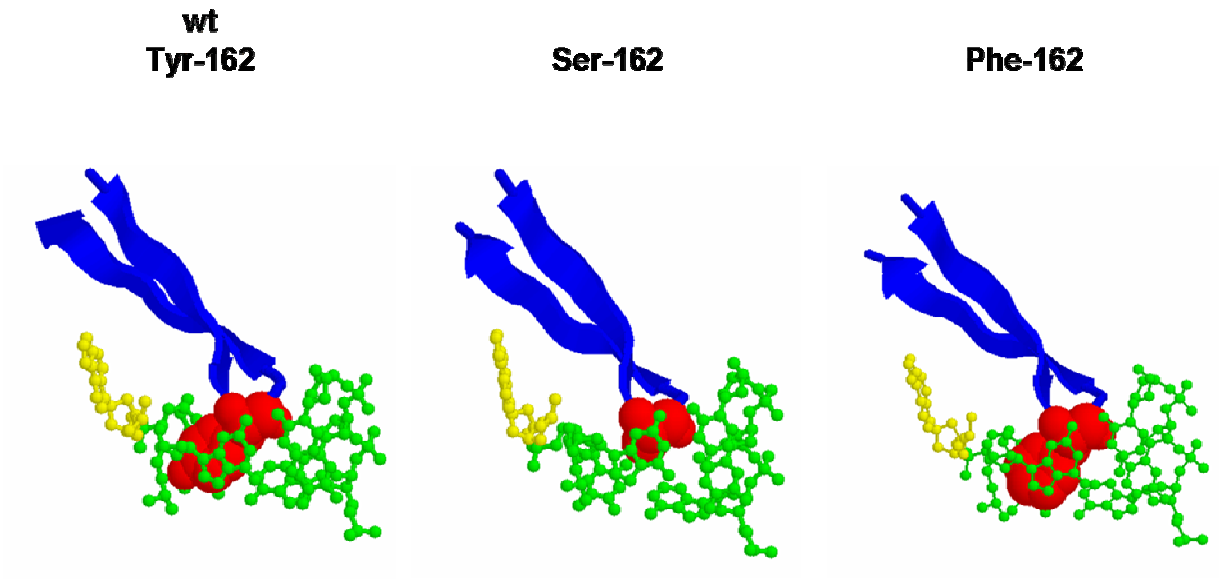

Figure4-2. Projected differences in intercalation ability of Ser-162 and Phe-162 when compared to the wild type residue, Tyr-162, based on the crystal structure of AAG bound to εA. Shown is a close- up view of the β-hairpin *(blue ribbons)* and the intercalating residue *(red space- fill)* positioned in the helix *(green ball and sticks)* to fill the space vacated by the flipped- out εA *(yellow ball and sticks)*. Ser and Phe may have different abilities to intercalate than Tyr *(see text)*.

Base Excision and DNA Binding Activities of the Y162S Mutant

Base excision activity for the Y162S mutant was measured in a chemical cleavage/gel assay for DNA substrates using saturating AAG concentrations, in which excision of all the substrate is expected based on previous kinetic studies. The strand containing the damage was end-labeled with ^{32}P, prior to annealing to its complementary strand to create duplexes of otherwise identical sequences that contained Hx•T and εA•T base pairs. In 60minute assays using 1600 nM Y162S and 50 nM DNA substrate, no detectable base excision was observed for either DNA substrate. We estimate that the Y162S mutant is at least 1000-fold less active than the wild type AAG enzyme based on this result and using the conservative assumption that 1 nM product (2% reaction) would have been detected if formed in these assays.

The DNA binding activity of the Y162S mutant was measured in electrophoretic mobility shift assays (EMSA) with the same damaged duplexes as used in excision assays, where the damage-containing DNA strand was 5'-end-labeled with ^{32}P. A damage-specific protein•DNA complex was not observed for the Y162S mutant with DNA substrates containing Hx or εA opposite T (Figure 4-3). At high Y162S concentrations in the EMSA, a general smearing of the DNA band was observed in a pattern similar to that for AAG with undamaged DNA (not shown). This smearing may represent weaker damage-independent DNA binding.

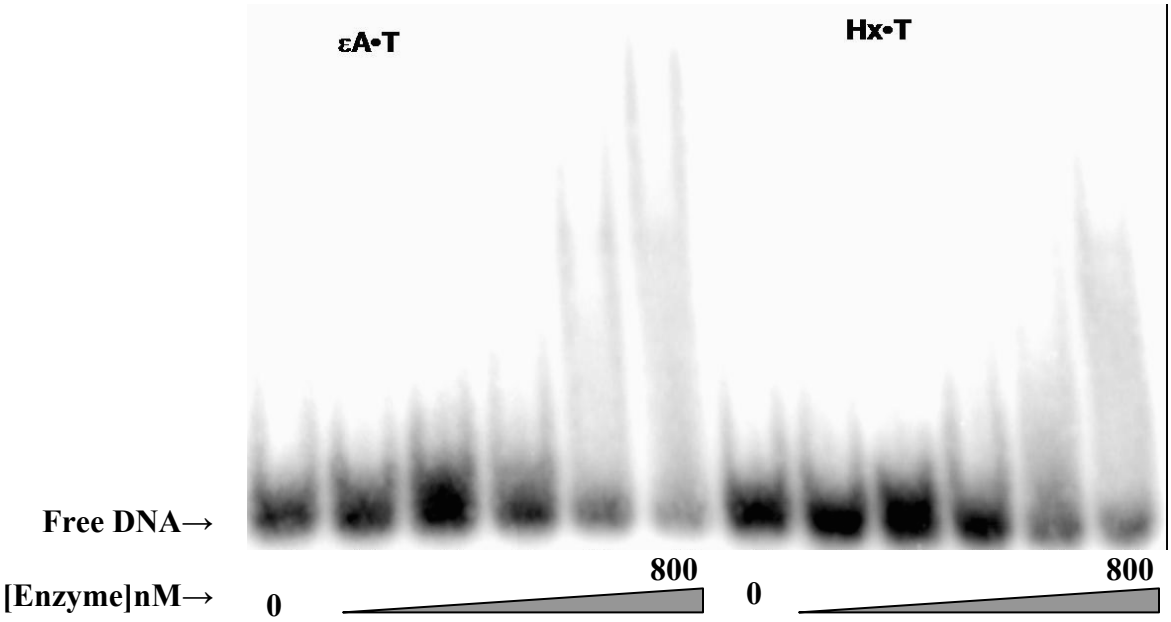

Figure4-3. Electrophoretic mobility shift assays to measure the affinity of the Y162S mutant for DNA containing an εA•T or a Hx•T base pair. 50nM labeled, duplex DNA was incubated with 0- 800nM Y162S mutant. A band corresponding to a damage-specific protein•DNA complex is not observed for the Y162S mutant in assays with either an εA•T pair (left panel) or an Hx•T pair (right panel). Smearing of the free DNA band is observed at 400 and 800 nM Y162S and may represent weaker damage-independent DNA binding.

Activity of the Y162F Mutant

Base Excision by the Y162F Mutant

Single turnover kinetics of excision of Hx when paired with T was measured in a chemical cleavage/gel assay for both AAG and the Y162F mutant. Enzymes, at concentrations of 400, 800, and 1600 nM, in two separate experiments at each concentration, were incubated with 50 nM ^{32}P-labeled 25-nt duplex DNA substrates at 37° C. Aliquots of each reaction mixture were withdrawn at several time points, quenched, and analyzed by PAGE to quantitate the concentration of products formed. For each enzyme, reaction time courses were essentially the same at all three concentrations demonstrating that single-turnover conditions were met. Individual time courses were fit empirically to an exponential rise to calculate observed rates *(k_{obs})*. Average values and standard deviations for k_{obs} calculated from all six experiments (two at each enzyme concentration) are shown in Table 4-2. Excision of Hx was 4-fold more rapid in assays with AAG than the Y162F mutant. The reaction course for 400nM enzyme is shown in Figure 4-4.

Because AAG catalyzes excision of a structurally diverse group of damaged purine bases, the possibility that the Y162F mutation may have differential effects on excision of different damaged bases was tested. Kinetics of excision of the structurally dissimilar *1,N^6*-ethenoadenine placed opposite T were measured in single-turnover assays containing 400 and 800 nM enzyme. Reaction courses are shown in Figure 4-5. For each enzyme, observed rates were the same at both enzyme concentrations. The Y162F mutation had a smaller effect on the single turnover excision rate for εA where AAG was 1.7-fold faster than the Y162F mutant (Table 4-2).

To determine whether rates of excision of Hx would increase by making the base easier to displace from the helix, the T opposite Hx was replaced by difluorotoluene (F), which does not form hydrogen bonds with Hx (Figure 4-1). Single-turnover kinetics of excision of Hx opposite F was measured in the chemical cleavage/gel assay with 50 nM DNA and 400, 800, and 1600 nM enzyme (Table 4-2). Excision rates were not dependent on enzyme concentration for either AAG or Y162F. Excision activities for both AAG and the Y162F mutant increased on the Hx•F DNA substrate relative to the Hx•T duplex (data for 400 nM enzyme are shown in Figure 4-4). The magnitude of the increase was greater for the Y162F mutant (3.5-fold) than for AAG (2-fold).

It is possible that the increased excision activity could be due to some effect of replacing T with F other than removing hydrogen bonding interactions. To rule out this possibility, excision was also measured for DNA substrates containing εA•T and εA•F base pairs. εA does not form Watson-Crick-type hydrogen bonding interactions with either T or F. Single-turnover kinetics of excision of εA opposite F were measured in chemical cleavage/gel assays using 50 nM DNA and 400 and 800 nM enzyme in separate experiments (Table 4-2). There was not a significant effect on excision rates of εA, as a 1.2-fold decrease in the excision rate for AAG and a 1.1-fold increase for the Y162F mutant were observed (Figure 4-5).

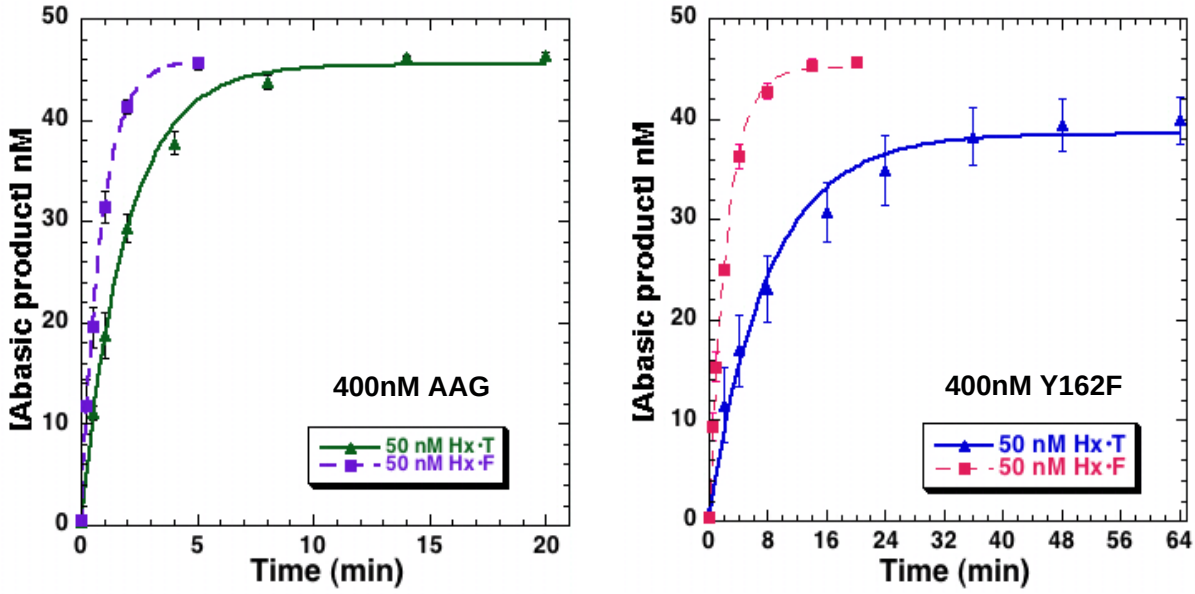

Figure 4-4. Plots of time courses for Hx excision by wt AAGΔ79 and Y162F**.** Plots of the concentrations of abasic DNA product formed as a function of time in assays containing 400 nM enzyme and 50 nM DNA are shown. Because there is a relatively large difference in rates of Hx excision, time courses for excision of Hx paired with T *(triangles)* and F *(squares)* are plotted in separate graphs on different time scales for AAG*(left)* and theY162F mutant *(right)*. Data plotted are average values from two independent experiments with standard deviations. Solid lines are the result of a single exponential fit to the data.

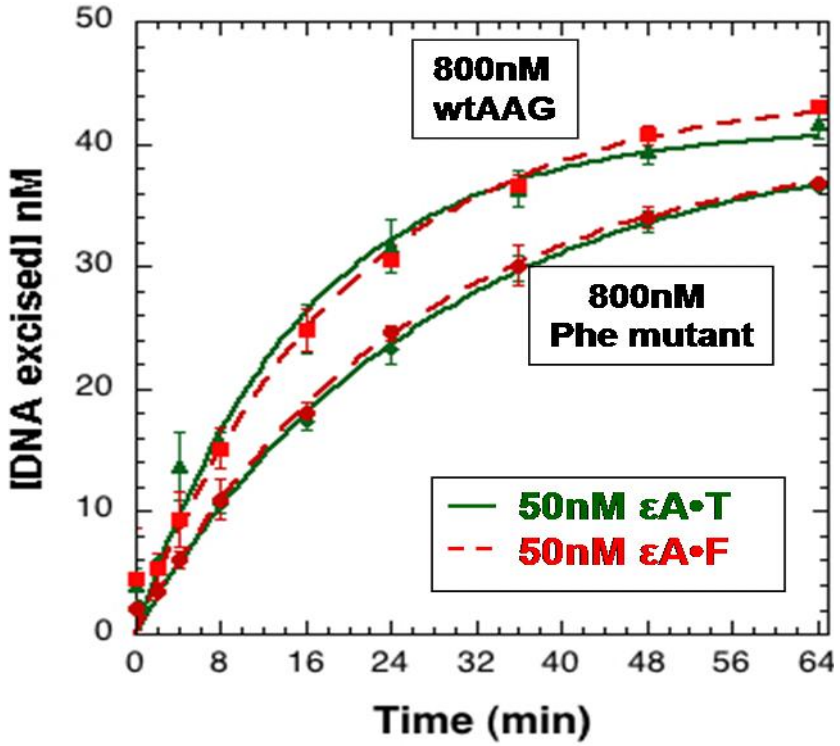

Figure 4-5.Plots of time courses for εA excision by wt AAGΔ79 and Y162F The base pairing partner, T or F, did not affect εA excision rates for either enzyme as demonstrated by overlapping time courses for excision of εA by AAG on εA•T (*green squares*) and εA•F (*blue squares*) DNA and Y162F on εA•T (*red diamonds*) and εA•F (*orange diamonds*) DNA. Data plotted are average values from two independent experiments with standard deviations. Solid lines are the result of a single exponential fit to the data.

Results obtained from removing hydrogen bonding interactions to Hx indicated enhanced rates of excision of Hx by both the wt and the Y162F mutant. Normal purines are not usually excised by AAG. Experiments were done to see if any enhanced excision of normal purines opposite F was seen. In control experiments in which DNA substrates containing no damaged base, but adenine or guanine opposite F (A/G•F), it was seen that removing hydrogen bonding interactions did not make these normal DNA bases substrates for AAG. Similar AAG assays were performed to confirm this fact (Figure 4-6). Some groups have observed excision of normal bases by AAG at low levels, but we have not been able to demonstrate this activity in the presence or the absence of hydrogen

bonding interactions. The observations of these groups may be due to different exposure times of the gels or very long assay times. The non- excision of normal purines opposite F goes on to further prove the fact that AAG uses flipping as an essential step in recognition but also co- ordinates flipping with the active site parameters that decide what a substrate is. So though A or G could be made easier to flip by putting opposite F, excision is not observed due to active site constraints.

Table 4-2. Observed excision rates and relative acitivities of AAG and Y162F mutant

Enzyme	Base pair	k_{obs} min^{-1a}	k_{rel} (AAG/Y162F)[b]
AAG	Hx•T	0.62±0.19	4.1
	Hx•F	1.3±0.1	2.5
	εA•T	0.062±0.003	1.7
	εA•F	0.052±0.005	1.2
Y162F	Hx•T	0.15±0.03	
	Hx•F	0.53±0.13	
	εA•T	0.037±0.001	
	εA•F	0.042±0.002	

a,Values for k_{obs} were calculated from single exponential fits to individual experiments. For Hx base pairs, two independent experiments were done at enzyme concentrations of 400, 800, and 1600 nM and average k_{obs} values and standard deviations are reported for all six experiments. For εA pairs, two independent experiments were done at 400 and 800 nM enzyme and average k_{obs} values and standard deviations are reported for the four experiments. b, Relative values, k_{rel}, were calculated from the ratio of the k_{obs} for wt to Y162F for each base pair.

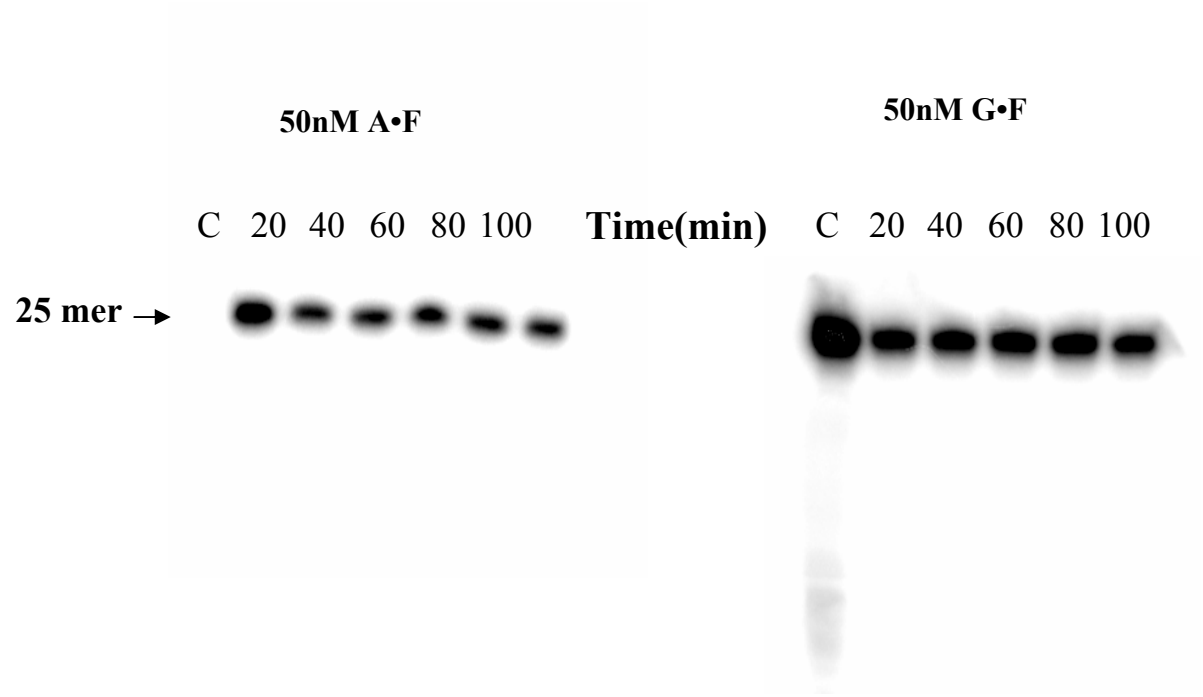

Figure 4-6. Control glycosylase assay to show that base pairing with F does not make A or G excisable by AAG. 100 minute time course gels are shown, with 50nM A•F and G•F DNA duplexes incubated with 800nM AAG at 37°C and quenched at the indicated time points. The C lane is the enzyme- less control reaction. Only 25-mer substrates are seen, no 12-mer product, indicative of excision by AAG is seen on the gel.

DNA Binding Ability of Y162F Mutant

Mutation of the Tyr-162 residue to Phe reduces the DNA binding activity measured in electrophoretic mobility shift assays (EMSA). For and EMSA, 50 nM ^{32}P-labeled duplex DNA substrates, identical to those used in excision assays, were incubated with increasing concentrations of enzyme (10 – 800 nM) prior to nondenaturing PAGE analysis. Since base excision would convert DNA substrates to products during the time course of EMSAs, catalytically inactive mutants (E125Q) of AAG and Y162F were used in these assays. The affinity of the Y162F/E125Q mutant for DNA containing a Hx•T pair is reduced relative to E125Q (Figure 4-7, upper panels). A concentration of 50 nM Y162F/E125Q is needed to form a similar fraction of enzyme•DNA complex as seen with

20 nM E125Q. At concentrations of 400 nM enzyme, about 70% of the DNA is bound by E125Q whereas about 25% is bound by Y162F based on the intensity of the bands. As reported previously (*100*), AAG binds to DNA containing an εA•T pair with greater affinity than a Hx•T pair (Figure 4-7 and Figure 4-8, upper left panels). This is also true for the Y162F/E125Q mutant (Figure 4-7 and Figure 4-8, upper right panels). The Y162F/E125Q mutant binds DNA containing an εA•T pair more weakly than E125Q as it takes 20 nM Y162F/E125Q to form about the same concentration of enzyme•DNA complex as 10 nM E125Q.

To determine what effect substitution of T with F would have on the DNA binding activity of AAG, assays were done for DNA substrates containing Hx•F and εA•F pairs. Binding assays contained 50 nM ^{32}P-labeled duplex DNA and increasing concentrations of AAG E125Q or Y162F/E125Q (10 – 800 nM). For both enzymes, binding was similar for DNA duplexes containing Hx•T and Hx•F pairs (Figure 4-7, lower panels), and binding was slightly enhanced on duplexes containing εA•F in comparison with εA•T (Figures 4-8, lower panels).

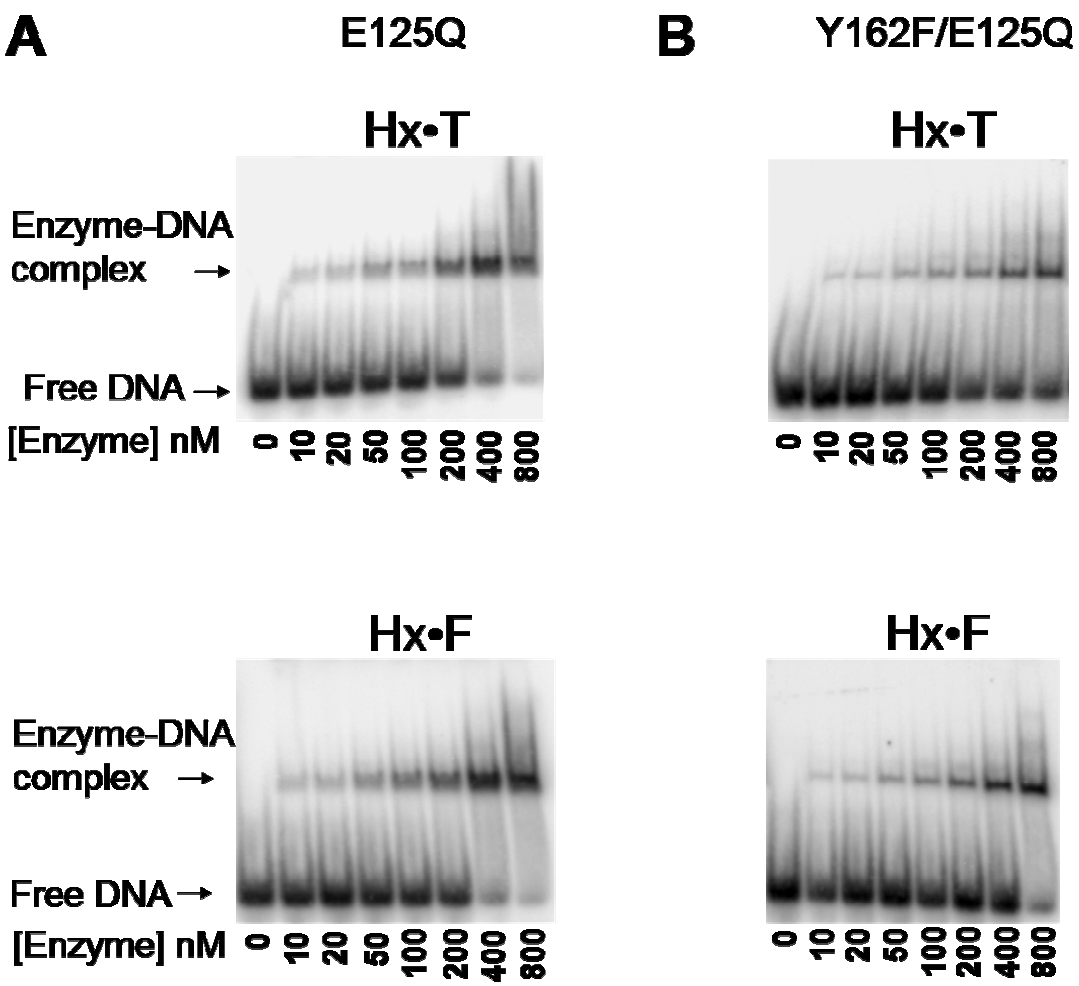

Figure 4-7. Binding of wt AAGΔ79 and the Y162F mutant to DNA containing Hx•T and Hx•F base pairs. Assays were done with duplexes containing either a Hx•T (upper panels) or Hx•F (lower panels) pair. Increasing concentrations (10 to 800 nM) of E125Q (left panels) and the E125Q/Y162F mutant (right panels) were incubated with 50 nM DNA. Both enzymes were catalytically inactive mutants of Δ79AAG and the Y162F mutant, respectively. They were used so that binding efficiency can be observed in the absence of excision. Binding constants were not obtained due to the high degree of smearing which hampered exact quantitation.

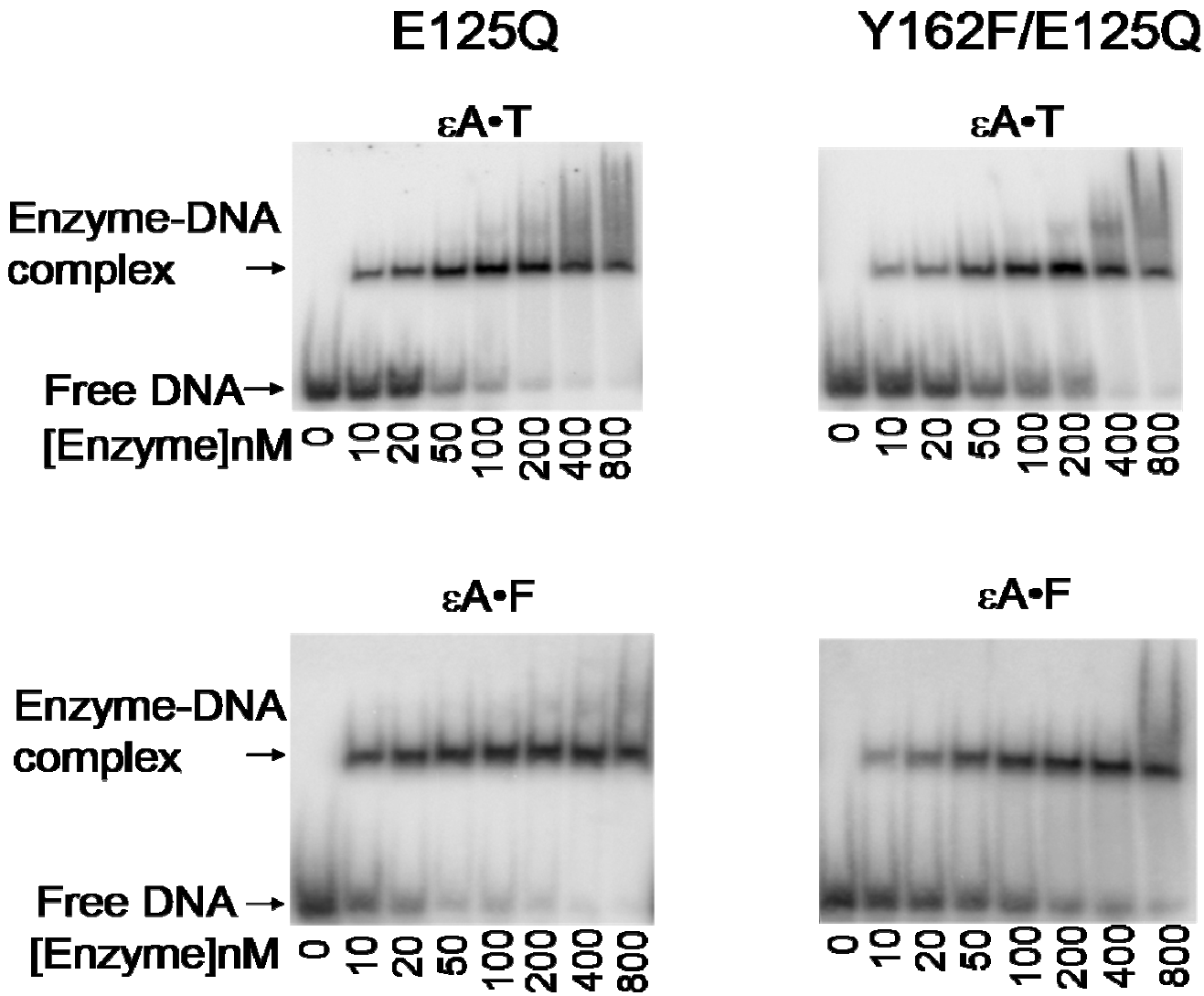

Figure 4-8. Binding of AAG and the Y162F mutant to DNA containing εA•T and εA•F base pairs. EMSA assays were done as in Figure 4.6 with 25-nt duplexes containing either an εA•T (upper panels) or εA•F (lower panels) pair at position 13. Increasing concentrations (10 to 800 nM) of wt AAG (left panels) and the Y162F mutant (right panels) were incubated with 50 nM DNA. Catalytically inactive mutants are used as in Figure 4.7.

Implications of Flipping in the Catalytic Efficiency of AAG

The ability of DNA glycosylases to identify and excise damaged DNA bases is key to the overall success of base excision repair. Structural studies of AAG reveal that

flipping of the damaged nucleotide is the first step in substrate recognition, and this is facilitated by intercalating Tyr-162 into the space vacated by the flipped out nucleotide.

In this study, the DNA-intercalating Tyr-162 residue of AAG was converted to serine (Y162S) and phenylalanine (Y162F) by site-directed mutagenesis. A decrease in the base excision activities of both mutants was observed as expected if the Tyr-162 residue contributed to nucleotide flipping by helping to push the damaged base from the helix. Base excision and damage- specific binding activities of the Y162S mutant were reduced to undetectable levels for DNA substrates containing Hx•T and εA•T pairs, indicating that this mutant must be at least 1000-fold less active than AAG. The fact that DNA binding activity of the Y162S mutant was not detectable by EMSA suggests that the enzyme•DNA complex seen for AAG is a nucleotide flipped complex.

A similar mutation in UDG converting the DNA-intercalating Leu residue to Ala resulted in an 8 to 80-fold decrease in excision activity and mutation of Leu to Gly reduced UDG's excision activity by a factor of 100 – 600 (*91, 92*). The comparatively large effect of the Y162S mutation on AAG's activity may reflect a greater contribution of the DNA-intercalating residue to the activity of AAG than UDG.

Mutation of Tyr-162 to Phe leaves the aromatic ring to intercalate in DNA but removes the hydroxyl group from the aromatic ring. This mutation decreases the size of the DNA-intercalating residue much less than the Ser mutation but still affects the excision activity of the enzyme. Excision of Hx when paired with T by the Y162F mutant is 4 times slower than excision by the AAG and excision of εA paired with T is 1.7 times slower. Interestingly, the activity of the Y162F mutant is "rescued" on a DNA substrate where Hx is paired with F. The excision rate for the Y162F mutant increases to

the rate measured for AAG excision of Hx paired with T. It is possible that making Hx easier to flip in the context of an Hx•F pair counterbalances a deficiency in the flipping ability of the Y162F mutant. An alternative explanation for the effect of the Y162F mutation on the excision activity of AAG is that the slightly smaller Phe residue is not able to "push" the displaced base as far into the enzyme binding pocket to align it properly for catalysis. If this were true then no difference in excision rates for Hx when paired with T and F would have been seen because the Phe mutant would have "pushed" Hx the same distance in both cases.

The rationale for replacing T with F in Hx base pairs was that F is isosteric with T having the same overall shape but will not form hydrogen bonds with Hx. The expectation was that the lack of hydrogen bonding will increase the ease of flipping Hx by decreasing the stability of the base pair. To rule out the possibility that F could have some other unanticipated effect on excision activity, excision of εA was measured when paired with T and F where neither pair forms hydrogen bonding interactions. Substitution of T with F had no significant effect on excision rates of εA for either AAG or the Y162F mutant whereas it increased the excision rate of Hx by a factor of 2 for AAG and about 3 to 4 for the Y162F mutant. Thus, the increase in Hx excision rates is likely to be due to changes in hydrogen bonding interactions in the Hx pair. These results are consistent with a model where the ease of flipping a damaged base contributes to the base pair specificity of AAG.

The kinetic mechanism for base excision by AAG is likely to contain a nucleotide flipping step in addition to the chemistry step where base excision occurs. Changing the ease of nucleotide flipping either by mutations to the enzyme or by changes to the

stability of a damaged base within the helix affects single turnover excision rates by altering the population of substrates stably flipped. The observation that substitution of T with F increases single turnover excision rates of Hx for both AAG and the Y162F mutant suggests that nucleotide flipping is important for Hx excision. An altered flipping equilibrium for Hx excision would also explain the base pair specificity observed previously (*75, 76*). Two explanations are possible to explain why excision of εA is not affected to a great degree by its base pairing partner. Either the nucleotide flipping step may not alter the flipping equilibrium as drastically as for Hx, or the flipping equilibrium is not affected by the base pairing partner since εA lacks hydrogen bonding interactions with its partner.

A Two-step Selection Model for AAG Activity

Based on these results that were published (*75*) and previous work, we have developed a working model that explains the damaged base and base pair specificity of AAG. We propose that the specificity of base excision by AAG is governed by two important selection steps, nucleotide flipping and chemistry of bond cleavage which is affected by many factors such as proper fit of the base, alignment of the bond, suitability of the leaving group etc. in the enzyme active site. The enzyme may use the ease of flipping a damaged base as the initial criterion for discriminating between damaged and undamaged bases and then use fit of the damaged base in the active site as a final check. The first nucleotide flipping selection step would be affected by changes in local DNA sequence or structure that affect the stability of a damaged base within the helix. Once a damaged base is flipped, it still must be aligned properly in the active site for hydrolysis of the glycosidic bond to occur. This second criterion, proper fit in the active site, would explain why Hx but not G is excised from a wobble-type base pair with T (*76*). The 2-

amino group may prevent G from fitting in the active site properly (*78*). The other factors in the active site may include suitability of the leaving group for chemistry, alignment of the glycosidic bond relative to the activated water and so on. An implication of this two step selection is that the overall efficiency of base excision repair may be a function of local DNA sequence and structure which affect the stability of damaged bases in the helix. A dependence on the efficiency of base excision on DNA sequence and structure could contribute to the formation of mutational "hot spots" and "cold spots". Both AAG DNA-intercalating mutants and the difluorotoluene base pairing partner will be useful tools for testing this model further.

CHAPTER 5
ACTIVITY OF HUMAN ALKYLADENINE DNA GLYCOSYLASE IS SENSITIVE TO THE LOCAL SEQUENCE CONTEXT OF THE DAMAGED BASE

The contribution of nucleotide flipping to the excision efficiency of DNA glycosylases is not yet fully understood. Especially with respect to a glycosylase like AAG, which has a diverse substrate range, the contribution of flipping could be critical to how the enzyme discriminates between substrates and non- substrates and also how it can accommodate a diverse group of substrates. The contribution of flipping to substrate specificity could be unique for AAG since many other glycosylases such as UDG act on a single substrate, in this instance, uracil only. But AAG acts on substrates ranging from 3-methyladenine and hypoxanthine (Hx) to *1, N^6*- ethenoadenine (εA), which are not structurally related enough to enable the enzyme to use a common mechanism of recognition. Though the crystal structure of AAG does not indicate any specific contacts between the enzyme and the base pairing partner to the flipped out damaged base, it has been shown by us that the excision efficiency of some damaged bases is dependent on the identity of the base pair and not the base alone (*75, 76*). The difference in excision can be directly related to the ease of flipping the damaged base in a given base pair because, removing hydrogen bonds which can make flipping easier, also increased excision efficiency, in the case of Hx (*75*). This indicated that stability in DNA could affect repair of Hx by AAG. The minimum two- step mechanism for recognition and binding to the substrate discussed in the end of chapter 4 served as an additional guide to come up with novel methods to understand the contribution of flipping to Hx excision. The first step

was to identify additional factors around Hx that could contribute to its flippability by AAG. Since base stacking in DNA is a major stabilizing source, changes to the flanking neighbors to Hx were made, using either relatively weak or strong base stacking partners. These may either further stabilize or destabilize the Hx base pair in DNA and thus affect its flipping by AAG. To the base stacking changes were added additional modifications in the base pairing partner within these sequence contexts. This allowed for understanding more about how effects on base flipping would affect excision by AAG.

DNA Substrates Indicating Base Stacking and Hydrogen Bonding Partners to Hx

DNA substrates were designed to include base stacking changes around the central damaged base which was base 13 in the 25-mer long substrate. Hx was either flanked by T –A base pairs (T*Hx*A) or G-C base pairs (G*Hx*C), the rationale being that, T-A and G-C nearest neighbors represent the weakest and strongest base stacking partners respectively (*100*). The G-C flanking base pairs may affect Hx accessibility in DNA due to their intrinsically stronger base stacking. It has been shown previously that hydrogen bonding within the base pair affected excision of Hx by AAG presumably by increasing or decreasing the stability of Hx in DNA (*75*). So, Hx was base paired with T, F or C, within these sequence contexts. As shown in Figure 5-1, Hx has different hydrogen bonding interactions with these bases, forming a wobble base pair with T, no base pairs with F, and a Watson-Crick base pair with C. In contrast, *εA*, which is also a substrate for AAG, forms no hydrogen bonding interactions at all (Figure 5-1) and serves as a good control as seen with the AAG mutants (Chapter 4). The above sequences were incorporated into 25-nucleotides long substrates, with Hx at position 13. The rest of the DNA sequence was the same as the sequence shown in Table 4-1. Substrates used for experiments were 5'-

end labeled with ^{32}P on the damaged strand and then annealed to the respective complement oligonucleotides.

The DNA substrate nomenclature is based on the base stacking partners and the hydrogen bonding partners to Hx or εA throughout this chapter. For example, a duplex substrate containing Hx with a 5'T and a 3'A in which Hx is paired with T will be referred to as THxA•T.

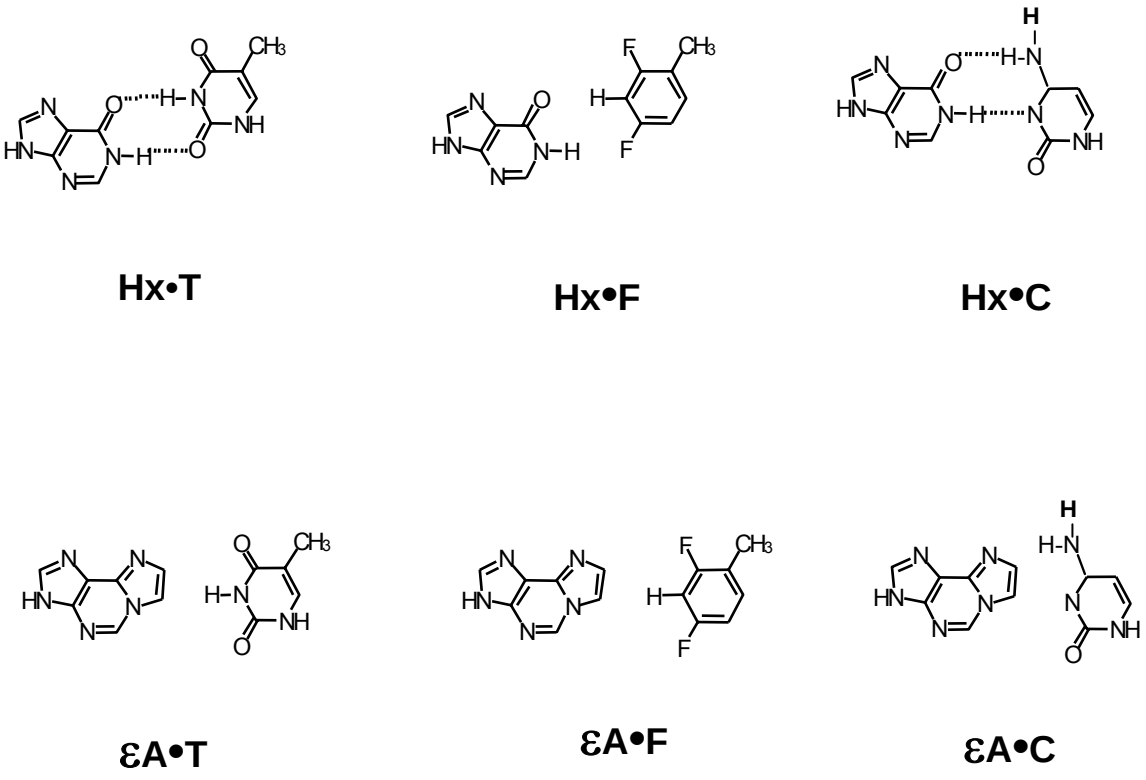

Figure 5-1. Chemical structures of Hx and εA base paired to thymine, diflorotoluene and cytosine. Hx forms wobble base pairs with T, no base pairs with F and Watson-Crick base pairs with C. εA forms no hydrogen bonds with any of the three base pairing partners.

Base Stacking and Hydrogen Bonding Effects on Hx

The flanking base pairs were designed to create strongest versus weakest base stacking interactions with Hx in DNA and hence reflect on the ability of the enzyme to flip εA or Hx. Base excision activity of AAG was measured using a chemical cleavage/ gel assay using labeled, double stranded DNA substrates with T-A or G-C base pairs flanking Hx, base paired to T. Increasing concentrations of enzyme (ranging from 20nM to 640nM) were incubated with 5nM substrate at 37°C. Aliquots were withdrawn at several time points from 0 to 80- min., quenched, and analyzed by denaturing PAGE for product formation. For each enzyme concentration, the reaction course was fit to an exponential rise to obtain observed rates (k_{obs}) which were used to compare excision efficiencies of Hx in the two sequence contexts. Increasing concentrations of enzyme were used until no change in the progress of the time courses were observed, indicating that single turnover conditions were achieved. For excision of Hx•T with G-C stacking partners, almost 4 times more enzyme was required to achieve single turnover conditions compared to Hx•T with T-A stacking partners (Figure 5-2) and the observed rates at these saturating enzyme concentrations showed that excision of Hx•T was 1.6- fold faster with T-A partners than with G-C base stacking partners. Rates are summarized in Table 5.1, at the end of the results section.

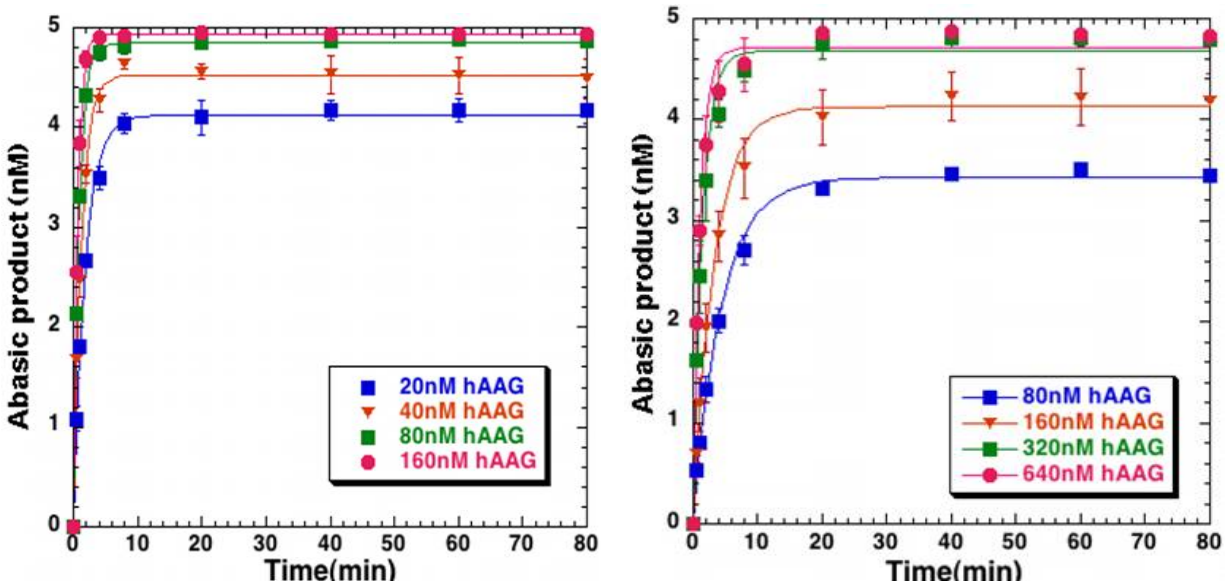

Figure 5-2. Single turnover excision of Hx opposite T with T-A and G-C base stacking partners. With T-A base stacking partners (*left*), saturation was observed with 80 and 160nM AAG, whereas with G-C base stacking partners (*right*), 640nM AAG was required to approach saturated excision of 5nM Hx•T. Saturation required almost 4- times more enzyme with the stronger base stacking partners (*See text*).

Effects of Hydrogen Bonding Partners on Hx Excision in the Strong and Weak Base Stacking Context

It is possible that making Hx less constrained in DNA may relieve the effects of the base stacking partners. This can be tested by replacing T with diflorotoluene (F), which does not form hydrogen bonds with Hx. In previous studies, removing hydrogen bonding to Hx was seen to improve its excision by AAG (*75*). In single turnover excision reactions, measured for 5nM Hx•F with both T-A and G-C base stacking partners with increasing concentrations of enzyme (20-160nM), it was seen that saturation was observed at relatively low enzyme concentrations (Figure 5-3). At these saturating concentrations, when compared to the rates of excision of the same sequences with Hx•T, Hx•F excision was enhanced. The enhancement was 2-fold for Hx•F over Hx•T with T-A stacking partners but the enhancement was dramatic for Hx•F over Hx•T with G-C

stacking partners, making Hx•F with G-C partners a better substrate than Hx•F with T-A partners. The excision time course for Hx•F with G-C partners was so fast that the early time points were not experimentally measurable by hand mixing. It is presumed that the enhancement in excision rates is at least 10-fold over Hx•T, as assumed from lower enzyme concentration excision assays.

In cells during replication, polymerases have a propensity to incorporate C, opposite Hx, with which it can form Watson-Crick hydrogen bonds, much like a G-C base pair (*101-104*). This preference makes Hx mutagenic because with another round of replication, Hx•C potentially becomes an AT→GC transition. Given the observations with the effect of base pairing partners on Hx excision, it is important to observe what effects base pairing with C will have on Hx excision, because even when Watson- Crick base paired with C, Hx is excisable by AAG. In previous experiments, it was shown that Hx excision was slower opposite C than opposite T (*76*). To determine how base stacking partners can affect Hx excision opposite C, single turnover excision reactions were done with 5nM Hx•C with T-A and G-C base stacking partners using 160 and 320nM AAG. Under these conditions, kinetics of excision of Hx was very slow (Figure 5-4). Notably, when base paired to C, Hx excision was unaffected by the base stacking partners, unlike when opposite T or F. Excision of Hx•C in both sequence contexts essentially proceeded at the same rate (Table 5-1).

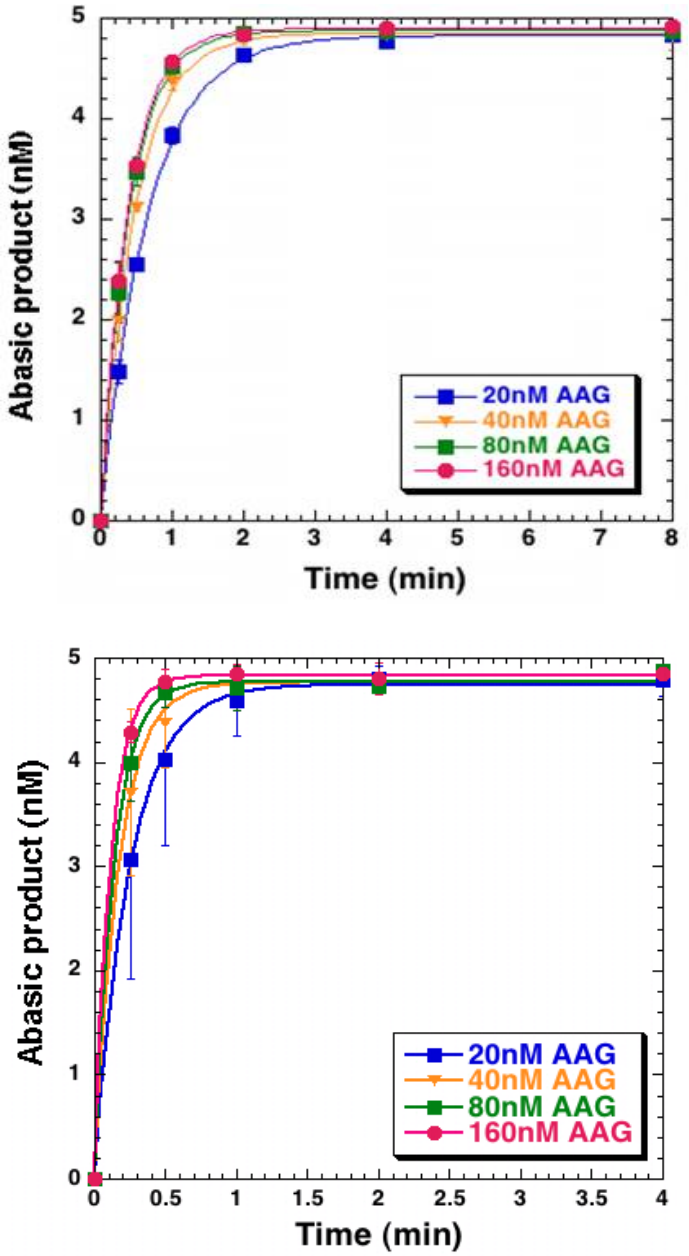

Figure 5-3. Single turnover excision of Hx with T-A and G-C base stacking partners opposite non- hydrogen bonding base pairing partner, F. Excision of Hx•F was much faster than opposite T. Increasing AAG concentrations of 20nM (*blue squares*), 40nM (*yellow triangles*), 80nM (*green squares*) and 160nM (*pink circles*) were used. With TA base stacking partners, 5nM Hx•F was excised to saturation by only 40nM AAG (*top, yellow triangles*). But with 5nm Hx•F with G-C base stacking partners, excision was fastest, with saturation achieved by only 20nm AAG (*bottom, blue squares*). A shorter time scale has been shown in these graphs when compared to Figure 5.2, to emphasize the faster excision achieved for these substrates.

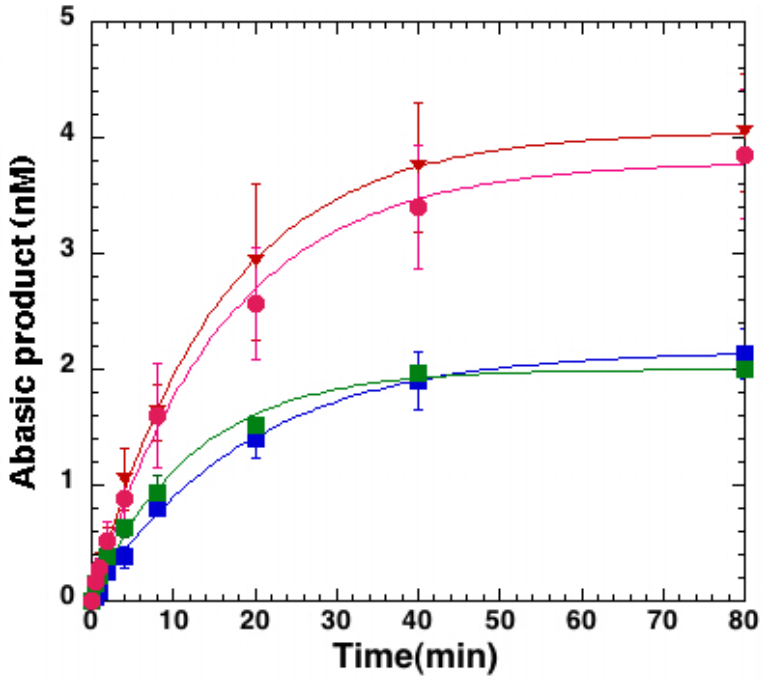

Figure 5-4. Single turnover excision of Hx with T-A and G-C base stacking partners opposite Watson-Crick hydrogen bonding partner, C**.** Excision of 5nM Hx•C with T-A base stacking partners did not saturate with 160nM (*blue squares*) or 320nM (*red triangles*) AAG. The same trend was seen with G-C stacking partners with 160nM (*green squares*) and 320nM (*pink circles*) AAG. Time courses for Hx•C excision in both sequence contexts closely mirror each other, indicating that excision of Hx was not affected by base stacking partners when Watson-Crick base paired with C.

Effects of Base Stacking Partners on Binding to Hx Substrates by AAG

It is possible that G-C base stacking partners made flipping Hx less favorable than T-A base stacking partners, by increasing its stability in DNA. The higher molecular weight band observed in our EMSA is indicative of a flipped base- enzyme complex, which would give a lower intensity shifted band with G-C stacking partners than with T-A stacking partners. Lesser intensity shifted bands were seen with the AAG mutants incapable or less capable of flipping the damaged base (*75*). To test this conclusion, 5nM ^{32}P- labeled substrates, identical to the ones used for excision assays, were incubated with

0-80nM enzyme and an EMSA was performed to separate free DNA from the higher molecular weight enzyme- DNA complex, indicative of specific binding. A catalytically inactive mutant of AAG, E125Q was used in binding assays, to overcome the problem of loss of substrate due to excision by AAG during the time course of the EMSA. The binding affinity of the enzyme for Hx•T with T-A base stacking partners was higher than with G-C base stacking partners. With T-A base stacking partners, at 80nM E125Q, almost all the substrate around 90%, was bound by the enzyme (Figure 5-5A, *upper panel*) whereas, with G-C base stacking partners, binding was less efficient and even at 80nM enzyme, only about 50% of the substrate was bound (Figure 5-5A, *lower panel*). This is also consistent with the observation that more enzyme was required to saturate GHxC•T in excision assays.

Effects of Hydrogen Bonding Partners on Binding to Hx in the Strong and Weak Base Stacking Context

The same enhancement shown with excision of Hx•F was also seen in improved binding affinity of E125Q to both substrates in assays performed with 5nM substrate and 0-80nM E125Q. The enzyme-DNA complex band appeared at lower E125Q concentrations than when opposite T with T-A stacking partners (Figure 5-5B, *upper panel*). With G-C base stacking partners, almost all the substrate around 90% was bound by 40nM enzyme with no free substrate detectable with 80nM enzyme (Figure 5-5B, *lower panel*). This is much improved binding when compared to Hx•T in the same sequence context, in which only 50% of the substrate was bound by 40nM enzyme (Figure 5-5B, *upper panel*. The improved binding affinity was more pronounced for the G-C substrates than for the T-A substrates, as was observed with excision efficiency.

Binding affinity of the enzyme for Hx•C mirrored the excision efficiency. Duplex substrate (5nM) was incubated with 0-320nM E125Q and then resolved by EMSA. But binding affinity was very weak for both DNA substrates (Figure 5-5C, *upper and lower panels*). A specific enzyme-DNA complex band was hardly visible even with 320nM E125Q.

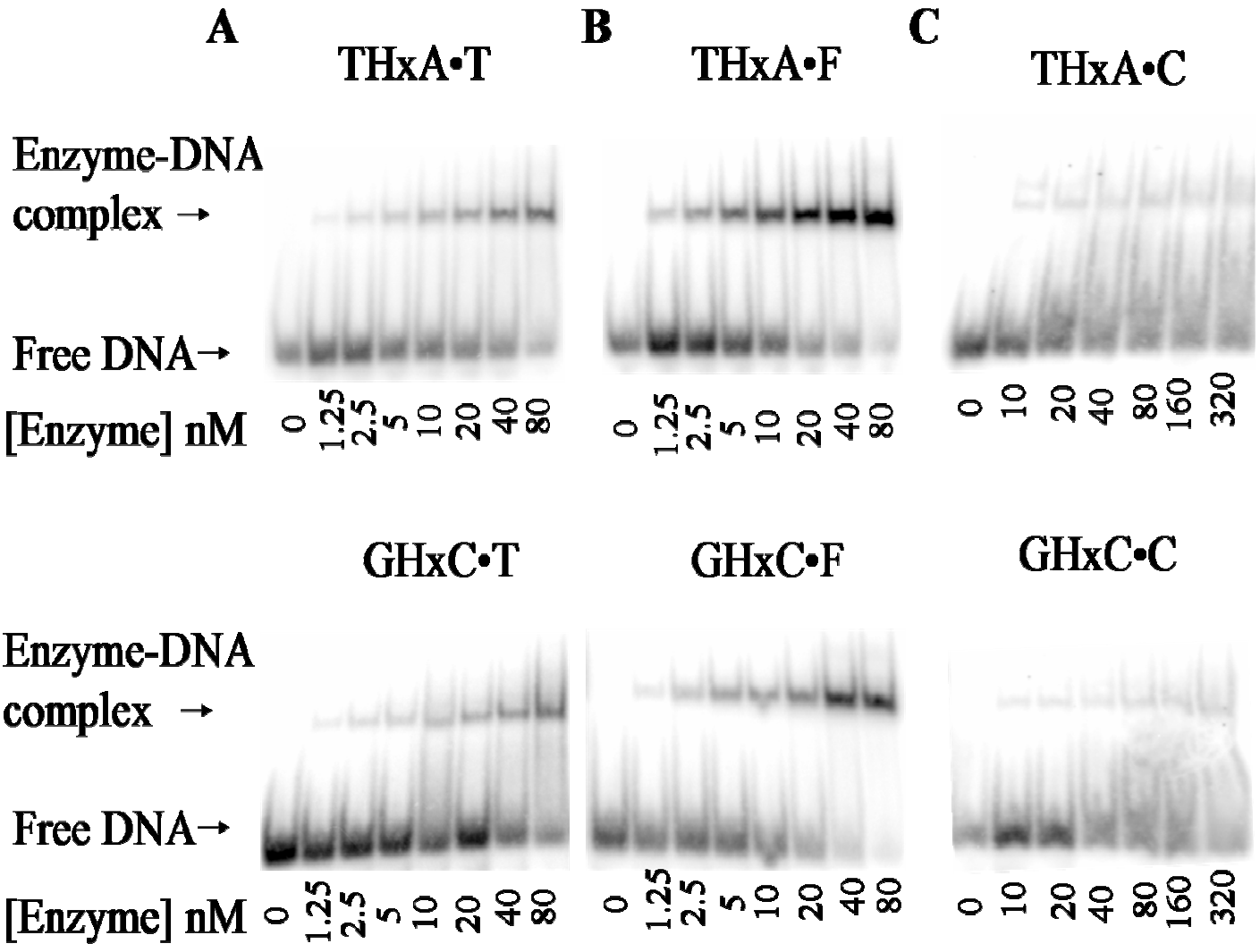

Figure 5-5. Electrophoretic mobility shift assays to measure binding of AAG to DNA containing Hx in different sequence contexts**.** Binding of E125Q to 5nM duplex DNA was observed as the appearance of the higher molecular weight band in EMSAs. Binding to Hx opposite when flanked by T-A stacking partners (*upper panel*) and G-C stacking partners (*lower panel*), with T (*A*), F (*B*) or C (*C*) base pairing partners are shown. (*See text*)

Base Stacking and Hydrogen Bonding Effects on εA

Effects of Base Stacking and Hydrogen Bonding Partners on εA Excision by AAG

In previous experiments it was seen that substitution of F for T opposite εA did not affect εA excision rates. We proposed that this was due to εA not making hydrogen bonding interactions with either T or F. Given the large magnitude of enhancement in excision seen for Hx•F with G-C base stacking partners, it would be interesting to determine whether base stacking partners may alter the effect of F on εA excision. Single turnover excision of εA•T and εA•F, both with G-C base stacking partners were measured for 5nM labeled substrate and 20nM-320nM AAG. There were few differences in the time courses, and rates of excision of εA was largely unaffected by substitution of F for T (Figure 5-6). The rate enhancement was 1.2-fold of εA•F over εA•T, which is similar to the rate enhancement observed for εA•F over εA•T when flanked by T-G base pairs (*75*). Excision of εA was much slower than excision of Hx, irrespective of the sequence context, highlighting the fact that AAG had a diverse substrate range which may differ intrinsically in their interaction with the enzyme. εA excision opposite C was also similar to excision when opposite T and F with G-C stacking partners (Figure 5-7). In all three sequences εA excision kinetics followed the same time course and showed similar rates of excision (Table 5-1). Strikingly, excision of Hx opposite C with both T-A and G-C stacking partners resembled the kinetics of excision of εA in any sequence context.

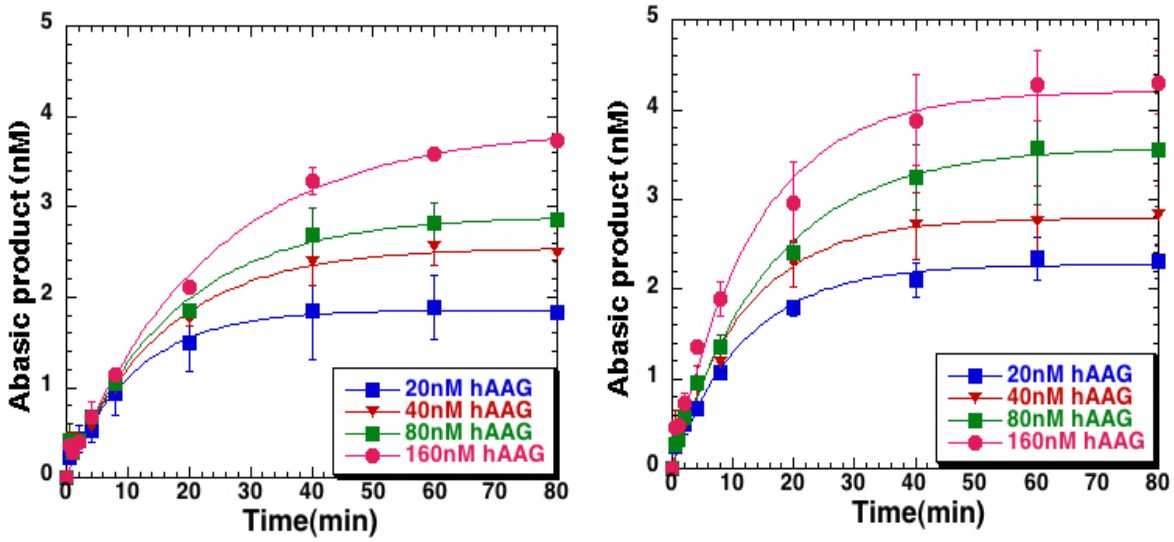

Figure 5-6. Single turnover excision of εA with G-C stacking partners. 5nM εA•T (left) and εA•F (right) were used in excision assays with 20 to 160nM AAG to acheve single turnover conditions. These sequences were used as controls because εA excision is not affected by base pairing partners. The dramatic effects seen for Hx excision with G-C stacking partners was not observed for εA excision, the time courses for both εA•T and εA•F substrates when with G-C stacking partners were very similiar.

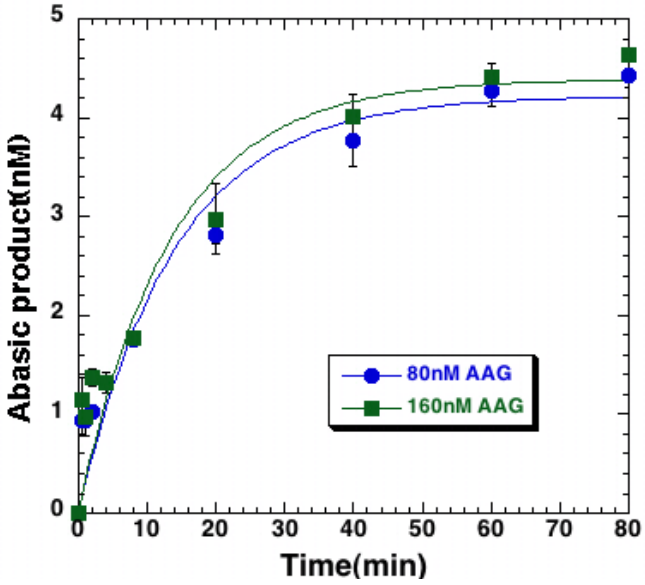

Figure 5-7. Single turnover excision of εA opposite C with G-C base stacking partners. 5nM εA•C was excised by 80 and 160nM AAG. The time courses and rates were similar to those observed for εA•T and εA•F.

Effects of Base Stacking and Hydrogen Bonding Partners on Binding to εA Substrates by AAG

No effect was seen on binding affinities to εA•T and εA•F flanked by G-C base pairs, in EMSAs (Figure 5-8A and B), requiring only 10-20nM enzyme to bind all of the substrate in both cases. Binding to εA•C DNA was as efficient as binding to the other two εA substrates (Figure 5-8C).

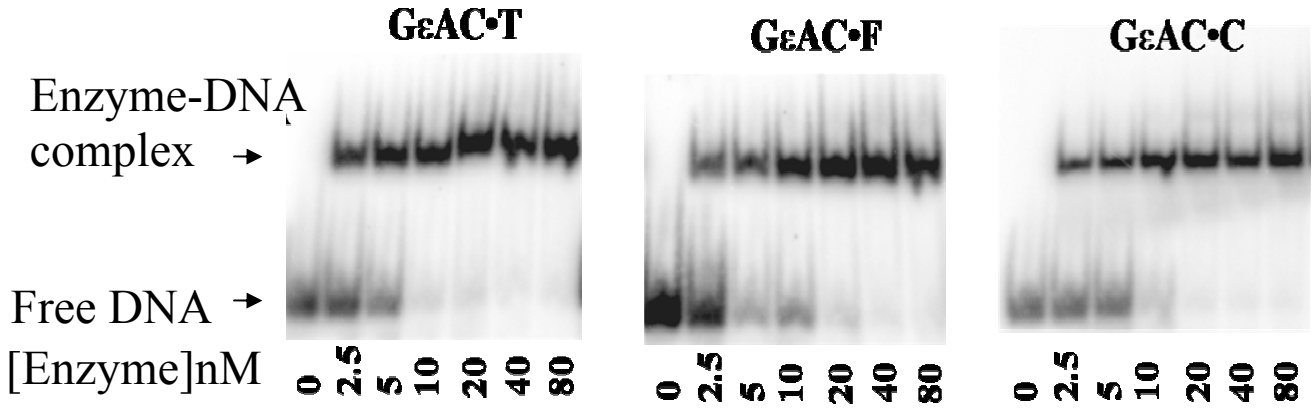

Figure 5-8. Binding of E125Q to εA substrates with G-C stacking partner**s.** Binding of 0-80nM E125Q to 5nM εA•T (*A*), εA•F (*B*) and εA•C (*C*) was observed in EMSAs. Binding affinity to all three εA substrates was essentially the same, with almost all DNA bound by 10nM E125Q.

Melting Temperatures of Hx and εA Substrates

The effects of base stacking and hydrogen bonding partners on the excision of Hx could be predominantly due to altered stability of Hx in the DNA in these sequence contexts, which in turn would reflect on how efficiently AAG can bind and flip Hx. These effects were seen in the amount of enzyme required to bring about saturated excision and the binding to DNA in different sequence contexts. To determine if base

stacking and hydrogen bonding partners bring about altered stability in DNA, melting temperatures were measured by monitoring the change in UV absorbance at 260nm over a controlled temperature ramp of 0.5°C per minute. A melting curve was obtained whose first derivative was taken to give a peak corresponding to the T_m. Mean T_m with standard deviation from two independent experiments for each substrate are given in Table 5-1. As a general trend, it was seen that the T_m for substrates with Hx and εA opposite C were the highest when compared to the same bases opposite T or F, within the same flanking base pairs. For Hx with G-C base stacking partners, the T_m was highest when base paired with C, intermediate when base paired with T and lowest when base paired with F. Generally, all three melting temperatures were higher than the corresponding ones for Hx with T-A base stacking partners. So it can be concluded that, the strong base stacking partners, may affect the stability of Hx considerably and hence the added effects of hydrogen bonding or removal of hydrogen bonding are more evident in this sequence context. This also agrees well with the excision rates of Hx in these sequence contexts. When placed between T-A base stacking neighbors, differences in T_m are not as distinct as for G-C neighbors. But the differences in Hx excision rates were also modest in this sequence context when T was replaced by F. εA did not show any differences in excision when T was replaced by F, and T_m for the εA substrates are not very varied. It must also be noted here that εA excision is much slower than Hx excision and may be mechanistically very different from Hx excision. Hence it is hard to correlate εA excision with the observed T_m and compare them with the other T_m for Hx substrates. It was also seen that for Hx with T-A base stacking partners and the εA substrates, the melting temperature was slightly higher when T was replaced by F. This may be because; F is a good stacker in DNA (*105,*

106). This stacking property of F may not affect the flipping effects due to lack of hydrogen bonds, but may just affect the T_m and hence the observation that for F in these two sequence contexts, reduced T_m may not necessarily implicate increased excision rates.

Table 5.1. Melting temperatures of Hx and εA substrates and corresponding single turnover excision rates

Substrate	Base pairing partner	T_m (°C)	k_{obs} (min^{-1})*
THxA	T	45.5±0.0	1.5±0.3
	F	46.5±1.0	2.6±0.4
	C	48.3±1.3	0.07±0.01
GHxC	T	51.5±0.5	0.95±0.07
	F	47.8±0.3	nd§
	C	53±0.0	0.06±0.01
GεAC	T	47.0±0.5	0.04±0.00
	F	48.5±0.0	0.07±0.00
	C	49.3±0.3	0.075±0.007

* k_{obs} values are based on mean single turnover excision rates for two independent experiments at saturation, with standard deviations.
§ k_{obs} values for GHxC opposite F were experimentally too fast to measure by hand. (*See text*).

Sequence Context Effects and Implications for AAG Activity

The active flipping mechanism of DNA glycosylases is very important for the overall efficiency of the base excision repair pathway. In the case of AAG, though flipping is facilitated by the intercalation of Tyr-162 into the helix, how the damaged base and its interactions in DNA can contribute to recognition, makes an interesting line of thought. Though the crystal structures of AAG, bound to a pyrrolidine abasic site analog (*77*) and *1, N^6*- ethenoadenine (*78*) show no specific contacts between the enzyme

with the base opposite the damaged base, excision efficiency of certain damaged bases is more an identity of the base pair than the base itself (*76*). It has been shown that AAG substrates vary in their sensitivity towards the base pairing partner and mutations to Tyr-162, which may decrease flipping efficiency (*75*). Only for Hx, removing hydrogen bonding could rescue the Y162F mutation, to the level of activity of the wild type enzyme. No rescue occurred for εA. This is a reminder of the diverse substrate range of AAG and that different steps in recognition and excision contribute to different levels for the substrates. The thymine analog, difluorotoluene, indicated that increasing the flexibility of Hx in DNA will also increase its flippability by AAG.

Added to the effect of the base pairing partner, flippability can potentially be affected by other changes around the damaged base, such as base stacking partners. Base stacking partners may increase or decrease the stability of base in DNA. In this chapter, the 5' and 3' base stacking partners to Hx were chosen as possible candidates to change and thereby affect flippability of Hx by AAG. Either T-A base pairs or G-C base pairs were chosen as the base stacking partners to represent relatively weak and strong base stacking neighbors to Hx. A working model for the activity of AAG has already been discussed based on the results from Chapter 4, in which the enzyme can use a two- step process to specifically identify and excise its substrates efficiently. In this model, the enzyme uses the flipping step as an initial test for destabilized bases in DNA, which could indicate possible substrates. After the base is flipped, AAG uses the factors in the active site like proper fit in the active site, alignment of the glycosylic bond for cleavage and suitability of the leaving group that lead to chemistry to finally identify the flipped base as a substrate and excise it from DNA. According to this model, flipping can be an

important determinant of the enzyme's efficiency. Factors that affect the "flippability" of a base may in turn contribute to excision efficiency too.

It required about 4 times more enzyme to saturate the rate of excision of Hx•T with G-C than T-A stacking partners and excision was also 1.6-fold slower than for TA neighbors. This shows that the strong base stacking contributed by the G-C base pairs probably increased the stability of Hx•T and made it much more difficult to be flipped by the enzyme, as can also be seen in the reduced binding affinity. If this were the case, then removing the constraint of hydrogen bonding must be able to destabilize Hx more and hence make it more easily flipped. This is exactly what happened when T was replaced by F, to which Hx cannot hydrogen bond. Both binding affinity and excision efficiency increase for Hx•F, in both sequences. Most striking was the enhancement of excision rates seen with G-C stacking partners, which was a 9-fold enhancement, compared to a 2-fold enhancement with T-A stacking partners. The stronger base stacking partners, G-C base pairs, seem to have exaggerated the effect of F on Hx excision by AAG, possibly owing to the fact that the effect of destabilization of Hx•F on flipping was more pronounced when in a stronger base stacking sequence. This could mean that the interactions between AAG and the DNA during the formation of a stable- flipped Hx complex were stabilized by the strong base stacking partners while at the same time, F destabilized Hx to enable easier flipping by AAG. The weaker base stacking sequence, T-A partners, may not have the same effect on the enzyme's interaction with DNA, and hence the base pairing partner effects on flipping were modest. The assumption that DNA stability is affected by the base stacking partners is backed by the melting temperatures measured for the various substrates.

In contrast, εA excision was not greatly altered when placed between G-C base pairs. The rate of εA excision and the binding of AAG to εA substrates when placed between G-C stacking partners mirrored the rates and binding properties of εA placed between T-G partners (*75*). It has been shown before that εA excision was not affected by the base pairing partner. Binding was unaltered too. Since εA lacks the ability to hydrogen bond with any base, the base pairing partners did not add to its destabilization in any way. It is also possible that its intrinsic instability in DNA makes εA adopt an extra helical conformation much more easily than Hx; hence making it more accessible to AAG.

For Hx the wobble base pair with T adds to its stability and impedes flipping, which can be overcome by other changes that decrease stability. This was seen when Hx is placed between T-A base pairs and when placed opposite a non-hydrogen bonding partner. Strikingly though, this neighboring base pair sensitivity was lost when Hx was Watson-Crick base paired with C. In the cell, Hx is formed opposite T due to deamination of A but; replicative polymerases have a high propensity to place a C opposite Hx, which leads to transition mutations. The fact that, when opposite C, Hx repair is impaired to the same degree irrespective of the base stacking partners indicates an important biological function. Hx repair opposite C would be mutagenic and a Watson-Crick base pair may overcome the base stacking partner effect to prevent repair. So stability of Hx in DNA may be an important factor in deciding its fate, a wobble base pair may make it more discernible by AAG while a Watson- Crick base pair may make it less discernible, possibly by shifting the flipping equilibrium. This difference in stability was partly reflected in the melting temperatures for the various substrates, especially for

the Hx base pairs between GC base pairs, with Hx•C substrates having the highest T_ms and Hx•F substrates having the lowest T_ms, with Hx•T being in between. Only a modest difference in T_ms was noticed for the Hx base pairs with T-A stacking partners, adding weight to the argument that base stacking partners can affect the stability of the Hx base pair in the substrates.

An important biological outcome of this scenario, in which local sequence context is seen to affect Hx removal by AAG, is its significance in understanding the presence of mutational "hot-spots and cold-spots" in the genome. The effect of local sequence context in the stability of Hx in DNA can play a major role in both enhancing and reducing its repair. This in turn may contribute to the complex interplay between factors dedicated to protecting the cell from mutations, like repair mechanisms and the limitations facing them.

CHAPTER 6
ACTIVITY AND STABILITY OF AAG DURING ASSAYS

The kinetics of AAG revealed a puzzling dilemma. The enzyme was not able to catalyze multiple rounds of excision. Under multiple turnover conditions, AAG performed anywhere from one to three turnovers and then seemed to stop catalyzing base excision. Under multiple turnover conditions, there is excess substrate over enzyme and ideally, an enzyme goes on catalyzing until all the substrate is depleted. But under these conditions, factors such as dissociation from product and reassociation with substrate will affect the catalysis by the enzyme. So single turnover conditions in which product dissociation will not contribute to the observed rate of catalysis were used in all experiments to study the properties and mechanism of action of AAG. Under single turnover conditions, there is a vast excess of enzyme over substrate and ideally, saturation of substrate is observed. The observed excision rates are a measure of the rate of excision when substrate is saturated with enzyme and reflects the rate of some step after binding the substrate and prior to product dissociation. Although single turnover excision kinetics offers a good measure of AAG's activity, the fact that the enzyme cannot catalyze several rounds of excision prompted several questions relating to its activity and stability. Is the enzyme losing activity during the experiment? Is this property also a function of the substrate and its sequence context? Are reaction conditions not ideal for AAG? These were important questions to address in order to design experiments in the future and make the most of the knowledge gained from previous experiments. In addition, evidence was mounting about similar activities observed for other glycosylases

like human thymine DNA glycosylase (*107*) and the human MutY homolog (*108*). These questions, when answered may reveal some missing links between glycosylase activity and probably, the BER pathway and its components. So, a systematic experimental design to address these questions was performed. In these experiments, enzyme death, the turnover issue as an effect of sequences and other conditions that could improve AAG activity were considered as possible candidates to test.

Loss of AAG Activity Can Contribute to Reduced Catalysis

AAG loses activity when stored below a final concentration of 40μM for periods longer than 6-8 months at -80°C. The enzyme also lost activity, both binding and excision, when stored for more than 10 days at -20°C. This indicated that, either the enzyme had to be stored above a critical concentration to preserve activity or the enzyme slowly loses activity over time, whatever concentration it may be. This loss of activity might be more significant at the higher temperature in which excision assays were performed. To determine if this is true, two simple enzyme "death assays" were performed. In both assays, 5nM THxA•T was used as the substrate with 40nM AAG. This was the substrate of choice because Hx was found to be efficiently excised by AAG but excision was not so fast that hand mixing experiments could not be used (Chapter 5). For single turnover excision assays, a 4X concentration of the enzyme was needed for the assay stored in ice and diluted directly into the assay mix to start the reaction. In the first enzyme death assay, 160nM AAG was pre-incubated for times ranging from 0 to 120 minutes at 37°C. Excision assays were performed to determine the loss of activity during the pre-incubation. Time points were taken as for a normal excision assay and the quenched samples were analyzed by PAGE and the product formed plotted over time

(Figure 6-1). The products formed and the rate of product formation was compared for various periods of pre-incubation at 37°C (Table 6-1). It was determined that the loss of activity was not drastic. When compared to the "No pre-incubation" control, there was a slight drop in the amount of product formed, progressively, with increasing times of incubation, from 4.8nM to 4.4nM. However the rates of excision did drop with increasing pre-incubation times, to almost two times lower than the control rate (Table 6-1). Even after 2 hours at 37°C, the loss of activity was much less than the activity of AAG on the slow substrates, for example, Hx•C for which, 160- 320nM AAG was required to observe comparable activity.

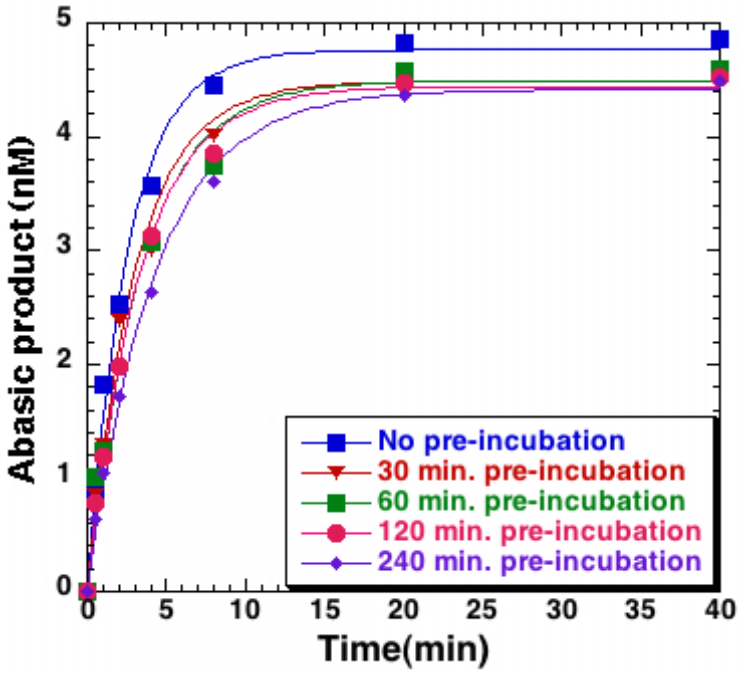

Figure 6-1. AAG death assay under single turnover conditions. 5nM THxA•T was excised by 40nM AAG diluted from a 160nm AAG stock which was incubated at 37°C for the indicated times (0 to 240 minutes). Reactions were started by diluting the stock 4-times into the tube. A serious loss of AAG activity was not seen even after 240 minutes at 37°C.

Table 6.1. Comparison of pre-incubation of 160nM AAG at 37°C with product formed and rates of product formation with 5nM THxA•T

Pre-incubation at 37°C (min)	Product formed (nM)	k_{obs} (min^{-1})
0	4.8	0.4
30	4.5	0.3
60	4.5	0.3
120	4.4	0.25
240	4.4	0.2

As there was not a significant loss of enzyme activity upon incubation of the 4X stock at 37°C, another approach was chosen, in which AAG was pre-incubated at 37°C with the assay buffer for the same time periods used before, but at a final assay concentration of 40nM instead of 160nM. The excision assay was started by adding 5nM substrate to the pre-incubated AAG. This will also mimic the condition of the usual assay carried out and may tell us more about whether AAG was losing activity during the assay itself. So, AAG was pre-incubated at 37°C for times ranging from 0-240 minutes and then the reactions were started by adding DNA to each mix, to give a final enzyme concentration of 40nM and substrate concentration of 5nM. The experiment was performed as before and product formed (Figure 6-2) with the single turnover excision rates (Table 6-2) was obtained. In this case, the observed loss of activity was considerable. Both the amount of product formed as well as the rate of product formation was reduced when compared to the "No pre-incubation" control. The progressive reduction was more pronounced for 40nM AAG than for 160nM AAG. In 60 minutes at 37°C, both the amount of product and the rate were only one-third of the "No pre-incubation" control. After 240 minutes of pre-incubation, there was no detectable product

formed. This means that the enzyme was totally inactive after this extended period at 37°C. However a significant drop occurred with every pre-incubation time at 37°C beginning at 30 minutes (Table 6-2), suggesting that AAG could be progressively losing activity during the time course of our single turnover assays. This may either be due to enzyme instability or the absence of an additional factor that could stabilize it. This factor may range from the right pH or ion to another specific protein.

These death assays were an important indication of the limitations faced in our experiments, the enzyme itself. The additional concentration-dependent loss of activity highlighted how enzyme death may be more evident when less AAG was used. Consequently, there could be a critical concentration below which enzyme death could be rapid. In the traditional multiple turnover assay with an excess of substrate over enzyme, this phenomenon may be contributing significantly to the lack of turnovers. According to Selwyn *(115)*, the test for enzyme inactivation during the course of an assay comes from the super-imposability of the progress curves at any concentration of the enzyme. When the enzyme loses activity over the progress of the assay, the enzyme itself will follow a first- order time dependence varying with concentration. Hence the product formed over time may vary with different enzyme concentrations, giving non- super-imposable progress curves. This property due to enzyme inactivation is called the “Selwyn’s test”. The behavior of AAG at the two different concentrations used, along with the progress curves obtained during single turnover titrations (Chapter 5) indicate similarities with the behavior under Selwyn’ test. This similarity may indicate possible loss of AAG activity during the assay and needs to be further investigated for designing strategies to explain the inactivity and to overcome the effects of inactivity.

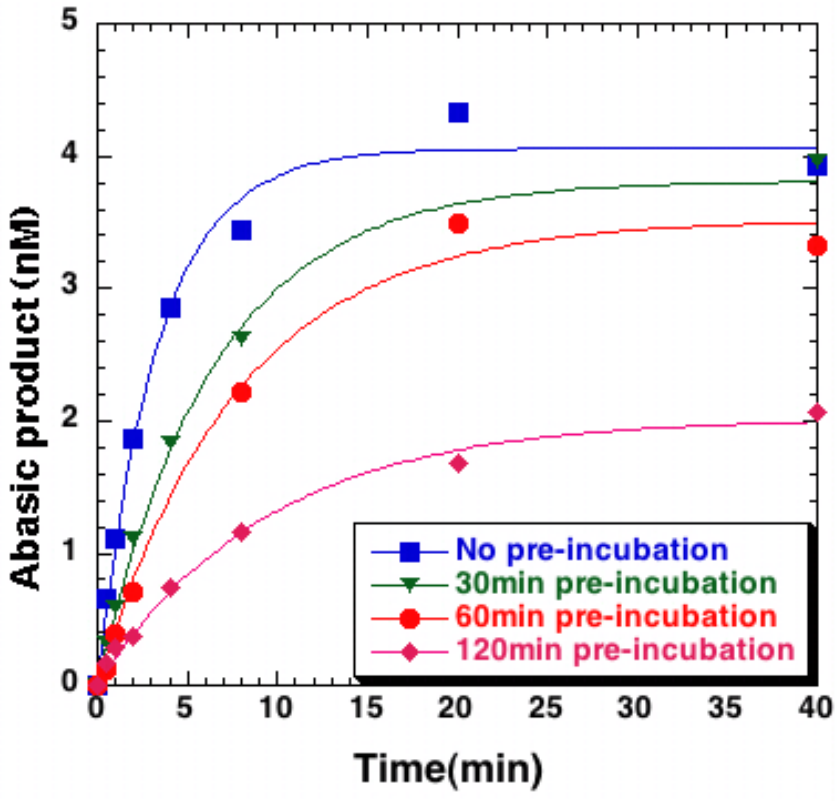

Figure 6-2. AAG death assay under single turnover conditions. Assays were done with 5nM THxA•T and 40nMAAG which were preincubated at 37°C for the indicated times (0 to 240 minutes). Reactions were started by adding substrate to preincubated AAG. A considerable loss of AAG activity was seen starting at 30 minutes to no detectable activity after 240 minutes.

Table 6.2. Comparison of pre-incubation of 40nM AAG at 37°C with the product formed and rate of product formation with 5nM THxA•T

Pre-incubation at 37°C (min)	Product formed (nM)	k_{obs} (min^{-1})
0	4.1	0.3
30	3.8	0.2
60	3.5	0.1
120	2.0	0.1
240	Not detectable	Not detectable

Multiple Turnover of Hx Is Dependent on the Base Pairing Partner

Based on the previous results which revealed base pairing and base stacking sensitivities in AAG mediated excision of Hx, it was clear that Hx excision depends more on local sequence context than εA. Under multiple turnover conditions, using a THxG substrate with T being the base pairing partner to Hx, approximately two or three turnovers were always observed. This meant that, AAG was able to catalyze more than one enzyme equivalent, but is limited by other factors and then is not able to catalyze excision of all the substrate. Removing hydrogen bonding to Hx was seen to improve its excision, especially with strong base stacking partners. A multiple turnover excision assay, in which 50nM Hx with GC stacking partners was used, opposite either T or F with 5nM AAG was performed. When opposite F, almost 45nM substrate was excised completing about 9 turnovers for AAG. On the other hand, the same substrate opposite T showed just 3nM substrate excised, meaning that AAG was unable to complete more than half a turnover (Figure 6-3). This was even less than the usual number of two or three turnovers seen for Hx•T substrates with TG base stacking partners. This inhibition of turnovers for Hx with GC stacking partners opposite T was observed again when 20nM AAG was used with 50nM substrate, while the same substrate opposite F was always

fully excised. In multiple turnover experiments done with the previous THxG substrate, which should be intermediate between TA and GC stacking sequences, F as the base pairing partner stimulated complete excision of Hx. Whereas T as the base pairing partner gave about two or three turnovers (Figure 6.4).

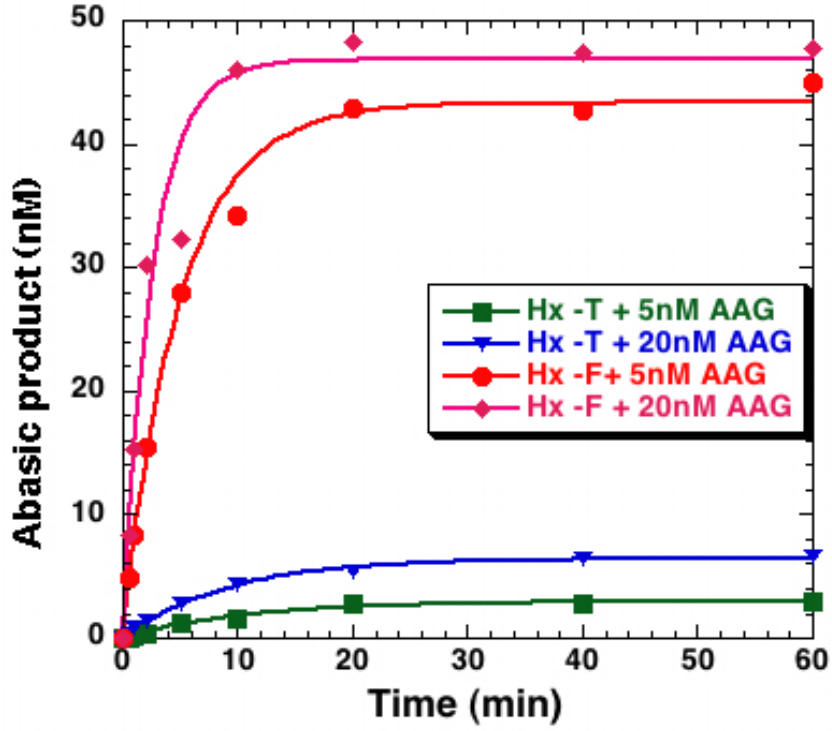

Figure 6-3. Multiple turnover of Hx•T and Hx•F with G-C stacking partners. 50nM substrate and either 5 or 20nM AAG were used in these assays. Hx•F was turned over completely by both concentrations of enzyme, meaning that AAG was able to do multiple turnovers of Hx when not hydrogen bonded. On the other hand, excision of Hx•T showed only half a turnover. This restriction on AAG turnovers seemed to be sensitive to the hydrogen bonding partner.

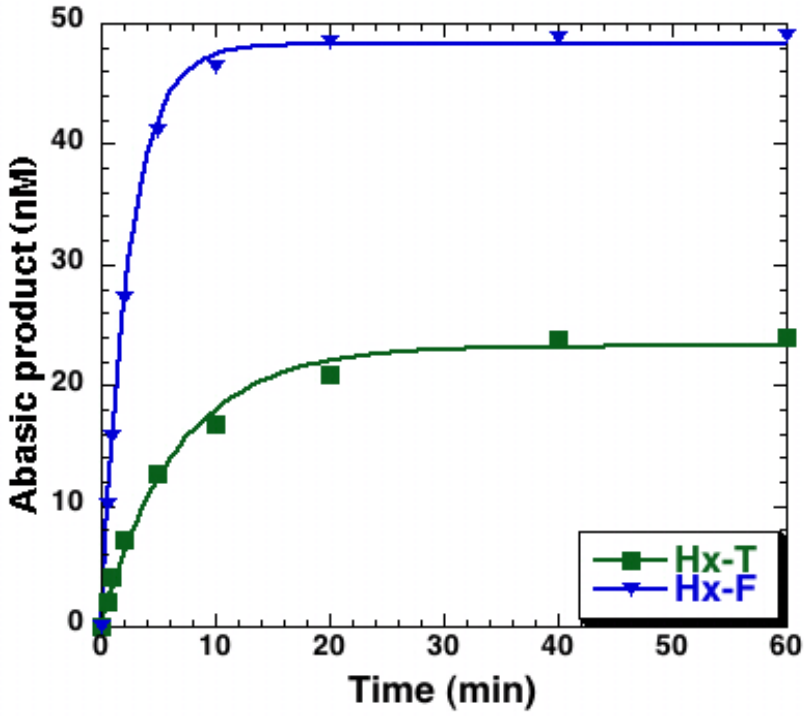

Figure 6-4. Multiple turnover of Hx•T and Hx•F with TG stacking partners. 50nM substrate and 10nM AAG were used. In the presence of stacking partners, intermediate between TA or GC base stacking partners, Hx•T excision showed around two or three turnovers with AAG, whereas, Hx•F was excised to completion by AAG.

There seemed to be a clear connection between the stability of Hx in DNA and the ability of AAG to turnover Hx. This could mean that the extremely fast excision of Hx•F in any sequence context is over shadowing the combined effects of loss of AAG activity and any other modes of inhibition possible in a multiple turnover reaction. A multiple turnover reaction may reflect product interactions with the enzyme that are not a factor in a single turnover reaction. So, the differences in turnover seen for Hx depending on the sequence context may be an exaggeration of the enzyme being slow due to the strong base stacking and hydrogen bonding sequence context and at the same time losing activity rapidly. It must also be recalled that in the stronger base stacking sequence, binding is much less efficient. The sequence context of the substrate DNA may play an

important role in taking into account product inhibition issues, which may make much less enzyme available to bind the substrate in addition to reduced binding affinity.

Multiple and Single Turnover of εA Present Different Pictures

Sequence context had little effect on the excision of εA. Whatever may be the base stacking or base pairing partners to εA, under single turnover conditions, product formed and the rate of product formation were virtually unchanged. This same behavior was observed under multiple turnover conditions too. Whatever the sequence context, exactly one equivalent of the amount of AAG used was excised when εA was the substrate. Whether it was εA opposite T or F, only one turnover was seen using GεAC DNA. 50nM substrate and 5 or 10nM AAG were used in multiple turnover reactions as described above. It was surprising that compared to the progress of single- turnover reactions, the burst of product to reach one turnover was much faster under multiple turnover conditions. Therefore, a titration of AAG to span multiple turnover and single turnover conditions was done with 5nM εA•T with GC stacking partners, the same substrate used before. It was seen that the lower the enzyme concentration, the faster the burst of product, though under multiple turnover conditions, only one turnover was seen (Figure 6-5). As the AAG concentration reached single turnover levels, above 5nM, the product formation curve resembled previous single turnover progresses and the rates of single turnover were much lower than multiple turnover. It was also observed that, as AAG concentration increased in the multiple turnover part of the titration, rates dropped whereas, in the single turnover part of the titration, rates remained constant throughout the concentration range (Table 6-3).

The above observations appeared to conflict with those made previously by Dr. Clint Abner, who conducted a similar titration with 50nM εA DNA and 10- 800nM AAG, final concentrations. He observed a concentration dependent rise in product formed consistent with a saturation curve. Interestingly, the observed rates of excision showed some anomalies with his experiments too, with rates dropping for the 50 and 100nM AAG experiments and remaining more or less constant for the other single turnover experiments. Together our results may indicate an AAG-dependent change in the excision kinetics of εA which needs further investigation to explain.

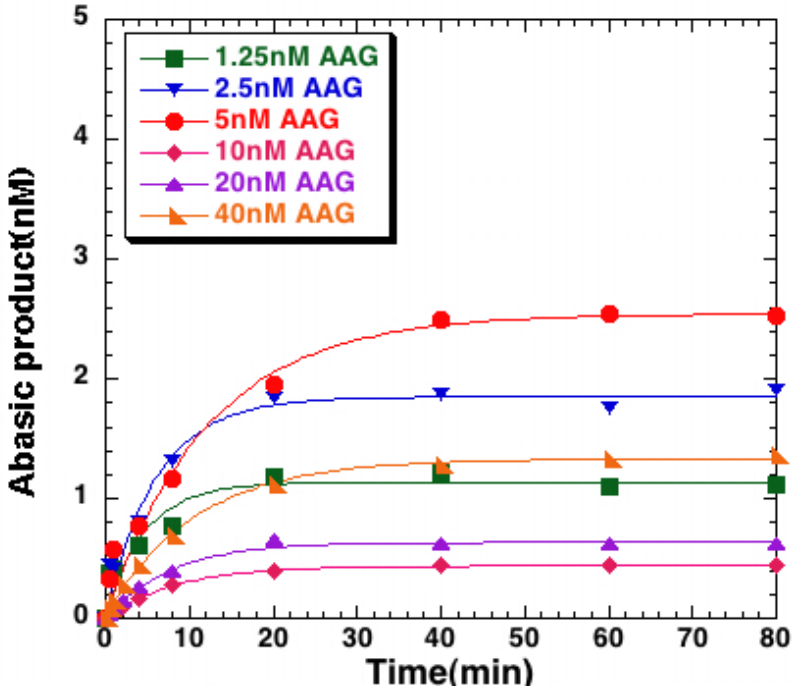

Figure 6-5. Multiple to single turnover titration of AAG with εA•T. 5nM substrate was used with 1.25 and 2.5nM AAG (*multiple turnover conditions*), 5nM AAG (*equal substrate and enzyme*) and 10, 20 and 40nM AAG (*single turnover conditions*). One turnover was seen at a faster rate under multiple turnover conditions (*See text and Table 6.3*)

Table 6-3. Observed rates of multiple to single turnover titration assays of AAG with 5nM εA•T

AAG (nM)	1.25	2.5	5.00	10.0	20.0	40.0
k_{obs} (min^{-1})	0.2	0.2	0.08	0.1	0.1	0.1
Product (nM)	1.0	1.8	2.60	0.4	0.6	1.2

Optimization of Assay Conditions for Maximum AAG Activity

The loss of AAG activity at 37°C may be due to non- optimum assay conditions, which may destabilize AAG especially at higher temperatures. Variations in buffer composition including pH, salts and other stabilizing agents like BSA may improve stability. A recent publication has suggested that for neutral substrates like Hx and εA, pH optimum for efficient excision by AAG is 6.0. The pH optimum is 6.0 for neutral substrates to make them favorable leaving groups upon excision (*109*). The assay buffer that we routinely use was based on previous data and stability assays and was at a pH of 8.0. To determine if excision was more efficient at pH 6.0, assays were done at pH 6.0, with sodium acetate pH 6.0/sodium chloride or potassium acetate pH 6.0/potassium chloride instead of HEPES pH 8.0/potassium chloride, which were the buffer and salt used in all our assays. Assays contained 50mM buffer and 100mM salt. The potassium buffer and salt were used at pH 6.0 because it was shown previously that potassium chloride was more suitable for storing and assaying AAG than sodium chloride. KCl stabilized AAG better than NaCl. An excision reaction was performed under these conditions with 5nM Hx•T with G-C base stacking partners and 50mM AAG diluted in the respective storage buffer to maintain salt and pH conditions. The substrate was so chosen that any increase or decrease in activity will be very evident, this being the

slowest excised substrate of all and probably the most stable substrate. The observations were interesting though by no means reflective of AAG activity being improved at pH 6.0. Only the potassium acetate pH6.0/potassium chloride buffer showed more products formed. The sodium acetate pH 6.0/sodium chloride buffer showed activity similar to the HEPES pH 8.0/potassium chloride, which was the previously used buffer/salt combination (Figure 6-6). The rate of product formation though remained essentially unchanged under all three conditions (Table 6-4). The argument that the right pH was not achieved to ensure maximum activity of AAG was not supported by these experiments. The effect of the potassium salts may be due to some other effect of salt on DNA structure and stability. To verify this, melting temperatures were measured as described for the same substrate used in these assays in the respective buffers. The overwhelming observation was the lower T_m with Potassium acetate, pH 6.0/Potassium chloride. The T_m was lower by about 3°C than the T_m of 51.5°C seen with HEPES, pH8.0/Potassium chloride and Sodium acetate, pH 6.0/Sodium chloride buffers (Table 6-4). Therefore, the effects of the potassium buffer may not be a pH effect but a salt effect on DNA stability or structure which may make Hx more flippable by AAG. The buffers used by the authors (*113, 114*) to illustrate the effects of lower pH on neutral substrates did not hold in the case of our assays since no enhanced excision of Hx was observed in the sodium buffer at pH 6.0 over our buffer at pH 8.0.

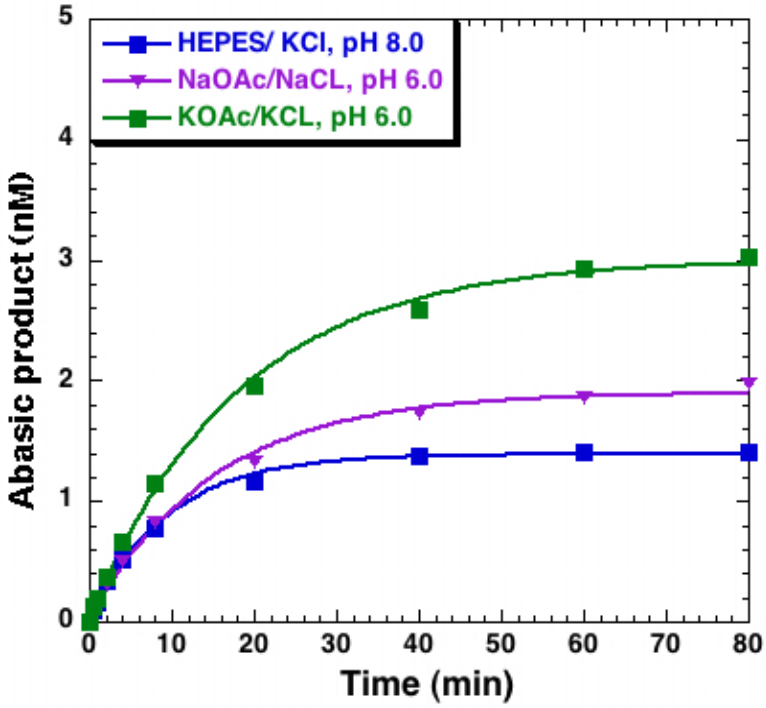

Figure 6-6. Effect of pH and salt on excision of Hx•T. 5nM Hx•T with G-C stacking partners was used as substrate to assess the activity of 50nM AAG at pH 6.0 with either NaOAC/NaCl buffer or KOAc/KCl buffer. The activity was compared to the control excision assay with the same amount of AAG at pH 8.0 in HEPES/KCl, which are the usual conditions used by us. NaOAC/NaCl buffer at pH 6.0, which was reported to be the optimum buffer, did not improve AAG activity over our buffer. When Na was replaced by K at pH 6.0, enhanced activity was seen.

Table 6.4. Comparison of the effects of pH and salt on AAG activity and stability with 5nM GHxC•T

Buffer	Product formed (nM)	k_{obs} (min^{-1})	T_m (°C)
HEPES/KCl, pH 8.0	1.4	0.1	51.5
NaOAc/NaCl, pH 6.0	1.8	0.1	51.5
KOAc/KCl, pH 6.0	2.9	0.05	47.5

Being convinced that the pH and salt in our assay buffer was in no way restricting enzyme activity, agents that were found to have stabilizing effects on proteins were considered. BSA is a common stabilizing agent, used to store proteins and in assay buffers to prevent protein denaturation. BSA has been used by some groups in AAG buffers, but no extensive study on what effects it had on AAG activity is available for

reference. To determine if BSA would stabilize AAG, 1mg/mL and 0.1mg/mL BSA were used in AAG storage buffer to dilute the protein. Excision of 5nMT with the GC stacking partners was observed with 50nM AAG using the standard AAG assay buffer at pH 8.0. A much less robust excision was noticed when compared to the "No BSA control", and lesser product was formed after 80 minute time course (Figure 6-7). Either BSA was not a good stabilizing agent or more concentration ranges of BSA must be tried before ascertaining its usefulness in stabilizing AAG.

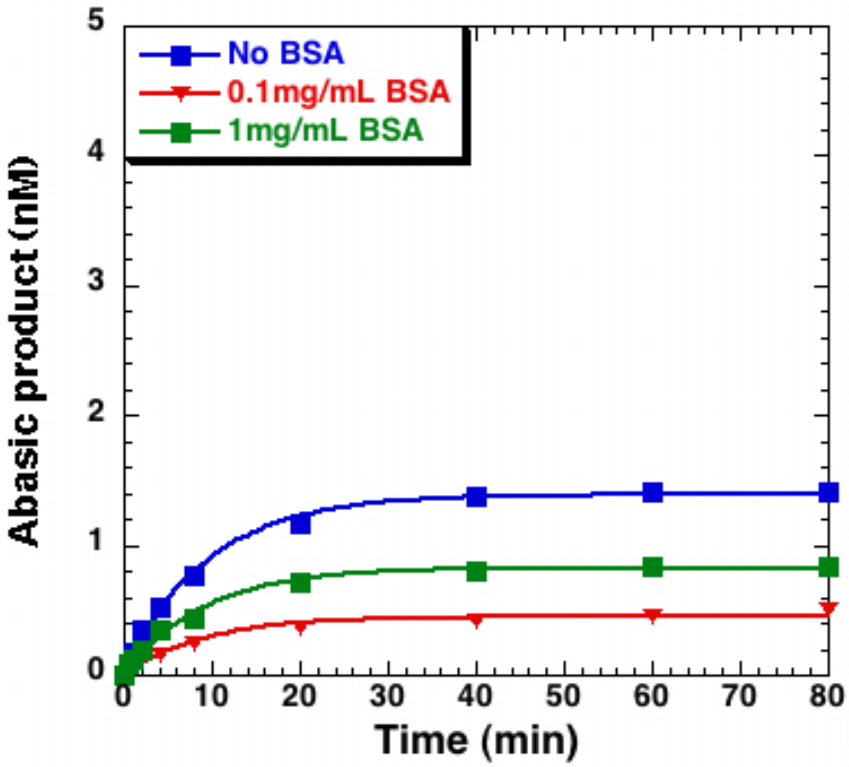

Figure 6-7. Effect of BSA on AAG stability and activity. Activity of 50nM AAG on 5nM Hx•T with GC stacking partners was assessed in the presence of 0.1mg/mL and 1mg/mLBSA. Activity in the presence of BSA was reduced when compared to the "No BSA" control.

Conclusions about Activity and Stability of AAG During Assays

It was clear from the above experiments that loss of activity at 37°C was contributing to reduced AAG activity and this when combined with slow product release

and product inhibition, could be the candidate issue preventing multiple turnovers by AAG. The issue of multiple turnovers due to instability, combined with poor substrate binding was seen to be exaggerated with slower substrates and not a factor with faster substrates. The reasons for loss of activity could be manifold, ranging from intrinsic instability of the protein to instability in the particular conditions used in the assays. Whatever be the reason, it is evident that a critical concentration exists, below which loss of activity is significant. Stabilizing agents like BSA were not useful. The suggestion that pH optima decide the excision efficiency of different substrates (*109,110*) did not hold under these assay conditions, rather, a more general effect of salt on DNA was seen. The instability of AAG could be an artifact of the *in vitro* system used in these assays, due to the lack of other cellular factors, including other BER proteins, acting downstream of AAG or other factors not yet discovered. Or, the instability may just be a biological property of the protein which could be important in the cell.

Additional experiments may give more details as to the best possible conditions for maximum activity and stability of AAG. The complexities associated with multiple turnover versus single turnover conditions may also begin to become more clear with experiments addressing the issue of stability at various conditions.

CHAPTER 7
FLUORESCENCE ASSAYS TO OBSERVE BINDING AND EXCISION OF ETHENOADENINE BY AAG IN REAL TIME

The need to develop an experiment which would allow us to look at base flipping and excision by AAG in real time is great, given the results obtained from the intercalating mutants and the sequence context effects. The most probable experiment would be to exploit the natural fluorescence properties of εA and use its changes to observe εA flipping and excision by AAG. This experiment will be valuable in validating our interpretations of the effect of the Tyr-162 mutations on flipping and the effects of base stacking neighbors. The difluorotoluene complement will also serve as another tool to test these conclusions. Real time measurements can also give equilibrium binding constants and a means to measure the rate of flipping, which can alleviate the limitations of the EMSA, which was the assay used to observe binding of AAG to its substrates. The crystal structure suggests that the fluorescence of εA has a potential to change when it is flipped out of the base stack into the active site and then released into solution upon excision of the glycosylic bond. There is also the possibility that the rate and magnitude of these changes is different and with the combination of the catalytically inactive E125Q mutant and the active AAGΔ79, flipping and excision can be monitored independent of each other to complement the ^{32}P assays for excision and binding respectively.

εA is naturally fluorescent, with an λ_{max} of excitation at 310nm and a λ_{max} of emission at 405nm(*94*). Its fluorescence is quite quenched when stacked in the DNA

double helix. But upon binding and excision by AAG, it shows an increase in intrinsic fluorescence as observed in the excitation and emission spectra (Figure 3-2)

Fluorescence of εA During Binding by AAG

In this experiment, εA fluorescence in duplex DNA was monitored at room temperature with saturating concentrations of E125Q (400-1600nM). These conditions mimicked the EMSA conditions, in which binding was observed independent of excision. The goal of the E125Q experiment was to see whether the flipping step could be observed and its rates measured. "Hand-mixing" experiments in which AAG was added to εA-DNA were done in the fluorimeter. Fluorescence of εA in DNA was largely quenched due to base stacking, so when εA is flipped out by AAG, a fluorescence intensity increase can help monitor the flipping step. No increase in fluorescence intensity of εA-DNA only was observed. Immediately following addition of enzyme to the DNA in the cuvette, there was a sharp increase in fluorescence intensity of εA and then constant fluorescence at 410nm. This jump in fluorescence could indicate a very fast εA flipping step, since the intensity was higher than that of stacked εA in DNA. But the increase was very fast and in the time scale used in this instrument, it was not possible to monitor the real change in fluorescence over time, as planned. Alternately, the increase in fluorescence could be due to Trp fluorescence when AAG was added to DNA. Titration experiments were done with 100nM duplex DNA containing εA and 25 to 800nM E125Q, which is the general scale used for EMSA experiments. There was a progressive increase in the intensity of εA fluorescence with increasing E125Q with the signal saturating with 400 and 800nM E125Q (Figure 7-1). If the increase in fluorescence was due to the addition of AAG, then the signal must not saturate but keep on increasing with increasing enzyme. The saturated signal and previous observations from the EMSA made

us interpret the fluorescence increase as a reflection of the rapid binding and flipping of εA. Hence, this jump in εA fluorescence intensity could be indicative of the flipped εA-E125Q complex. Interestingly, the magnitude of the fluorescence increase was the same for εA in any sequence context (T*εA*G substrates or G*εA*C substrates) (Figure 7-1). It is important to recall that neither the base pairing partner nor base stacking neighbors changed the binding and excision of εA by AAG (*75*). εA does not hydrogen bond to any other base and is bulkier than the other AAG substrate studied in this work Hx. This similarity in the fluorescence intensity changes of εA in both sequence contexts complements the EMSA, which showed very little change in the fraction bound for both DNA substrates.

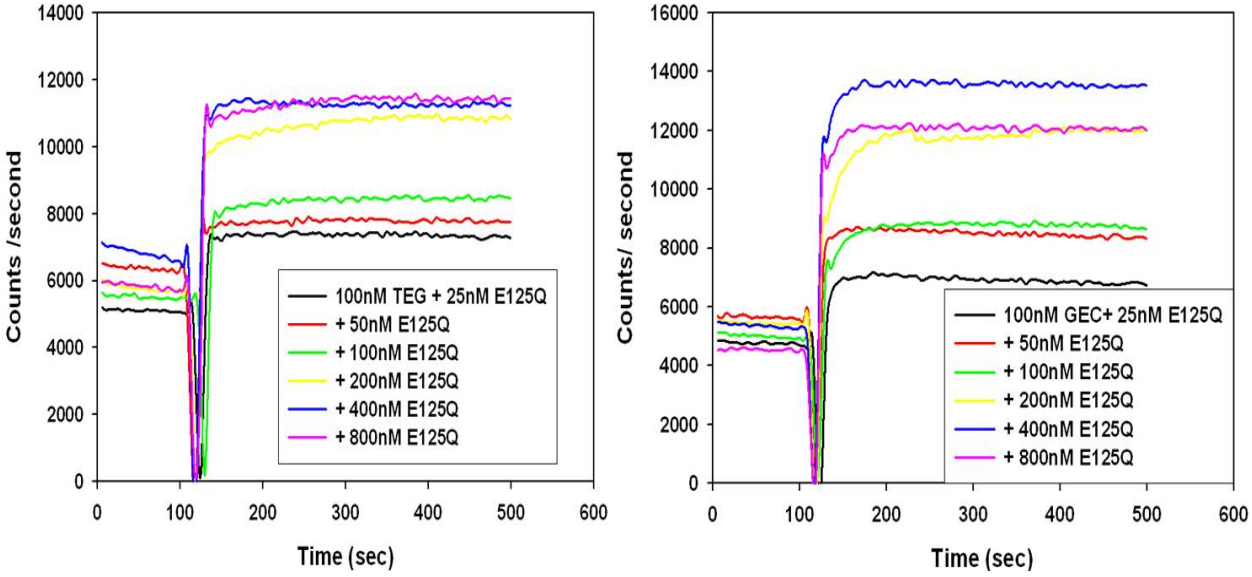

Figure 7-1. 500 second time based fluorescence of εA when bound by increasing concentrations of E125Q**.** 100nM DNA with εA in two sequence contexts, T*εA*G (left panel) and G*εA*C (right panel) was used. Excitation was at 320nM and fluorescence emission was observed at 410nM with the band pass set at 4nM. The DNA only background was recorded for 100 seconds after which the shutter was opened and the enzyme added. A sharp jump in fluorescence emission upon closing the shutter was observed, followed by constant fluorescence. The sequence context did not affect the change (*See text*)

Blueshift of εA Emission upon Binding by E125Q

Upon titrating increasing concentrations of E125Q with DNA substrates containing εA as the damaged base, as discussed above, emission spectra were taken to observe the λ_{max} of emission when excited at 310-320nm. With increasing E125Q concentrations, a blue shift occurred in the emission maximum from 410nm, which is the εA emission λ_{max} to 390nm with 800nM E125Q with the shift being gradual with increasing enzyme (Figure 7-2). This shift was similar with both εA substrates used and the progress of the blue shift coincided with the increase in fluorescence intensity observed over time in Figure 7-1. Interestingly, a corresponding spectrum of increasing concentrations of the enzyme only did not show any emission maxima or blue shift when excited at 320nm (Figure 7-3). This control was incorporated to rule out any possible fluorescence change in the enzyme, as, it is possible that at the UV range, protein fluorescence is significant and may affect the observed signal.

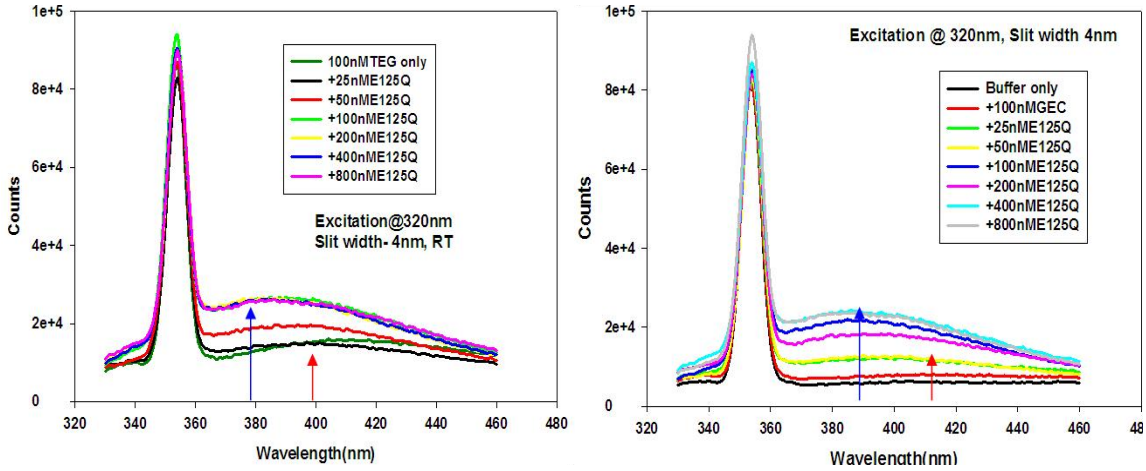

Figure 7-2. Emission spectra of 100nMεA substrates, after adding 25-800nM E125Q at room temperature, after excitation at 320nm. εA was placed in two sequence contexts, T*εA*G (left panel) and G*εA*C (right panel). The red arrow indicates the normal emission maximum of εA at 410nm, as can be seen with the free DNA spectrum. The blue arrow indicates the shifted λ^{max} with increasing E125Q.

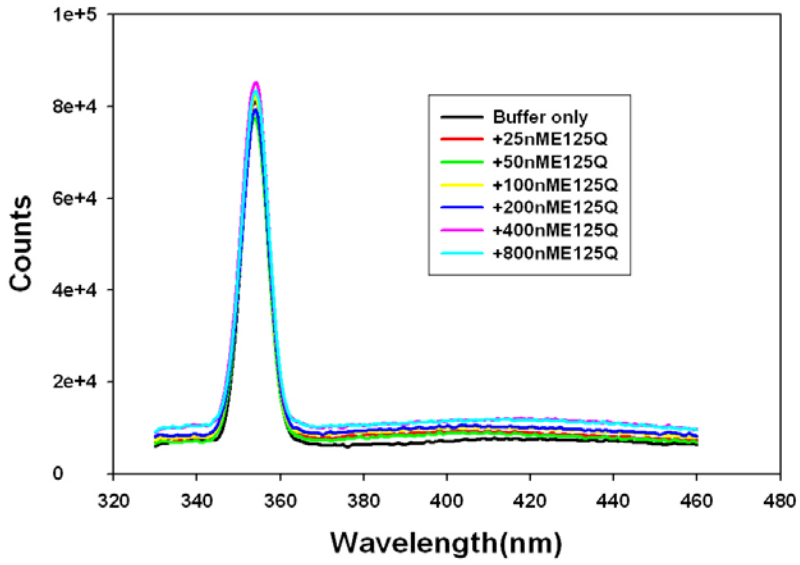

Figure 7-3. Emission scans of increasing concentrations of E125Q only when excited at 320nm. No appreciable fluorescence of the protein was observed and no blue shift was observed, contrary to when e125Q bound εA- DNA (*See Figure 7.2 and text*)

The Y162S mutant, which did not show a shifted band with εA and Hx containing DNA in the mobility shift assays (Chapter 4), did not show any appreciable increase in fluorescence with εA. The Y162S mutant did not blue shift with increasing concentrations of enzyme when excited at 320nm at room temperature (Figure 7-4). The blue shift with E125Q was interpreted as a possible electrostatic change in the active site of E125Q upon flipping the εA base out of the DNA. Hence the gradual blue shift with increasing enzyme- flipped εA complex formation. The electrostatic change upon flipping would also explain the lack of the shift with the enzyme only and with a flipping-deficient mutant, Y162S. Again, the Y162S experiment proves that this mutant was deficient in flipping the damaged base, and Tyr-162 is responsible largely for bringing and stabilizing the enzyme-flipped base complex.

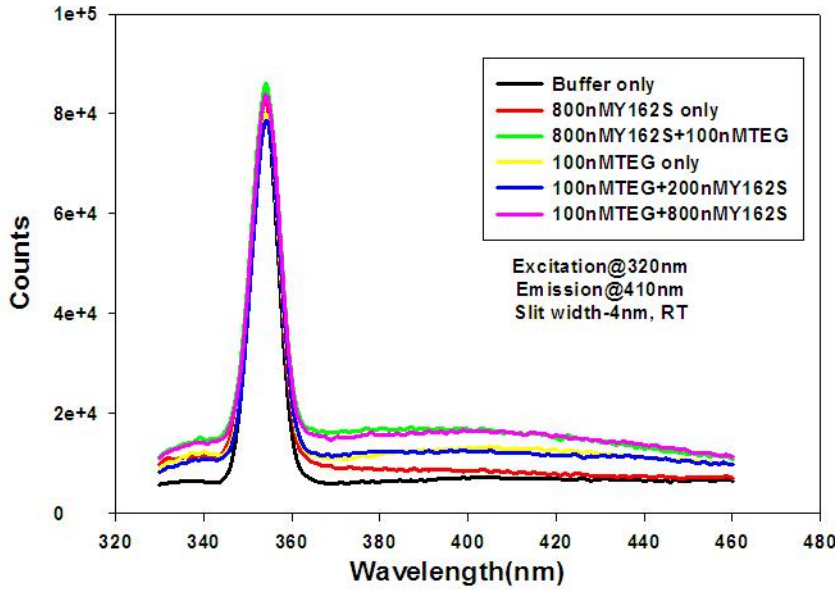

Figure 7-4. Emission spectra of 100nM TEG with 100, 200 and 800nM Y162S. The Y162S only, DNA only and buffer only control spectra are also shown to bring out the lack of the blue shift observed with E125Q. There is neither an increased fluorescence emission from εA nor a blue shift accompanying the increase.

Fluorescence of εA upon Excision of εA by AAG

Experiments were also done under excision conditions to observe the change in fluorescence when εA was excised by AAG. Excision of εA may give a much higher change in signal than that observed with E125Q mediated binding. If the excision reaction can be monitored by observing εA fluorescence change and found to complement the ^{32}P-based gel assays, we could have another real- time technique which can give us many more time points than the gel- based excision assays.

When AAGΔ79 was added to the cuvette containing DNA and the fluorescence of εA recorded at 37°C, an increase in fluorescence of εA was observed when excited at 310nm with an emission maximum at 420nm. After observing the background fluorescence of 100nMDNA only, 400 or 800nM enzyme were added and the shutter was closed. A sharp jump in εA fluorescence was observed. But in contrast to E125Q binding,

after the sharp jump, a slow and gradual increase in fluorescence intensity over a long time, up to 60 minutes was observed, when the enzyme was capable of excision (Figure 7-5). The progress of the fluorescence increase matched the progress of a εA excision curve obtained from ^{32}P-based excision assays. The magnitude of the first jump in fluorescence was also smaller than the increase seen with E125Q mediated binding. The jump is interpreted as binding and flipping of εA into the active site, whereas the slower, time- based increase is the release of free εA after excision by AAG. Interestingly the magnitude of the initial jump was higher for E125Q than for wtAAG. The difference in the initial increase was interpreted for now as possibly arising from the mutation which removes the charged glutamate and replaces it with neutral glutamine. The loss of glutamate could increase the fluorescence of the base-flipped complex. In contrast to binding only, excision of εA by AAG did not cause a blue shift the in the excision λ_{max} (Figure 3-2).

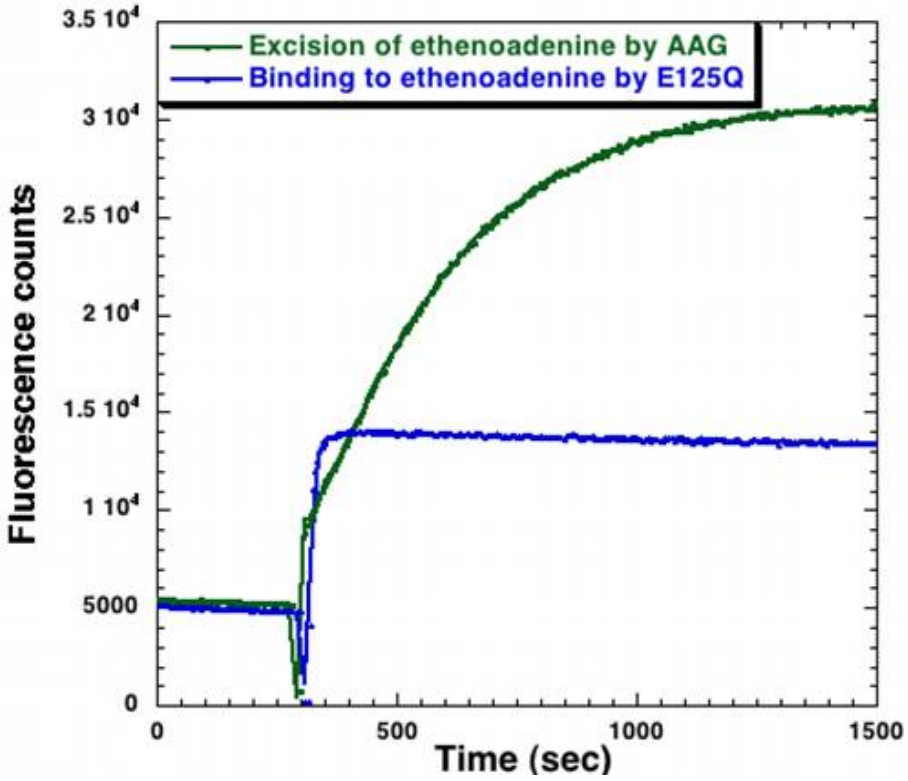

Figure 7-5. Time- based increase in εA fluorescence upon excision by 800nM AAG at 37°C (*green trace*). 100nM TεAG was incubated at 37°C and excited at 310nm and its emission observed at 420nm. After 300 seconds (flat part of the curve) 800nM AAG was added and the shutter closed. A sharp increase in εA fluorescence was observed, followed by a gradual time-based increase in fluorescence indicative of excision of εA. The progress of the curve is reminiscent of a curve obtained by fitting ^{32}P-based excision assays. The contrast between fluorescence change during excision and change during binding only is highlighted by the *blue trace*, which represents binding by E125Q *(see text).*

Stopped-flow Analysis of εA Flipping by AAG

It was clear from the experiment detailed above and the observation of Figure 7-4, that even if the first jump in fluorescence was indicating flipping of εA, it was too fast to allow any kinetic measurements of flipping. To directly measure the rate of this rapid increase in fluorescence, a stopped-flow analysis of εA flipping was done, so that the changes associated with εA flipping can be monitored on a millisecond time-scale. After measuring initial signals with free εA and 100 and 200nM εA•T substrate, 200nM

substrate was chosen for binding experiments because it provided a relatively intense signal. From EMSAs shown in chapter 4 and 5, it was noted that good binding of AAG to εA substrates was seen with as little as 4-fold less enzyme than substrate. To rule out the possibility of binding of εA by AAG being too rapid as is the case with hand- maxing experiments, the stopped-flow was maintained at a temperature of 20°C, at which the binding reaction is slower. The binding assay was done by rapidly mixing to give a final concentration of 100nM AAG and 200nM εA substrate as described in Chapter 3. The change in fluorescence was monitored using 385nm cut- on filters and a 5 milliseconds dwell time to collect data points. After trials with 4-8 fold more enzyme than substrate, the fluorescence signal upon rapid mixing was seen to be saturated. A gradual time-based change was not seen. This rapid change could either mean that the fluorescence change was not indicative of flipping or that the binding reaction is too fast that the signal is saturated at the onset. So, in an attempt to slow down the binding reaction, lower enzyme concentrations at which saturated binding may not be seen were used. After referring back to a previous EMSA, 100nM AAG was chosen as a concentration at which binding could be slower due to the fact that saturation of the substrate by E125Q was not observed at this concentration in the EMSA. With 100nM AAG and 200nM εA•T substrate, a gradual increase in fluorescence, spanning the first 10 seconds of the binding reactions was observed (Figure 7-6). The signal change was very small in magnitude when normalized with the fluorescence signals associated with the AAG only and the DNA only controls. The signal: noise ratio was also very small. These two factors made any kinetic interpretation of the fluorescent increase highly error-prone. Nevertheless,

this could be the beginning of a real-time experiment to measure the rate of base-flipping.

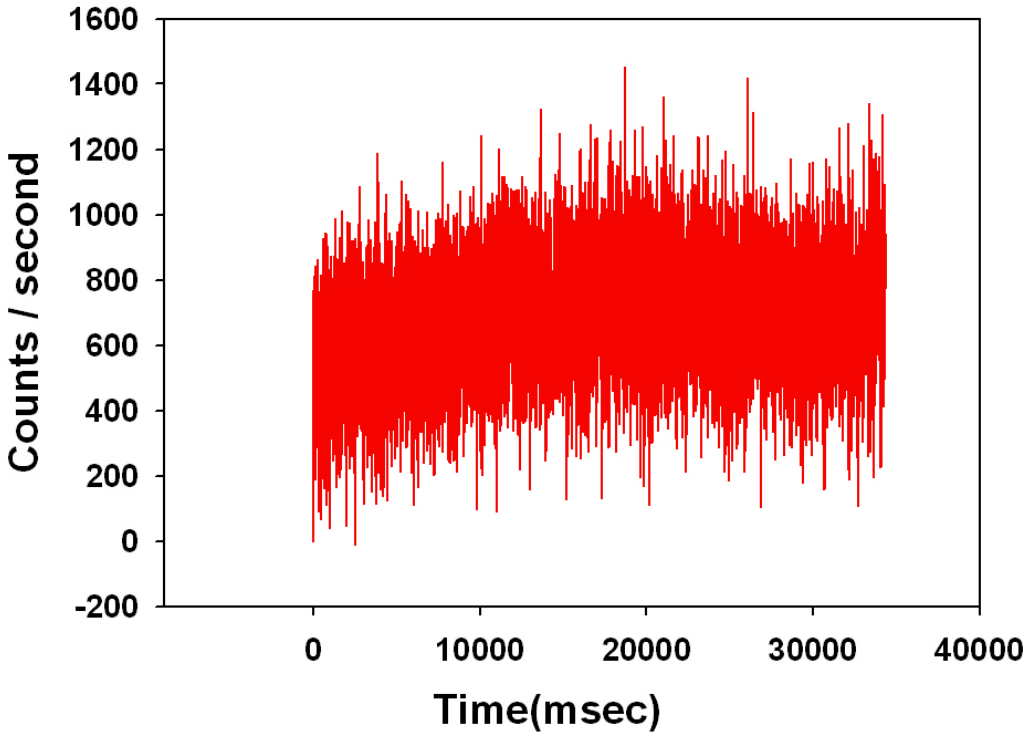

Figure 7-6. Stopped-flow analysis of εA flipping by AAG. 200nM εA•T and 100nM AAG were mixed in the stopped-flow machine at 20°C and the fluorescence change associated with binding was monitored after excitation at 310nm , using 385nm cut-on filters. A gradual change in εA fluorescence was noticed very early in the reaction.

Contribution of Fluorescence Experiments to Understanding of AAG

The need for a real time assay for glycosylases cannot be overstated, especially for AAG for which base flipping makes an important contribution to activity. The availability of the naturally fluorescent substrate, εA for development of a real time assay was also very fortunate. In the first group of experiments described in this chapter, it was clear that εA fluorescence changes when flipped and excised by AAG. The Y162 mutants whose properties were analyzed and detailed in Chapter 4 are valuable reagents to use with εA. The fluorescent base and flipping mutants, when combined tell us more about

the contribution of flipping to the activity and diversity of AAG, which is the primary objective of this dissertation. The EMSA which was the binding assay used quite successfully to delineate the differences between the Y162 mutants on one hand and the sequence context effects on the other hand, is not an equilibrium technique. So, the development of an assay to determine rates of flipping in real time would be very useful in ascertaining the conclusions made in Chapters 4 and 5. To this end, the fluorescent assays looking at the changes in the emission spectra and εA intensity upon binding by AAG are significant. The blue shift observed upon binding and the real time increase in fluorescence observed in the stopped- flow analysis are important indications that with more fine tuning, a real time assay to measure flipping rates is possible. That is the most important conclusion made from the experiments reported in this chapter.

CHAPTER 8
DISCUSSION AND FUTURE DIRECTIONS

This dissertation has attempted to address the question of the extent of the contribution of flipping to the overall efficiency of DNA glycosylases by studying flipping in AAG. AAG is the ideal glycosylase to use in such a study owing to its diverse substrate range and the availability of structural data to plan an effective strategy to test our hypotheses. The expectation that the contribution of base flipping could be considerable to AAG's activity was vindicated by the results obtained from mutagenesis of both the protein and the DNA. But how can these results be combined to explain the effects of flipping efficiency on the overall activity of the protein based on our preliminary two- step model for AAG activity? The two-step model proposed, served as a basis for partitioning the activity of AAG outside the active site (such as substrate recognition, DNA binding and base flipping) and the actual catalysis activity accomplished by the active site (*75*). But this partitioning is strictly theoretical, a good first step to understand two complex activities, infinitely useful in formulating strategies to look at flipping effects. The truth is that, both steps are interdependent and affect each other, reflecting on the activity of the enzyme. If ever the purpose of this dissertation can be achieved, it would be by formulating a model that can explain this inevitable connection between the two steps. A good way to do that would be to revisit the basic two-step model and incorporate the kinetic interpretations detailed in the preceding chapters. The purpose of this discussion is to accomplish the goal to applying the kinetic

conclusions made in chapters 4 and 5 to come up with a better understanding of the mechanism of AAG activity and substrate diversity.

The Night-Watchman Model for AAG Activity

The Night-watchman model for AAG activity is a comprehensive two- step model (Figure 8-1). According to this model, AAG can scan along the minor groove randomly looking for bases that are susceptible to flipping. It must be recalled here that AAG substrates like 3-MeA, Hx and εA have different properties in DNA from the normal bases, and hence will be flippable during this process, while normal bases will not. Once flipped, various factors in the active site of AAG including proper fit, alignment of the nucleotide for excision and suitability of the leaving group, all play a role in deciding the efficiency by which base excision proceeds to complete AAG activity. This second step is an effective check for any accidentally flipped normal bases. A general acid- base mechanism of excision serves to accommodate diverse substrates. This whole process is akin to how a night- watchman checks for open doors along an alley and, when he does encounter an open door, checks for any possible problems associated with the open door. Hence, the name “Night- watchman model” for AAG activity is an apt coinage.

This model can delineate the 2 steps enough to test them separately but at the same time allows for a common mechanism in which one factor can affect both steps in tandem and hence affect both the substrate recognition and excision of the damaged base by AAG. This model is also very useful in propagating the mechanism of AAG to include other possible steps like product dissociation and recycling back to the substrate, and this possible addition is a very important future goal in understanding AAG mechanism and action.

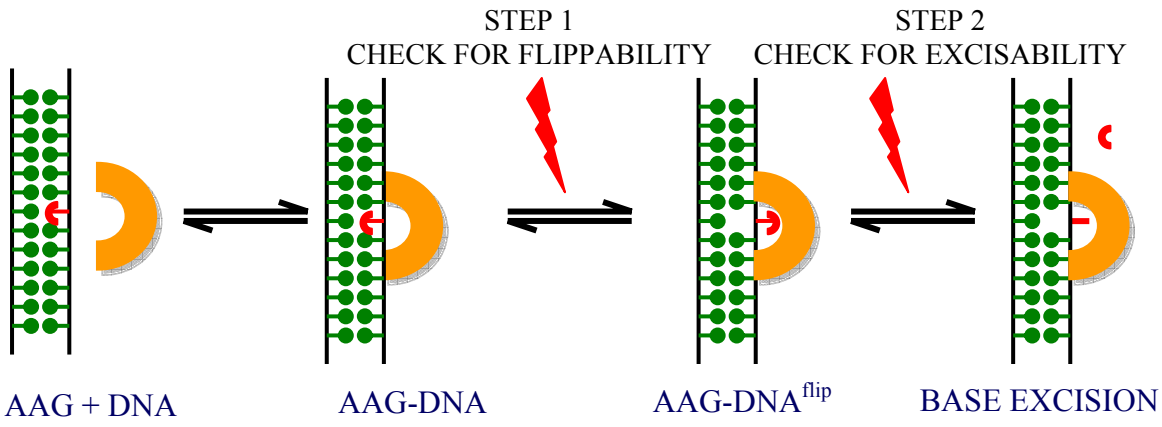

Figure 8-1. The Night-watchman model for AAG activity. AAG scans the minor groove for possible substrates by checking first for flippabilty and second for excisability once flipped into the active site. This two- step mechanism provides for enough leeway to act on multiple substrates and at the same time control over excising normal bases and non- substrates.

There are many variables that can affect Step1. This thesis has examined two such variables that could potentially affect Step1-Tyr-162, the AAG residue responsible for intercalating into the minor groove and enabling the flipped- out conformation of the *AAG- DNA*^{flip} complex and local sequence context which can impede or facilitate the achievement of the . *AAG- DNA*^{flip} complex.

Tyr-162 and the Flipping Equilibrium

As seen in figure 8-1, the flipping equilibrium can affect the active site- mediated catalysis by making less substrate available for excision by AAG. Tyr-162 is the AAG residue responsible for bringing about flipping and stabilizing the resultant flipped out base- AAG complex to enable excision. This complex function is accomplished by Tyr-162's ability to intercalate into the DNA and occupy the space vacated by the damaged base. When compared to the binding mechanisms of other well- studied glycosylases like

UDG, which uses a "pinch-push-pull" mechanism (*85*) to flip out uracil from DNA, the crystal structure of AAG bound to εA did not reveal any such distorting mechanisms for flipping εA. The contribution of Tyr-162 mediated intercalation, therefore, was thought to be very important in flipping the damaged base. This model was tested by mutating Tyr-162 to Phe and Ser. The Y162S mutant had undetectable activity, whereas, the Y162F mutant had reduced activity. In EMSAs, it was seen that binding affinity was much reduced for the Y162F mutant with both Hx and εA substrates. This reduced activity can be attributed to impaired intercalation due to the mutation. Ser, lacking the aromatic residue of Tyr was severely impaired, while Phe lacking the hydroxyl group of Tyr was significantly impaired. This impairment can reflect on Step-1 of the Night-watchman model, by making flipping inefficient, and thus move the equilibrium to the left, leaving less substrate flipped and hence less substrate excised (Figure 8-2). The combined effect of the mutation would be less efficient binding and slower rates of excision, both resulting from less efficient flipping as a result of the mutation.

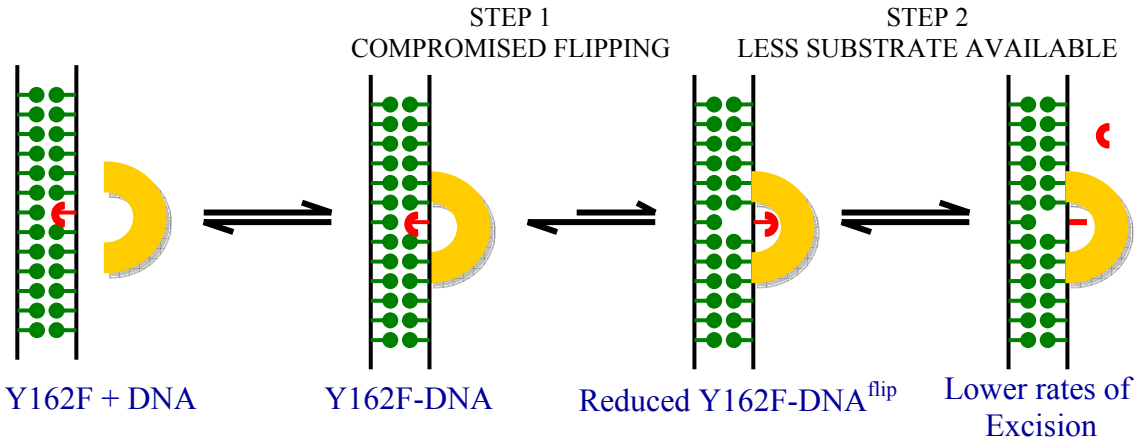

Figure 8-2. Compromised flipping due to Tyr-162 mutation. Reduced intercalation ability in the Y162F mutant can reflect on the flipping equilibrium and result in compromised flipping. Less Y162F-flipped base complex formation makes excision rates lower owing to less substrate availability in the active site. The effect of the mutation was overcome by removal of hydrogen bonds to Hx, hence making it less stable in DNA and more easily flipped

Stability of Hx and the Flipping Equilibrium

The activity of the Y162F mutant was rescued when Hx was base paired with F, the reason being that Hx cannot form hydrogen bonds with F. The additional energy needed to break the hydrogen bonds and flip out the base may also be primarily provided by the stabilizing effect of Tyr-162 intercalation into DNA. In the absence of Tyr-162, the less stable a substrate is in DNA, the more likely it is to be flipped out by the mutant. The reduced stability of Hx in a non- hydrogen bonded Hx•F context compared to the wobble base- paired Hx•T context can thus, move the flipping equilibrium in opposite directions, reflected in enhanced or slower rates of excision.

The success with the Tyr-162 mutants and the effects of base pairing partners on Hx excision prompted to look at other means to perturb the flipping equilibrium. This time around, Hx was placed in either the strongest or the weakest base stacking context and base paired with T, F or C.

The resulting single turnover excision rates reflect the flipping equilibrium with no change in the intrinsic rate of chemistry in any way. The flipping equilibrium, moved either way based on the sequence context around Hx. This is attested by the EMSAs shown in Chapter 5, in which the intensity of the higher molecular weight band, indicative of a flipped base-AAG complex, is inversely proportional to the stability of Hx. More bound Hx is seen at a lower AAG concentration when in a weaker base stacking/ non-hydrogen bonding context. In a stronger base-stacking/ hydrogen bonding context, less Hx is bound and more AAG is required to bind that Hx. This property is reflected in the amount of AAG required to bring about saturated excision of Hx in the respective sequences. That these sequence changes could intrinsically affect DNA

stability was also verified by measuring melting temperatures which also complemented the excision and binding results.

So, for Hx, perturbing the flipping equilibrium changed the way it is perceived as a substrate by AAG. The stability of Hx made it either a better or worse substrate solely by affecting how well it is flipped by AAG. This may mean that, for Hx, the rate- limiting step in its excision by AAG could be flipping, as illustrated in Figure 8-3. The hydrogen bonding potential of Hx to T and C also supports this concept. A rate-limiting flipping step for Hx can have a biological significance owing to the fact that, flipping decides whether Hx is a substrate for excision or not, and flipping Hx•T and Hx•C will have totally different consequences. Hx•T flipped, relatively well by AAG must be excised before an additional round of replication to reverse the pro- mutagenic effects of Hx. On the other hand, Hx•C is highly mutagenic. Flipping Hx•C and thereby excising Hx may confirm an AT→GC transition even before a round of replication. Hence, there seems to be a biologic imperative to control flipping of Hx by AAG. The base stacking effects add another layer to this story. and the combination of sequence effects may decide the occurrence of mutations in particular sequences of the genome, adding leverage to the existence of possible mutational “hot-spots” versus “cold-spots”, which are regions of the genome prone to having mutations versus mutation- free regions. The difference may be as simple as slower repair of lesions versus faster repair of lesions as is possible based on the sequence context a lesion like Hx is found. The objective of this dissertation of studying the contribution of flipping to the activity of AAG has thus been completed to its limits in coming up with this interpretation.

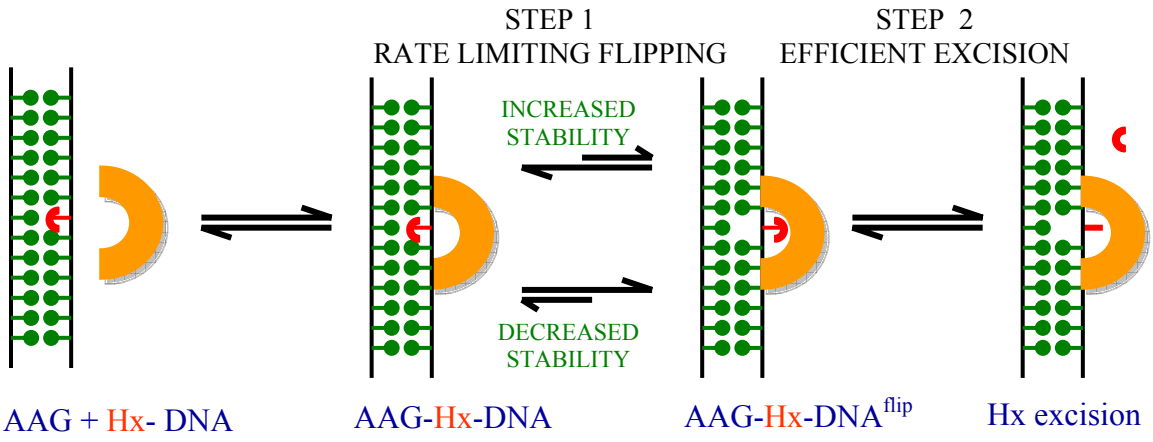

Figure 8-3. The effect of Hx stability on the Night-watchman model. Stability of Hx in DNA is affected by the sequence context of Hx which in turn affects the flipping equilibrium in Step 1. A rate-limiting flipping step would mean that enhanced or compromised flipping would increase or decrease rates of excision without any intrinsic changes in the actual rate of chemistry

Not All Bases Are Born Equal

Another question that pops up from the results obtained in Chapters 4, 5 and 6 is, *what about εA? What makes εA practically immune to the sequence context effects that so dramatically affected Hx?* The answer lies in the fact that the two bases are not the same. εA, in contrast to Hx, does not form hydrogen bonds in DNA and is a bulky base. The stability of εA is not likely to be compromised by sequence changes around the base. Progressive degradation of εA leads to many intermediates which can be mutagenic (*74*). The lack of hydrogen bonding in DNA and bulky nature combine to make εA a much more distorting lesion in DNA and confer the possibility of it being partially extra helical. This property may enable easy flipping by AAG. Binding assays using the EMSA show that εA is bound very efficiently, with low nanomolar binding constants, and needs only twice as much enzyme than substrate to bind all. This is contrasting to the binding properties of Hx. The efficient binding in the EMSA is indicative of very efficient flipping of εA by AAG. What these assays indicate is that the flipping equilibrium is

moved to the far right with εA, leaving about 90% substrate flipped at a concentration of AAG at which only 10% Hx will be flipped. So sequence changes like base stacking and base pairing partners do not have the same effect on εA as they have on Hx, since no hydrogen bonds need to be broken to flip εA and the flipping equilibrium is always tilted to the right. It is clear then that, unlike for Hx, flipping is not the rate- limiting step in εA excision.

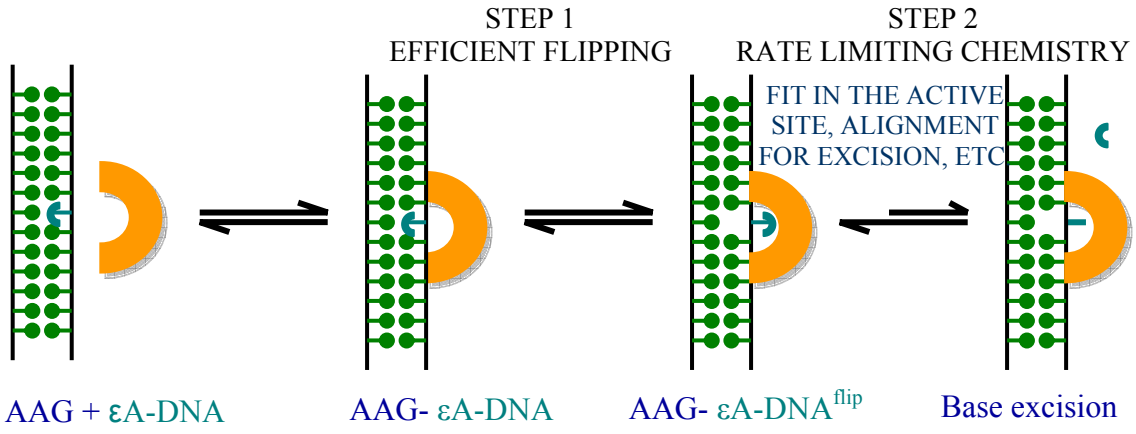

Figure 8-4. Effect of εA excision on the Night-watchman model. Rate limiting chemistry would follow efficient flipping of εA to lead to compromised excision in the active site due to many factors.

Then what else is likely to limit εA excision? Single turnover excision of εA have always shown almost invariant rates of excision with increasing AAG, with those rates being almost 4-times slower than the rates of Hx excision. The bulky nature of εA may make chemistry in the active site compromised due to many factors, like a proper fit in the active site, alignment of the glycosidic bond etc. So, it is likely that for εA, chemistry is rate-limiting and not flipping. So, Step 2 of the Night-watchman model is limiting for εA while Step 1 is limiting for Hx as is illustrated in Figure 8.4. This kinetic partitioning may be an important contributor to the ability of AAG to excise structurally diverse substrates.

Future Directions

The most important out come of this dissertation has been an understanding of the underlying complexity of DNA glycosylase activity, especially owing to AAG's diverse substrate range. The use of novel and appropriate methods to further the understanding afforded by the kinetic data discussed is important for future projects. The following are some suggestions as to what directions further research on AAG can take.

Completing the Need for a Real Time Assay to Measure Flipping

A most important corroboration to the conclusions made in this chapter would be real time rates of base flipping by AAG. A direct measure of the ease of flipping would confirm the model postulated and have a tremendous impact in the DNA glycosylase field, where the flipping mechanism is a major interest. An attempt towards developing such a technique was made and has been detailed in chapter 7. But as concluded in chapter 7, further experiments and conditions need to be worked out before the data can be kinetically interpreted to give flipping rates, which were beyond the scope of this dissertation. So, further trials with the stopped-flow fluorescence of εA are essential. It can be argued that, only for Hx will such a technique be useful in corroborating the model since εA was not affected by possible changes in the flipping equilibrium. An important avenue of research must be ways to report on Hx flipping by AAG. Fluorescent bases such as 2-aminopurine are available, which can be incorporated into DNA in such a way that, their fluorescence intensity can change with the conformation of the neighboring base, say Hx. Such an experiment will be an enormous step forward in realizing the goal of a real- time assay for flipping rates. With all the reagents made available by the projects undertaken for this dissertation, once such an experiment is established, the volume of information obtainable is very large.

Continuing Research on Sequence Context Effects

The dramatic effect of local sequence context on Hx excision and not on εA excision, combined with the rescue of the Y162F mutant, told an important story about the preferences and fine-tuning of AAG's multiple substrate specificity. To continue the research started in this dissertation to include more sequence changes, not just to flanking neighbors but to more extensive neighboring bases will not only add on to the conclusions made, but also be relevant in the sense of the genome. Another weapon in this arsenal, is the availability of the non- native base, zebularine (Z), which is a thymine analog that can form only one hydrogen bond with Hx (Figure 8-5). The use of zebularine as a base pairing partner can help to touch the middle ground between T, with which Hx forms two wobble base pairs, C, with which Hx forms two Watson- Crick base pairs and F, with which Hx forms no base pairs. The outcome of these experiments could be very interesting and may ultimately provide the ground work to assess the effects of higher order DNA structures like chromatin and methylation on AAG activity.

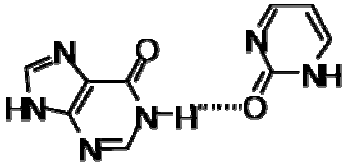

Figure 8-5. A hypoxanthine• zebularine base pair. Hx can form one hydrogen bond with Z in contrast to two hydrogen bonds with T and C and none with F.

Possible Strategy to Explain εA Excision

The only conclusion about the fate of εA which is only excised by AAG was that, perturbing the flipping equilibrium did not affect its excision by AAG. The additional indication from the kinetic studies indicated that, chemistry of bond cleavage may be the most important step in εA excision. The bulky nature of εA, compared to the other AAG

substrates, due to the presence of the etheno adduct on adenine, could be making it fit less productively in the active site for fast chemistry. This hypothesis can be tested by making the base binding pocket more amenable to fit a bulky base. The crystal structure of AAG bound to εA shows an active site residue, Met-169 making contacts with the etheno bridge of εA (Figure 8-6). The contact may be the factor limiting a proper fit in the active site thereby limiting chemistry. Mutating Met-169 to a smaller residue like alanine may make a proper fit more possible for εA. Single turnover excision assays can then de done to compare the properties of this mutant on wild type AAG to see if εA excision is improved in anyway. Binding controls by way of EMSAs need to be done to ascertain that the binding and flipping of εA is the same for the mutant and the wild type. These experiments will be a way to propagate from analyzing Step 1 of the Night- watchman model to analyzing step-2.The availability of two substrates, Hx and εA is fortuitous in allowing both steps to be tested. The Met-169 mutant will also be an interesting way to look at Hx excision, since the binding pocket may allow movement of Hx in a way that could disrupt its alignment in the active site for chemistry. So, the Met-169 mutant will also add on to furthering the horizons of this dissertation.

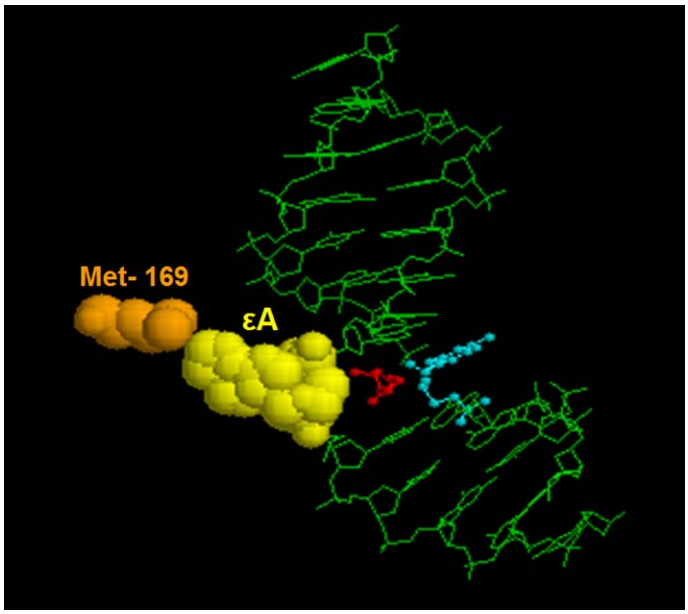

Figure 8-6. Crystal structure of the AAG-εA complex showing the proximity of Met-169 (*orange space- fill*) to the etheno bridge of the flipped out εA (*yellow space-fill*) in the active site. The *green sticks* in the DNA

Coordination of the Activity of AAG to Other Downstream Steps in BER

It must be remembered that, though the DNA glycosylases perform the important function of ridding the genome of harmful damages, the product they leave behind is in fact, more harmful than their initial substrates. The abasic site which is the product of glycosylase activity is cytotoxic. In contrast to around half a dozen known human glycosylases, only one AP endonuclease, APE1, is known to process the abasic sites in humans. Moreover, spontaneous generation of abasic sites proceeds at a considerable rate too, leading to around 10,000 abasic sites/cell/day. Evidence is mounting on the possible co- ordination between glycosylases and endonucleases hOGG1 and APE1(*111*), hMutY homolog and APE1(*112*) as well as E. coli MutY and EndoIV and ExoIII(*113*). A possible handover of product to successive enzymes in BER is now considered acceptable. The discovery of direct protein- protein interaction between APE1 and Polβ and between Polβ and ligase III through XRCC1 also add to this concept. Numerous

glycosylases and a single APE1 may not indicate direct protein- protein interactions, but may have functional interactions that help to protect the cell from accumulating abasic sites. The single turnover kinetics explored extensively in this dissertation can be a very good place to start addressing the possibility of functional interactions between AAG and APE1. The single turnover kinetics has explored the product- independent part of AAG mechanism. The complex effects of product dissociation, substrate re-association and enzyme inactivity need to be studied to further the understanding of the pathway and look for functional interactions with downstream enzymes in the pathway. The observation that multiple turnovers by AAG were impaired can indicate a possible role for APE1, which is the next enzyme in the pathway, in relieving possible product inhibition on AAG. If a functional interaction does exist, it may also be responsible for stabilizing AAG and may also relieve the loss of AAG activity noticed at lower concentrations. A functional interaction between the first two enzymes of the BER pathway will strengthen the growing perception of *passing the baton in BER*.

It can be finally concluded that the kinetic analysis of AAG activity on Hx and εA, undertaken in this dissertation has contributed significantly to the glycosylase field and will serve as the necessary ground work for more novel research in the critical field of base excision repair and the ultimate goal of safe guarding the genome.

LIST OF REFERENCES

1. Shapiro, R., and Klein, R. S. (1966) *Biochemistry 5*, 2358-62.

2. Mosbaugh, D. W., and Bennett, S. E. (1994) *Prog. Nucleic Acid Res. Mol. Biol. 48*, 315-70.

3. Lindahl, T. (1993) *Nature 362*, 709-15.

4. Peng, W., and Shaw, B. R. (1996) *Biochemistry 35*, 10172-81.

5. Marnett, L. J., and Plastaras, J. P. (2001) *Trends Genet. 17*, 214-21.

6. Marnett, L. J., Riggins, J. N., and West, J. D. (2003) *J. Clin. Invest. 111*, 583-93.

7. Atamna, H., Cheung, I., and Ames, B. N. (2000) *Proc. Natl. Acad. Sci. U. S. A. 97*, 686-91.

8. Podlutsky, A. J., Dianova, II, Wilson, S. H., Bohr, V. A., and Dianov, G. L. (2001) *Biochemistry 40*, 809-13.

9. Gros, L., Saparbaev, M. K., and Laval, J. (2002) *Oncogene 21*, 8905-25.

10. Moncada, S., Palmer, R. M., and Higgs, E. A. (1991) *Pharmacol. Rev. 43*, 109-42.

11. Prior, J. J., and Santi, D. V. (1984) *J. Biol. Chem. 259*, 2429-34.

12. Burney, S., Caulfield, J. L., Niles, J. C., Wishnok, J. S., and Tannenbaum, S. R. (1999) *Mutat. Res. 424*, 37-49.

13. Caulfield, J. L., Wishnok, J. S., and Tannenbaum, S. R. (1998) *J. Biol. Chem. 273*, 12689-95.

14. Spencer, J. P., Whiteman, M., Jenner, A., and Halliwell, B. (2000) *Free. Radic. Biol. Med. 28*, 1039-50.

15. Nilsen, H., and Krokan, H. E. (2001) *Carcinogenesis 22*, 987-98.

16. Scharer, O. D., and Jiricny, J. (2001) *Bioessays 23*, 270-81.

17. Memisoglu, A., and Samson, L. (2000) *Mutat. Res. 451*, 39-51.

18. Lindahl, T. (2000) *Mutat. Res. 462*, 129-35.

19. Lindahl, T., and Wood, R. D. (1999) *Science 286*, 1897-905.

20. Krokan, H. E., Nilsen, H., Skorpen, F., Otterlei, M., and Slupphaug, G. (2000) *FEBS Lett. 476*, 73-7.

21. Sandigursky, M., Yacoub, A., Kelley, M. R., Xu, Y., Franklin, W. A., and Deutsch, W. A. (1997) *Nucleic Acids Res. 25*, 4557-61.

22. Sobol, R. W., Prasad, R., Evenski, A., Baker, A., Yang, X. P., Horton, J. K., and Wilson, S. H. (2000) *Nature 405*, 807-10.

23. Weiss, B. (1976) *J. Biol. Chem. 251*, 1896-901.

24. Mol, C. D., Hosfield, D. J., and Tainer, J. A. (2000) *Mutat. Res. 460*, 211-29.

25. Weiss, B. (2001) *Mutat. Res. 461*, 301-9.

26. Chan, E., and Weiss, B. (1987) *Proc. Natl. Acad. Sci. U. S. A. 84*, 3189-93.

27. Demple, B., Herman, T., and Chen, D. S. (1991) *Proc. Natl. Acad. Sci. U. S. A. 88*, 11450-4.

28. Robson, C. N., and Hickson, I. D. (1991) *Nucleic Acids Res. 19*, 5519-23.

29. Osheroff, W. P., Beard, W. A., Wilson, S. H., and Kunkel, T. A. (1999) *J. Biol. Chem. 274*, 20749-52.

30. Bhagwat, A. S., Sanderson, R. J., and Lindahl, T. (1999) *Nucleic Acids Res. 27*, 4028-33.

31. Scheuermann, R. H., and Echols, H. (1984) *Proc. Natl. Acad. Sci. U. S. A. 81*, 7747-51.

32. Dianov, G. L., Prasad, R., Wilson, S. H., and Bohr, V. A. (1999) *J. Biol. Chem. 274*, 13741-3.

33. Fortini, P., Pascucci, B., Parlanti, E., Sobol, R. W., Wilson, S. H., and Dogliotti, E. (1998) *Biochemistry 37*, 3575-80.

34. Lieber, M. R. (1997) *Bioessays 19*, 233-40.

35. Matsumoto, Y., Kim, K., and Bogenhagen, D. F. (1994) *Mol. Cell. Biol. 14*, 6187-97.

36. Sobol, R. W., Horton, J. K., Kuhn, R., Gu, H., Singhal, R. K., Prasad, R., Rajewsky, K., and Wilson, S. H. (1996) *Nature 379*, 183-6.

37. Prasad, R., Dianov, G. L., Bohr, V. A., and Wilson, S. H. (2000) *J. Biol. Chem. 275*, 4460-6.

38. Prasad, R., Lavrik, O. I., Kim, S. J., Kedar, P., Yang, X. P., Vande Berg, B. J., and Wilson, S. H. (2001) *J. Biol. Chem. 276*, 32411-4.

39. Sung, J. S., and Mosbaugh, D. W. (2003) *Biochemistry 42*, 4613-25.

40. Bennett, R. A., Wilson, D. M., 3rd, Wong, D., and Demple, B. (1997) *Proc. Natl. Acad. Sci. U. S. A. 94*, 7166-9.

41. Kubota, Y., Nash, R. A., Klungland, A., Schar, P., Barnes, D. E., and Lindahl, T. (1996) *Embo. J. 15*, 6662-70.

42. Marintchev, A., Mullen, M. A., Maciejewski, M. W., Pan, B., Gryk, M. R., and Mullen, G. P. (1999) *Nat. Struct. Biol. 6*, 884-93.

43. Prasad, R., Singhal, R. K., Srivastava, D. K., Molina, J. T., Tomkinson, A. E., and Wilson, S. H. (1996) *J. Biol. Chem. 271*, 16000-7.

44. Caldecott, K. W., Aoufouchi, S., Johnson, P., and Shall, S. (1996) *Nucleic Acids Res. 24*, 4387-94.

45. de Murcia, G., and Menissier de Murcia, J. (1994) *Trends Biochem. Sci. 19*, 172-6.

46. de Murcia, J. M., Niedergang, C., Trucco, C., Ricoul, M., Dutrillaux, B., Mark, M., Oliver, F. J., Masson, M., Dierich, A., LeMeur, M., Walztinger, C., Chambon, P., and de Murcia, G. (1997) *Proc. Natl. Acad. Sci. U. S. A. 94*, 7303-7.

47. Nilsen, H., Otterlei, M., Haug, T., Solum, K., Nagelhus, T. A., Skorpen, F., and Krokan, H. E. (1997) *Nucleic Acids Res. 25*, 750-5.

48. Takao, M., Aburatani, H., Kobayashi, K., and Yasui, A. (1998) *Nucleic Acids Res. 26*, 2917-22.

49. Ohtsubo, T., Nishioka, K., Imaiso, Y., Iwai, S., Shimokawa, H., Oda, H., Fujiwara, T., and Nakabeppu, Y. (2000) *Nucleic Acids Res. 28*, 1355-64.

50. de Souza-Pinto, N. C., Eide, L., Hogue, B. A., Thybo, T., Stevnsner, T., Seeberg, E., Klungland, A., and Bohr, V. A. (2001) *Cancer Res. 61*, 5378-81.

51. Croteau, D. L., ap Rhys, C. M., Hudson, E. K., Dianov, G. L., Hansford, R. G., and Bohr, V. A. (1997) *J. Biol. Chem. 272*, 27338-44.

52. Croteau, D. L., Stierum, R. H., and Bohr, V. A. (1999) *Mutat. Res. 434*, 137-48.

53. Vaughan, P., Lindahl, T., and Sedgwick, B. (1993) *Mutat. Res. 293*, 249-57.

54. Moore, M. H., Gulbis, J. M., Dodson, E. J., Demple, B., and Moody, P. C. (1994) *Embo. J. 13*, 1495-501.

55. Lindahl, T. (1974) *Proc. Natl. Acad. Sci. U. S. A. 71*, 3649-53.

56. Matijasevic, Z., Sekiguchi, M., and Ludlum, D. B. (1992) *Proc. Natl. Acad. Sci. U. S. A. 89*, 9331-4.

57. Bjelland, S., Bjoras, M., and Seeberg, E. (1993) *Nucleic Acids Res. 21*, 2045-9.

58. Riazuddin, S., and Lindahl, T. (1978) *Biochemistry 17*, 2110-8.

59. Thomas, L., Yang, C. H., and Goldthwait, D. A. (1982) *Biochemistry 21*, 1162-9.

60. Samson, L., Derfler, B., Boosalis, M., and Call, K. (1991) *Proc. Natl. Acad. Sci. U. S. A. 88*, 9127-31.

61. Chakravarti, D., Ibeanu, G. C., Tano, K., and Mitra, S. (1991) *J. Biol. Chem. 266*, 15710-5.

62. O'Connor, T. R., and Laval, J. (1991) *Biochem. Biophys. Res. Commun. 176*, 1170-7.

63. Vickers, M. A., Vyas, P., Harris, P. C., Simmons, D. L., and Higgs, D. R. (1993) *Proc. Natl. Acad. Sci. U. S. A. 90*, 3437-41.

64. Pendlebury, A., Frayling, I. M., Santibanez Koref, M. F., Margison, G. P., and Rafferty, J. A. (1994) *Carcinogenesis 15*, 2957-60.

65. Bouziane, M., Miao, F., Bates, S. E., Somsouk, L., Sang, B. C., Denissenko, M., and O'Connor, T. R. (2000) *Mutat. Res. 461*, 15-29.

66. Engelward, B. P., Weeda, G., Wyatt, M. D., Broekhof, J. L., de Wit, J., Donker, I., Allan, J. M., Gold, B., Hoeijmakers, J. H., and Samson, L. D. (1997) *Proc. Natl. Acad. Sci. U. S. A. 94*, 13087-92.

67. Elder, R. H., Jansen, J. G., Weeks, R. J., Willington, M. A., Deans, B., Watson, A. J., Mynett, K. J., Bailey, J. A., Cooper, D. P., Rafferty, J. A., Heeran, M. C., Wijnhoven, S. W., van Zeeland, A. A., and Margison, G. P. (1998) *Mol. Cell. Biol. 18*, 5828-37.

68. Miao, F., Bouziane, M., Dammann, R., Masutani, C., Hanaoka, F., Pfeifer, G., and O'Connor, T. R. (2000) *J. Biol. Chem. 275*, 28433-8.

69. Asaeda, A., Ide, H., Asagoshi, K., Matsuyama, S., Tano, K., Murakami, A., Takamori, Y., and Kubo, K. (2000) *Biochemistry 39*, 1959-65.

70. Dosanjh, M. K., Chenna, A., Kim, E., Fraenkel-Conrat, H., Samson, L., and Singer, B. (1994) *Proc. Natl. Acad. Sci. U. S. A. 91*, 1024-8.

71. Dosanjh, M. K., Roy, R., Mitra, S., and Singer, B. (1994) *Biochemistry 33*, 1624-8.

72. van der Kemp, P. A., Thomas, D., Barbey, R., de Oliveira, R., and Boiteux, S. (1996) *Proc. Natl. Acad. Sci. U. S. A. 93*, 5197-202.

73. Leithauser, M. T., Liem, A., Stewart, B. C., Miller, E. C., and Miller, J. A. (1990) *Carcinogenesis 11*, 463-73.

74. el Ghissassi, F., Barbin, A., Nair, J., and Bartsch, H. (1995) *Chem. Res. Toxicol. 8*, 278-83.

75. Vallur, A. C., Feller, J. A., Abner, C. W., Tran, R. K., and Bloom, L. B. (2002) *J. Biol. Chem. 277*, 31673-8.

76. Abner, C. W., Lau, A. Y., Ellenberger, T., and Bloom, L. B. (2001) *J. Biol. Chem. 276*, 13379-87.

77. Lau, A. Y., Scharer, O. D., Samson, L., Verdine, G. L., and Ellenberger, T. (1998) *Cell 95*, 249-58.

78. Lau, A. Y., Wyatt, M. D., Glassner, B. J., Samson, L. D., and Ellenberger, T. (2000) *Proc. Natl. Acad. Sci. U. S. A. 97*, 13573-8.

79. Klimasauskas, S., Kumar, S., Roberts, R. J., and Cheng, X. (1994) *Cell 76*, 357-69.

80. Reinisch, K. M., Chen, L., Verdine, G. L., and Lipscomb, W. N. (1995) *Cell 82*, 143-53.

81. Slupphaug, G., Mol, C. D., Kavli, B., Arvai, A. S., Krokan, H. E., and Tainer, J. A. (1996) *Nature 384*, 87-92.

82. Yamagata, Y., Kato, M., Odawara, K., Tokuno, Y., Nakashima, Y., Matsushima, N., Yasumura, K., Tomita, K., Ihara, K., Fujii, Y., Nakabeppu, Y., Sekiguchi, M., and Fujii, S. (1996) *Cell 86*, 311-9.

83. Barrett, T. E., Savva, R., Panayotou, G., Barlow, T., Brown, T., Jiricny, J., and Pearl, L. H. (1998) *Cell 92*, 117-29.

84. Fuxreiter, M., Luo, N., Jedlovszky, P., Simon, I., and Osman, R. (2002) *J. Mol. Biol. 323*, 823-34.

85. Parikh, S. S., Mol, C. D., Slupphaug, G., Bharati, S., Krokan, H. E., and Tainer, J. A. (1998) *Embo. J. 17*, 5214-26.

86. Fraser, C. M., Casjens, S., Huang, W. M., Sutton, G. G., Clayton, R., Lathigra, R., White, O., Ketchum, K. A., Dodson, R., Hickey, E. K., Gwinn, M., Dougherty, B., Tomb, J. F., Fleischmann, R. D., Richardson, D., Peterson, J., Kerlavage, A. R., Quackenbush, J., Salzberg, S., Hanson, M., van Vugt, R., Palmer, N., Adams, M. D., Gocayne, J., and Venter, J. C. (1997) *Nature 390*, 580-6.

87. Morohoshi, F., Hayashi, K., and Munkata, N. (1993) *J. Bacteriol. 175*, 6010-7.

88. Santerre, A., and Britt, A. B. (1994) *Proc. Natl. Acad. Sci. U. S. A. 91*, 2240-4.

89. Cole, S. T., Brosch, R., Parkhill, J., Garnier, T., Churcher, C., Harris, D., Gordon, S. V., Eiglmeier, K., Gas, S., Barry, C. E., 3rd, Tekaia, F., Badcock, K., Basham, D., Brown, D., Chillingworth, T., Connor, R., Davies, R., Devlin, K., Feltwell, T., Gentles, S., Hamlin, N., Holroyd, S., Hornsby, T., Jagels, K., and Barrell, B. G. (1998) *Nature 393*, 537-44.

90. Labahn, J., Scharer, O. D., Long, A., Ezaz-Nikpay, K., Verdine, G. L., and Ellenberger, T. E. (1996) *Cell 86*, 321-9.

91. Handa, P., Roy, S., and Varshney, U. (2001) *J. Biol. Chem. 276*, 17324-31.

92. Jiang, Y. L., and Stivers, J. T. (2002) *Biochemistry 41*, 11236-47.

93. Jiang, Y. L., Stivers, J. T., and Song, F. (2002) *Biochemistry 41*, 11248-54.

94. Secrist, J. A., 3rd, Barrio, J. R., Leonard, N. J., and Weber, G. (1972) *Biochemistry 11*, 3499-506.

95. Stivers, J. T., Pankiewicz, K. W., and Watanabe, K. A. (1999) *Biochemistry 38*, 952-963.

96. Savva, R., McAuley-Hecht, K., Brown, T., and Pearl, L. (1995) *Nature 373*, 487-493.

97. Mol, C. D., Arvai, A. S., Slupphaug, G., Kavli, B., Alseth, I., Krokan, H. E., and Tainer, J. A. (1995) *Cell 80*, 869-878.

98. Jiang, Y. L., Kwon, K., and Stivers, J. T. (2001) *J. Biol. Chem. 276*, 42347-42354.

99. Asaeda, A., Ide, H., Asagoshi, K., Matsuyama, S., Tano, K., Murakami, A., Takamori, Y., and Kubo, K. (2000) *Biochemistry 39*, 1959-1965.

100. Wyatt, M. D., and Samson, L. D. (2000) *Carcinogenesis 21*, 901-8.

101. D'Ambrosio, S. M., Gibson-D'Ambrosio, R. E., Brady, T., Oberyszyn, A. S., and Robertson, F. M. (2001) *Environ. Mol. Mutagen. 37*, 46-54.

102. Hill-Perkins, M., Jones, M. D., and Karran, P. (1986) *Mutat. Res. 162*, 153-63.

103. Myrnes, B., Guddal, P. H., and Krokan, H. (1982) *Nucleic Acids Res. 10*, 3693-701.

104. Sidorkina, O., Saparbaev, M., and Laval, J. (1997) *Mutagenesis 12*, 23-8.

105. Kool, E. T. (2001) *Annu. Rev. Biophys. Biomol. Struct. 30*, 1-22.

106. Kool, E. T., Morales, J. C., and Guckian, K. M. (2000) *Angew Chem. Int. Ed. Engl. 39*, 990-1009.

107. Waters, T. R., and Swann, P. F. (1998) *J. Biol. Chem. 273*, 20007-14.

108. Porello, S. L., Leyes, A. E., and David, S. S. (1998) *Biochemistry 37*, 14756-64.

109. O'Brien, P. J., and Ellenberger, T. (2003) *Biochemistry 42*, 12418-29.

110. O'Brien, P. J., and Ellenberger, T. (2004) *J. Biol. Chem. 279*, 9750-7.

111. Hill, J. W., Hazra, T. K., Izumi, T., and Mitra, S. (2001) *Nucleic Acids Res. 29*, 430-8.

112. Yang, H., Clendenin, W. M., Wong, D., Demple, B., Slupska, M. M., Chiang, J. H., and Miller, J. H. (2001) *Nucleic Acids Res. 29*, 743-52.

113. Pope, M. A., Porello, S. L., and David, S. S. (2002) *J. Biol. Chem. 277*, 22605-15.

114. Fasman, G. (ed) (1975) *Handbook of Biochemistry. Nucleic Acids, Vol. 1,* CRC Press

115. Selwyn, M. J. (1965) *Biochim. Biophys. Acta 105*, 193-195

BIOGRAPHICAL SKETCH

Aarthy Vallur was born on 11.19.1975 in the garden city of Bangalore, India. She obtained an undergraduate degree in nutrition and dietetics and a master's degree in biochemistry and molecular biology from the University of Madras, Madras, India. She joined the interdisciplinary program in biomedical sciences in the University of Florida in 2000 for graduate studies. She was awarded an alumni fellowship to continue her research and obtain a PhD degree under the mentorship of Dr. Linda Bloom.